ABSTRACT

Title of Dissertation: ASSESSMENT OF SELECT KINEMATIC AND KINETIC GAIT OUTCOMES ACROSS THREE STANDARD SINGLE-EVENT MULTILEVEL SURGERY GROUPS

Rana Karimpour, Doctor of Philosophy, 2025

Dissertation directed by: Professor Jae Kun Shim
Kinesiology

Single-event multilevel surgery (SEMLS) is commonly performed in ambulatory children with cerebral palsy (CP) to address musculoskeletal deformities contributing to pathological gait. Although instrumented gait analysis (IGA) is widely used to evaluate postoperative outcomes, uncertainty remains regarding the sensitivity, specificity, and clinical interpretability of commonly reported gait metrics across heterogeneous surgical

protocols and patient presentations. The objective of this dissertation was to explore the behavior of kinematic, spatiotemporal, kinetic, and frontal-plane knee loading outcomes following three standardized SEMLS protocols and to evaluate how these outcomes respond to surgical context, developmental factors, and postoperative recovery.

Retrospective gait data were analyzed from ambulatory children with CP undergoing bilateral soft-tissue lengthening (TDR-B), bilateral femoral derotational osteotomy with soft-tissue procedures (TDFR-B), or unilateral femoral derotational; osteotomy with soft-tissue procedures (TDFR-U). Linear modeling frameworks were used to examine associations between gait outcomes and predictors including time post-surgery, surgical group, normalized walking speed, age, and anthropometry, as well as within-group pre–post changes and between-group differences. Effect sizes were emphasized alongside statistical significance to characterize outcome sensitivity.

Results demonstrated marked outcome-specific and SEMLS-context-dependent patterns of postoperative change. Global kinematic indices, spatiotemporal asymmetry measures, joint kinetic and energetic outcomes, and knee adduction moment (KAM)-based metrics captured distinct and sometimes dissociated aspects of postoperative adaptation and were not interchangeable. For example, improvements in global gait pathology were not consistently accompanied by parallel changes in joint kinetic or energetic measures, indicating dissociation between overall gait appearance and underlying mechanical demand. Temporal asymmetry differentiated hemiplegic and diplegic involvement patterns more consistently than spatial asymmetry, highlighting domain-specific sensitivity to clinical presentation. Developmental and speed-related associations varied by outcome and surgical protocol, indicating construct-specific behavior rather than uniform maturation effects. Modest

reductions in frontal-plane knee loading metrics were observed following SEMLS with differential patterns across protocols and between peak and impulse-based measures. Furthermore, changes in KAM metrics did not consistently correspond to changes in sagittal-plane kinematics commonly referenced as influential for knee loading, underscoring the complementary information captured by these outcomes when considering implications for long-term joint health.

Collectively, these findings support a validation-oriented interpretation of postoperative gait outcomes, emphasizing sensitivity to biomechanical constructs and clinical context rather than uniform responsiveness or direct inference of treatment efficacy. The observed heterogeneity underscores the need for structured, interdisciplinary, and condition-specific consensus approaches to outcome selection in SEMLS research. SEMLS should be viewed as an enabling intervention within a prolonged recovery process, with gait outcomes reflecting interactions among surgical correction, rehabilitation, neuromuscular adaptation, and individual patient characteristics. Future work should prioritize longitudinal designs, consensus-driven outcome frameworks, and integration of biomechanical measures with functional and patient-centered assessments to improve clinical interpretability.

ASSESSMENT OF SELECT KINEMATIC AND KINETIC GAIT OUTCOMES ACROSS THREE STANDARD SINGLE-EVENT MULTILEVEL SURGERY GROUPS

by

Rana Karimpour

Dissertation submitted to the Faculty of the Graduate School of the
University of Maryland, College Park in partial fulfillment
of the requirements for the degree of
Doctor of Philosophy
2025

Advisory Committee:
Professor Jae Kun Shim, Chair/Advisor
Associate Professor Tim Kiemel
Associate Professor Ross H. Miller
Associate Professor Moon Seok Park
Professor Norman M. Wereley

© Copyright by
Rana Karimpour
2025

Acknowledgements

I would first like to express my deepest gratitude to my advisor, Dr. Jae Kun Shim, for his continued mentorship, guidance, and support throughout this dissertation. I am especially thankful that, during Dr. Moon Seok Park's sabbatical at the University of Maryland, he facilitated the collaboration that made this work possible.

I am sincerely grateful to Dr. Moon Seok Park of the Seoul National University Bundang Hospital and their Motion Analysis Laboratory for generously sharing the gait analysis data that formed the foundation of this research. The scientific rigor and effort involved in building and maintaining such a valuable dataset are deeply appreciated, and I am honored to have been entrusted with its use.

I also thank my committee members, Drs. Kiemel, Miller, Park, and Wereley, for their thoughtful feedback and encouragement, as well as the faculty and staff of the School of Public Health for their support.

Finally, I am profoundly grateful to my family and friends for their unwavering patience, understanding, and love throughout this journey.

Table of Contents

Acknowledgements ii
Table of Contents iii
List of Abbreviations vi
Chapter 1: Introduction 1
1.1. Cerebral Palsy 1
1.2. Single-Even Multi-Level Surgeries 4
1.2.1. SEMLS Protocols Considered in the Present Study 5
1.3. Motivation and Study Rationale 8
1.4. Aim 11
Chapter 2: Kinematics 14
2.1. Introduction 14
2.2. Methods 16
2.2.1. Participants 16
2.2.2. Data Collection 16
2.2.3. Data Processing 17
2.2.4. Outcome Measures 18
2.2.5. Statistical Analysis 20
2.3. Results 21
2.3.1. Predictor Associations with Outcome and Baseline Asymmetry Correlations 22
2.3.2. Within-Group Changes Following Surgery 24
2.3.3. Between-Group Differences in Pre–Post Changes Following Surgery 26
2.4. Discussion 26
2.5. Limitations 29
2.6. Conclusion 29
Chapter 3: Gait Task-Related Joint Kinetics and Energetics 31
3.1. Introduction 31
3.2. Methods 35
3.2.1. Participants 35
3.2.2. Data Collection 35
3.2.3. Data Processing 36
3.2.4. Outcome Measures 37
3.2.5. Statistical Analysis 39
3.3. Results 40
3.3.1. Predictor Associations 40
3.3.2. Within-Group Changes Following Surgery 43
3.3.3. Between-Group Differences in Pre–Post Changes Following Surgery 45
3.4. Discussion 45
3.5. Limitations 48
3.6. Conclusion 49
Chapter 4: Knee Adduction Moment–Based Indicators of Joint Loading 51
4.1. Introduction 51
4.2. Methods 53

4.2.1. Participants 53
4.2.2. Data Collection 54
4.2.3. Data Processing 54
4.2.4. Outcome Measures 55
4.2.5. Statistical Analysis 56
4.3. Results 57
4.3.1. Cross-Sectional Associations Between Crouch Knee Posture and Outcomes 58
4.3.2. Predictor Associations with Outcomes 58
.4.3.3 Within-Group Changes Following Surgery 58
4.3.4. Between-Group Differences in Pre–Post Changes Following Surgery 59
4.4. Discussion 59
4.5. Limitations 62
4.6. Conclusion 63
Chapter 5: Integrated Synthesis, Clinical Implications, and Future Directions 64
5.1. Synthesis 64
5.1.1. Predictor Effects 65
5.1.2. Within-Group Ghanges and Between-Group Differences 67
5.2. Clinical Implications 69
5.3. Future Directions 70
Appendices 72
Appendix A: Statistical Methods 73
A.1. Regression Model Analysis 73
A.1.1. Assumption Checks 74
A.1.2. Model Selection 76
A.1.3. Model Results 76
A.1.4. Adjustment for Multiple Outcome Comparisons 78
Appendix B: Kinematic Models and Diagnostics 80
B.1. GDI 81
B.1.1. Model Assumption Checks 81
B.1.2. Model Selection 83
B.2. Normalized Walking Speed 85
B.2.1. Model Assumption Checks 85
B.2.2. Model Selection 87
B.3. Normalized Step Length 89
B.3.1. Model Assumption Checks 89
B.3.2. Model Selection 91
B.4. Normalized Step Time 93
B.4.1. Model Assumption Checks 93
B.4.2. Model Selection 95
B.5. Normalized Step Length Asymmetry 97
B.5.1. Model Assumption Checks 97
B.5.2. Model Selection 99
B.6. Step Time Asymmetry 102
B.6.1. Model Assumption Checks 102
B.6.2. Model Selection 104
B.7. Double-limb Support Time 107

B.7.1. Model Assumption Checks 107
B.7.2. Model Selection 110
Appendix C: Joint Kinetics and Energetics Models and Diagnostics 112
C.1. Ankle Positive Work in Late Stance 112
C.1.1. Model Assumption Checks 112
C.1.2. Model Selection 115
C.2. Knee Extensor Impulse in Stance Phase 116
C.2.1. Model Assumption Checks 116
C.2.2. Model Selection 119
C.3. Hip Flexor Moment Impulse in Pre-Swing 120
C.3.1. Model Assumption Checks 120
C.3.2. Model Selection 123
C.4. Sum of Lower Body Net Joint Work 124
C.4.1. Model Assumption Checks 124
C.4.2. Model Selection 127
C.5. Ratio Of Ankle To Hip Peak Propulsive Power 128
C.5.1. Model Assumption Checks 128
C.5.2. Model Selection 129
Appendix D: Knee Adduction Moment–Based Indicators of Joint Loading Models and Diagnostics 131
D.1. Peak KAM 131
D.1.1. Model Assumption Checks 131
D.1.2. Model Selection 133
D.2. KAM Impulse 135
D.2.1. Model Assumption Checks 135
D.2.2. Model Selection 137
References 140

List of Abbreviations

$AI_{\overline{sL}}$	Step length asymmetry
$AI_{\overline{st}}$	Step time asymmetry
GDI	Gait deviation index
$\overline{sL}$	Normalized step length
$\overline{v_{L_0}}$	Normalized walking speed
J_{PreSw}^{HipFlx}	Hip flexor moment impulse in pre-swing phase
W_{tot}^{LB}	Sum of lower body net joint work
W_{LSt}^{Ank+}	Ankle positive work in late stance
J_{St}^{KneExt}	Knee extensor moment impulse in stance phase
$R_{p^+}^{A/H}$	Ratio of ankle to hip peak propulsive power
J_{KAM}	Knee adduction moment impulse in stance phase
$\overline{st}$	Normalized step time
gls_ident	Generalized least squares model with identity (equal) variance structure
gls_varExp	Generalized least squares model that accounts for nonconstant variance, i.e., heteroskedasticity, by allowing error variance to increase exponentially with a fitted covariate

DHL	Distal Hamstring Lengthening
DLS	Double-limb support time
FDO	femoral (varus) derotational osteotomy
TAL	Tendo Achilles Lengthening
RFT	Rectus Femoris transfer
CP	Cerebral Palsy
GLS	Generalized Least Squares
OLS	Ordinary Least Squares
LLR	Likelihood ratio test
SEMLS	Single-event multi-level surgery

Chapter 1: Introduction

1.1. Cerebral Palsy

Cerebral palsy (CP) is the most common cause of motor disability in childhood, affecting 2.7–3.4 per 1000 live births (McIntyre et al., 2022), and is associated with high medical burden (Whitney et al., 2019). CP is not a diagnosis in the conventional sense; that is, it does not infer specific information about the underlying pathology, etiology, or prognosis (Badawi et al., 1998). Rather, it is an umbrella term encompassing disorders of posture and movement resulting from non-progressive lesions to the developing brain (Smithers-Sheedy et al., 2014). Damage to the brain's motor pathways interferes with the development of selective motor control, defined as the ability to activate muscles independently and in a coordinated manner (Sanger et al., 2006). The cause of the brain injury, along with its timing, location, and extent, gives rise to substantial heterogeneity in CP severity and motor impairment profiles(Metz et al., 2022).

One aspect of the heterogeneity in cerebral palsy is variation in motor type with the most common being spastic (Novak et al., 2025). Spasticity has been associated with alterations in muscle structure and function, which have been implicated in the development of shortened muscle–tendon units (Lieber et al., 2004). These alterations involve both passive muscle properties, such as increased collagen content within the extracellular matrix (Smith et al., 2011), and active muscle properties, including reduced myofibrillar development that limits force-generating capacity (Herskind et al., 2016; Lieber et al., 2004). Functionally, these changes manifest as reduced muscle length, strength and increased stiffness (Lieber et al., 2004). Over time, extreme shortening of muscle–tendon units leads to joint contractures, which together with the primary neuromuscular deficits place the developing skeletal system under abnormal

loading, leading to progressive bony deformities (Morrell et al., 2002).

These secondary musculoskeletal abnormalities further impact motor function as they augment the primary neuromuscular deficits during the growth spurt (Bell et al., 2002; Gage et al., 2009a). Depending on the severity of movement disorders, Gross Motor Function Classification System (GMFCS) classifies the children's motor function abilities into five levels as relevant to the functions of daily life and age (Palisano et al., 2008) (Fig. 1.1). The levels indicate the extent to which the child needs physical or powered assistance for mobility. GMFCS has been associated with children's quality of life, feelings about functioning, community participation, and physical health (Keawutan et al., 2018; Shelly et al., 2008). Walking, as one of the most frequent forms of locomotion, significantly impacts children's independence.

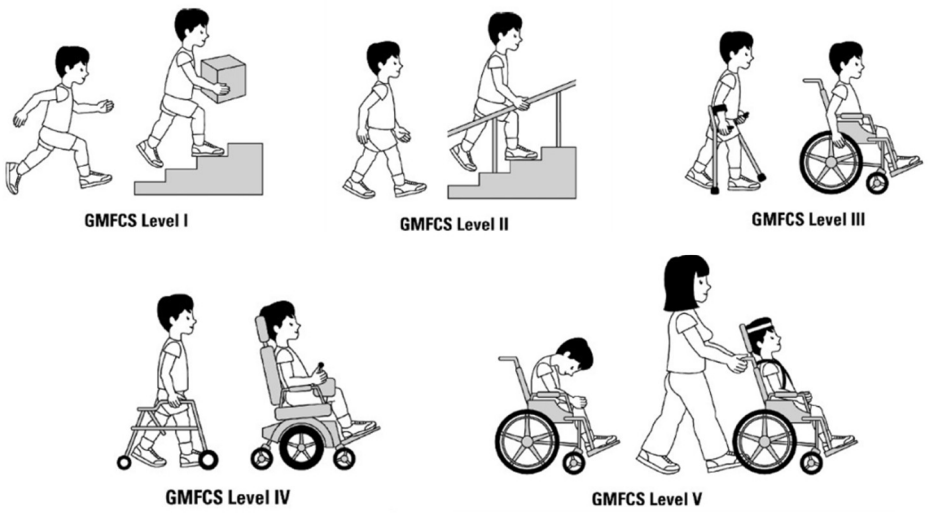


Fig 1.1: Gross Motor Function Classification System. Graham et al., 2016 (Graham et al., 2016), minor edits applied.

Gait impairments have been associated with decreased community participation and quality of life in children with CP (Bjornson et al., 2008; Palisano et al., 2009). Beyond these functional associations, qualitative studies suggest that walking also carries substantial symbolic and social value for children

with CP and their families. Parents often describe a strong imperative to "do something" or "try everything" to preserve or improve walking, equating continued intervention with hope and good parenting, while tapering of walking-focused treatments can evoke guilt and doubt (Gibson et al., 2012). Complementing these findings, parents of ambulatory children with CP participating in gait-focused rehabilitation trials have emphasized not only the importance of walking itself, but specifically the value of "correct" walking as a marker of their children's present and future well-being (Beveridge et al., 2015). In contrast, children may perceive walking primarily as exercise rather than a functional necessity, while simultaneously internalizing societal attitudes toward disability (Gibson et al., 2012). These perspectives indicate that walking is not solely a biomechanical or physiological outcome, but a deeply value-laden construct that shapes rehabilitation priorities and expectations. These perspectives help contextualize why interventions aimed at modifying gait remain a central focus of clinical management in children with CP.

One method of intervention involves surgical correction of musculoskeletal deformities that disrupt gait. "Lever arm dysfunction" refers to the altered moment arm of forces acting and moving the body due to such deformities (Gage et al., 2009b; Theologis, 2013). Orthopedic surgeries target lever arm dysfunctions that cause "imbalance" between anatomical levels (joints) and disrupt gait (Rodda et al., 2004; Silver et al., 1985). Previously these surgeries were done in a sequential single-level manner based on emerging problems. This approach required multiple anesthesia exposures, hospital admissions, and prolonged cumulative rehabilitation. This approach resulted in the child's fluctuating function after each of the staged procedures, a phenomenon described by Mercer Rang as "birthday syndrome" (Saraph et al., 2002) (Fig. 1.2). Furthermore, when problems are addressed only at the most closely related level, residual imbalances may contribute to the development of additional pathologies. A well-known example is crouch gait, characterized by excessive knee and hip flexion. Iatrogenic crouch gait was reported

following isolated gastrocnemius lengthening, which worsens the sagittal plane imbalance between the ankle and unaddressed knee and hip contractures (Stout et al., 2008; Sutherland & Davids, 1993) To mitigate the medical and indirect costs associated with staged procedures, the correction of multiple soft-tissue and/or bony deformities in a single surgical session, first described by Norlin and Tkaczuk in 1985(Norlin & Tkaczuk, 1985), has become standard practice.

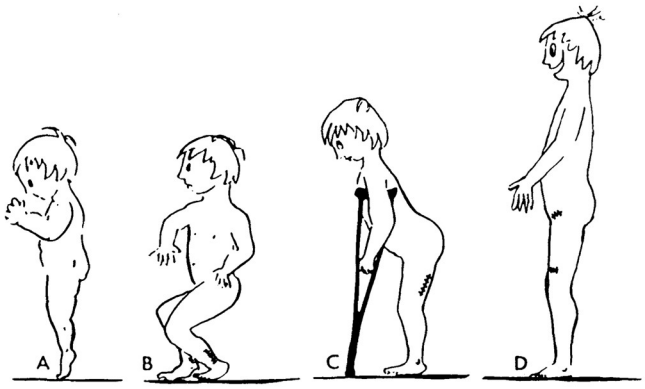


Fig 1.2: The sequence of a typical scenario of staged sequential surgeries. (a)ankle deformity addressed by isolated lengthening of Achilles tendon, in the presence of spastic hamstrings leads to (b)crouch gait, when addressed by isolated hamstring lengthening, leads to trunk collapse caused by the unopposed flexion moments, which was finally addressed in (d) by hip flexor lengthening. Original Drawing by Mercer Rang. Gage 1990 (Gage, 1990)

1.2. Single-Even Multi-Level Surgeries

Single-Event Multi-Level Surgery (SEMLS) is commonly performed in ambulatory children with cerebral palsy (GMFCS I–III). The procedure addresses multiple musculoskeletal deformities within a single operative session, with the aim of modifying structural contributors to pathological gait patterns (Gage et al., 2009b; Narayanan, 2007), and has been reported to have generally favorable and lasting effects on gait (Sung et al., 2018; Thomason et al., 2013). SEMLS typically consists of combinations of soft-tissue procedures, such as tendon lengthening or transfers, and may also include bony realignment procedures performed during the same surgical episode. The intervention has been shown to improve

gait function, quality of life, and functional independence in children with cerebral palsy (Amen et al., 2018; Cuomo et al., 2007; Himpens et al., 2013). SEMLS is inherently individualized, with procedure selection tailored to each child's pattern of musculoskeletal impairments and gait deviations (Chang et al., 2010; Cook et al., 2003; McCarthy et al., 2020; Rasmussen et al., 2019). When evaluating postoperative changes following SEMLS, it is important to recognize that concurrent procedures can influence one another within the interconnected neuromuscular system(Adolfsen et al., 2007; Õunpuu et al., 2015). Therefore, the present study focused on patients undergoing isolated SEMLS protocols consisting of four specific procedures.

1.2.1. SEMLS Protocols Considered in the Present Study

The present study focused on gait changes following three standard SEMLS protocols. These protocols were selected to represent commonly implemented combinations of three or four procedures, while minimizing the influence of additional concurrent interventions. Each procedure addresses a soft-tissue or bony deformity directly associated with pathological gait patterns commonly observed in children with cerebral palsy. The following sections describe each procedure and the characteristic kinematic and kinetic gait features with which it is commonly associated.

I. **Femoral derotational osteotomy (FDO):** FDO is commonly performed to address the in-toeing gait that is due to femoral anteversion (excessively internally rotated femur) and is associated with tripping (Cimolin et al., 2011b; Gresits et al., 2026; Rethlefsen et al., 2006). Femoral anteversion and in-toeing cause lever arm dysfunctions at the hip and foot (Fig. 1.3). FDO has been reported to restore the hip abductor moment arm, the knee extensor moment arm of ground reaction forces (Novacheck & Gage, 2007). Excessive internal rotation observed during gait analysis is a common indication for FDO (McCarthy et al., 2020), which has been shown to

improve abnormal hip and pelvic rotational kinematics during gait (Gresits et al., 2026).

II. **Tendo Achilles lengthening (TAL):** TAL is commonly performed to increase ankle dorsiflexion range of motion and has been associated with normalization of sagittal-plane ankle moments (Kay et al., 2004; Rutz et al., 2011). However, effects on ankle push-off mechanics remain inconsistent, with studies reporting reductions, preservation, or increases in ankle positive power following TAL (Davids et al., 2011; Dreher et al., 2012; Horsch et al., 2024; Rose et al., 1993; Tylkowski et al., 2009). From a biomechanical perspective, TAL increases tendon slack length, which may reduce plantarflexor force-generating capacity and alter the timing of ankle power production during stance (Delp et al., 1995; Dreher et al., 2012).

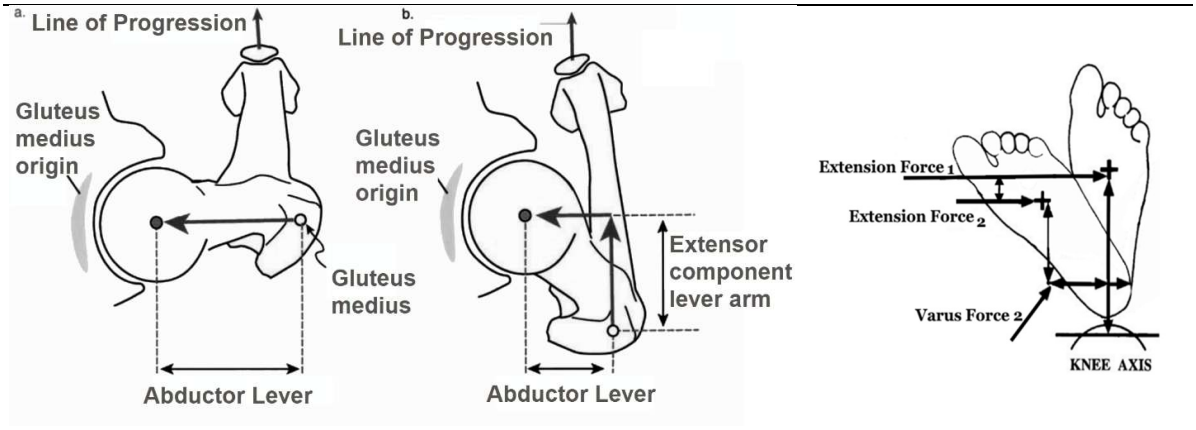


Fig 1.3: Lever arm dysfunctions associated with femoral anteversion (excessive internal rotation) at the hip (left panel), and with in-toeing gait pattern at the foot (right panel). Left panel: (a) shows the typical skeletal morphology when the adductor muscle gluteus medius works exclusively as an adductor, while (b) shows femoral anteversion carrying its insertion point posteriorly, reducing its adductor capacity and introducing extensor and internal rotation moments arms for this muscle's force. Modified from Paley (2002). Right panel: lever arm dysfunction at the foot from in-toeing gait pattern observed in patients with femoral anteversion. Abnormal foot progression angle changes the moment arm ground reaction force decreasing its extensor effect from $Force_1$ to $Force_2$ and introducing varus moments at the knee. Modified from Novacheck & Gage (2007).

III. **Distal hamstring lengthening (DHL):** DHL addresses hamstring contractures through surgical lengthening or distal tendon transfer (Haberfehlner et al., 2018; Park et al., 2009) and is commonly performed as part of multi-level surgical management in individuals with crouch

gait. Crouch gait characterizing features, i.e. excessive knee and hip flexion during stance, alter lower-limb lever arms such that the ground reaction force vector passes posterior to the knee directly increasing the external knee flexor moment (Fig. 1. 4). This biomechanical configuration is associated with elevated quadriceps demand to generate a compensatory knee extensor moment during stance (Gage et al., 2009b; Hsu et al., 1993; McNee et al., 2004; Steele et al., 2012).

IV. **Rectus femoris transfer (RFT):** Rectus RFT is used to address stiff-knee gait by transferring the tendon of an overactive rectus femoris to the posterior aspect of the knee (Dreher et al., 2012; Lee et al., 2014). The procedure is intended to preserve the rectus femoris contribution to hip flexion while reducing its knee extensor action, although the extent to which the transfer adds to its knee flexor function has been debated (Asakawa et al., 2002; Fox et al., 2009). Independent of the precise mechanism, RFT has been associated with improvements in the reduced or delayed knee flexion moment characteristic of stiff-knee gait (Lee et al., 2014; Ounpuu et al., 1993; Thawrani et al., 2012).

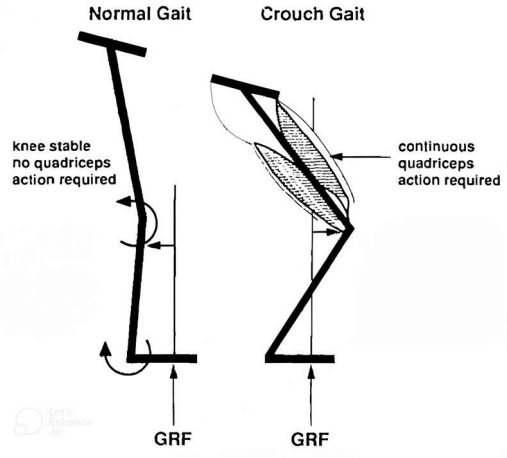


Figure 1.4: Left panel: In normal gait, the GRF passes anteriorly to the knee. The knee extensor and ankle plantarflexion moment stabilize the knee in midstance and terminal stance. Right panel: Crouch gait moves GRF posterior to the knee, generating a flexion moment that requires the action of the quadriceps to support the posture (Gage, 1993).

The SEMLS procedure combinations examined in this study were: 1- bilateral soft-tissue–only surgery (**TDR-B** = [TAL + DHL + RFT] on both sides), 2- bilateral femoral derotational osteotomy with soft-tissue procedures (**TDFR-B =** [TAL + DHL + RFT + FDO] on both sides), and unilateral femoral derotational osteotomy with soft-tissue procedures (**TDFR-U =** [TAL + DHL + RFT + FDO] on one side). These SEMLS protocols represent commonly employed surgical approaches for addressing multilevel musculoskeletal impairments that contribute to pathological gait patterns in children with cerebral palsy (Adolfsen et al., 2007; Õunpuu et al., 2015; Saglam et al., 2016). Distinguishing unilateral from bilateral FDO is clinically relevant because asymmetric internal hip rotation during gait presents a common surgical decision point. Evidence that unilateral correction of the more involved limb can yield outcomes comparable to bilateral correction highlights the importance of evaluating gait responses across unilateral and bilateral correction contexts (Desailly et al., 2020; Niklasch et al., 2015). These SEMLS protocols are tailored to the individual patient based on clinical examination and instrumented gait analysis (IGA)(Chang et al., 2010; Gage, 1993). IGA has played a central role in the classification of pathological gait patterns in cerebral palsy patterns (Rodda et al., 2004; Winters et al., 1987) and has become increasingly integrated into surgical planning and evaluation of SEMLS over time (Narayanan, 2007; Smith et al., 2021; Wren et al., 2020).

1.3. Motivation and Study Rationale

Despite its central role in SEMLS planning, broader clinical impact of IGA has been limited by persistent challenges in interpretation, clinical relevance, and integration into decision-making (Fregly, 2021; Sharma et al., 2024; Theologis et al., 2025). IGA outcomes provide objective assessment of gait, and substantial research efforts have focused on improving the reliability and repeatability of the outcomes(Carollo et al., 2025; McDowell et al., 2000; McGinley et al., 2009). Surgical planning and

evaluation of SEMLS protocols have increasingly incorporated IGA to support decision-making and outcome assessment in children with CP(Gage, 1993; Smith et al., 2021; Wren et al., 2020). For example, its use has been shown to improve agreement among clinicians regarding problem identification and surgical recommendations (Cook et al., 2003; DeLuca et al., 1997; Franki et al., 2014; Lofterød et al., 2007), and integration of IGA into clinical practice has been associated with significant reductions in iatrogenic crouch gait (Vuillermin et al., 2011). However, the broader clinical adoption of IGA outcomes remains limited(Fregly, 2021; Sharma et al., 2024; Theologis et al., 2025), particularly beyond preoperative decision-making and into postoperative evaluation and rehabilitation (Hobani et al., 2022; Hulleck et al., 2022; Wren et al., 2020). This limited uptake reflects persistent challenges in interpreting gait analysis outcomes and translating biomechanical change into clinically meaningful information.

A central contributor to this interpretability challenge is the substantial heterogeneity inherent to CP. Variability in neurological involvement, musculoskeletal impairments, surgical prescriptions, and rehabilitation pathways has been shown to obscure consistent patterns of postoperative change, resulting in variable and context-dependent responses across individuals and procedures (Lamberts et al., 2016; McGinley et al., 2012). From a technical perspective, this heterogeneity complicates identification of gait outcomes that demonstrate stable, interpretable behavior at the group level (Damiano, 2014). Clinically, such variability has been reported to reduce confidence in the usefulness of gait metrics(Van Ooteghem et al., 2020); particularly when changes are difficult to relate to functional performance or treatment goals(Almoajil et al., 2020; Hebda-Boon et al., 2023; Wren et al., 2011a).

A second barrier to clinical adoption centers on the interpretability of gait analysis outcomes and their alignment with constructs routinely used in clinical assessment and patient- and caregiver-centered decision-making. Qualitative and mixed-methods studies examining barriers to clinical use of gait

analysis have identified limited data expertise among clinicians, including variability in interpretation across clinicians (Saraph et al., 2002; Skaggs et al., 2000), difficulty with understanding and interpreting (Sharma et al., 2024) as key impediments to their integration into practice (Sharma et al., 2024; Wren et al., 2020).

From a clinical perspective, this interpretability challenge is closely tied to the outcomes clinicians are accustomed to using. Clinical assessment in CP often prioritizes functional performance measures (e.g., walking speed or timed walking tests) and patient- or caregiver-centered concerns related to gait appearance, mobility, and participation (Almoajil et al., 2020; Wilson et al., 2014). Gait outcomes that are difficult to relate to these familiar constructs or to observable movement patterns are therefore less likely to influence clinical decision-making, even when biomechanically informative (Arnold et al., 2006; Fregly, 2021; Hicks et al., 2011; Theologis et al., 2025). In current clinical practice, kinematic measures are the most widely used gait outcomes (Gómez-Pérez et al., 2019) and were the primary metrics reaching consensus in recent outcome-selection efforts in cerebral palsy gait analysis (McCarthy et al., 2020). While this emphasis supports clinical interpretability, it may also limit consideration of underlying mechanical demands and compensatory strategies that are more directly captured by kinetic and energetic outcomes.

A third challenge arises from the volume and complexity of gait analysis data. IGA generates high-dimensional, multifaceted datasets that are difficult to summarize in ways that preserve both biomechanical meaning and clinical interpretability (Shore et al., 2020). Data-reduction techniques have been proposed to address this challenge (Zwick et al., 2004); however, such approaches can be complex, difficult to interpret clinically, and may impose artificial groupings that obscure individual variability (Dobson et al., 2007; Nieuwenhuys et al., 2016). Alternatively, discrete gait outcomes are often used, but

this strategy introduces additional limitations. Reducing continuous waveforms to isolated time-point features may obscure temporally distributed biomechanical behavior (Kean et al., 2012), and there remains limited consensus regarding which discrete outcomes are most clinically meaningful, resulting in substantial heterogeneity across studies (Almoajil et al., 2022; McCarthy et al., 2020; Nieuwenhuys et al., 2016).

These challenges motivate an exploratory, validation-oriented examination of gait outcomes that aims to balance clinical interpretability with biomechanical relevance, particularly in the context of multilevel surgical interventions such as SEMLS.

1.4. Aim

The aim of this dissertation was to conduct an exploratory, validation-oriented evaluation of the behavior and interpretability of selected kinematic and kinetic gait outcomes across three standard Single-Event Multi-Level Surgery (SEMLS) procedure combinations.

These SEMLS groupings were selected to serve as well-defined clinical contexts, reducing procedural heterogeneity and enabling assessment of whether gait outcomes that are mechanistically linked to the targeted surgical corrections demonstrate stable, interpretable, and clinically meaningful behavior following intervention. This exploratory study is motivated by the recognition that gait outcomes reflect the behavior of a complex system rather than direct, proportional responses to isolated structural changes. Human gait arises from a highly nonlinear dynamical system shaped by the interaction of mechanical structure, neuromuscular control, and environmental constraints (West & Scafetta, 2003). Even in the absence of muscle activation and neural control, gait mechanics exhibit inherent nonlinearity, as demonstrated in passive dynamic walking models (Kurz et al., 2008), with additional state-dependent

nonlinearities introduced by muscle force production and neural coordination(Frank et al., 2010; Zajac, 1989). Within this nonlinear systems framework, bilateral correction of femoral malalignment is expected to perturb gait mechanics more extensively than unilateral correction; however, responses of derived gait outcomes are not necessarily expected to scale linearly or additively with the extent of structural correction.

Accordingly, to address challenges related to heterogeneity, the three SEMLS protocols were treated as distinct clinical containers within which outcome behavior could be explored rather than pooled across disparate surgical presentations. To address challenges related to clinical relevance, outcomes were selected that are directly related to surgical targets and are conceptually linked to gait appearance, functional walking, and long-term joint health. To address challenges related to data volume and interpretability, emphasis was placed on outcomes that either provide global characterization of gait behavior (e.g., Gait Deviation Index) or capture temporally distributed mechanical information through kinetically meaningful measures such as joint impulse and work.

The investigation was structured hierarchically to reflect increasing biomechanical specificity, progressing from kinematic gait outcomes (Chapter 2) to gait-task–related joint kinetics and work-based energetics (Chapter 3), and finally to frontal-plane knee joint kinetics commonly used as surrogates of internal joint loading and long-term joint health (Chapter 4). Together, these chapters provide a tiered, exploratory validation of gait analysis outcomes, examining their sensitivity, consistency, and clinical interpretability within stable surgical contexts, rather than their ability to differentiate surgical effectiveness.

Chapter 2: Kinematics

2.1. Introduction

Cerebral palsy (CP) is the most common cause of motor disability in childhood, affecting 2.7–3.4 per 1000 live births(McIntyre et al., 2022), and is associated with a high medical burden (Whitney et al., 2019). CP is an umbrella term for disorders of posture and movement caused by non-progressive lesions in the developing brain (Smithers-Sheedy et al., 2014). Spasticity, a common neural deficit in CP, alters muscle properties and leads to functional changes such as muscle weakness and shortening (Lieber et al., 2004). Over time, these neural deficits and shortened muscle–tendon units contribute to secondary bony deformities and joint contractures (Kerr Graham & Selber, 2003). "Lever-arm dysfunction" describes the resulting musculoskeletal deformities that alter the moment arms of forces acting on the body during movement (Rethlefsen & Kay, 2013; Theologis, 2013). Together, abnormal loading and impaired neuromuscular control progressively compromise functional mobility(Bell et al., 2002; Gage et al., 2009a).

In ambulatory individuals, orthopedic surgery interventions aim to correct contractures and dysfunctional lever arms to improve gait and reduce pain (Himpens et al., 2013). Single-event multilevel surgery (SEMLS), which involves musculoskeletal corrections at multiple anatomical levels within a single surgical session, is the standard orthopedic surgical approach for ambulatory children with CP as it reduces the number of hospitalizations and recovery periods and minimizes the risk of residual imbalances associated with staged procedures (Gage et al., 2009b; Saraph et al., 2002; Schwartz et al., 2004; Zwick et al., 2001). Following surgical intervention, objective evaluation of gait outcomes is essential, and kinematic measures provide a widely used and interpretable means of characterizing

postoperative gait changes.

Kinematic gait measures are inherently descriptive of movement patterns while also reflecting functional coordination across joints. Their descriptive value is clinically meaningful, as gait appearance ranks as a top treatment priority for children with CP and their caregivers, often even ahead of function and mobility (Karpati et al., 2011). Beyond appearance, kinematic measures also capture aspects of gait function. For example, the Gait Deviation Index (GDI) (Schwartz & Rozumalski, 2008) is a validated composite score derived from joint angle patterns across the gait cycle (Molloy et al., 2010) and reflects global deviations in overall gait pathology, encompassing both gait appearance and coordinated kinematic function.

Similarly, spatiotemporal variables provide clinically interpretable indicators of global walking function and interlimb coordination in children with CP. For example, in diplegic spastic CP, they have been reported to correlate with clinical outcomes like muscle spasticity, skeletal deformities, and gross motor function(Gómez-Pérez et al., 2023). Typically children with CP demonstrate lower walking speed and step length, along with increased step time and double-limb support time (Chakraborty et al., 2020; Dimakopoulos et al., 2022; Kim & Son, 2014). Walking speed, often termed the "sixth vital sign" (Fritz & Lusardi, 2009), is central to clinical assessments of walking capacity (Bjornson et al., 2013), as it reflects overall gait efficiency and integrates neuromuscular control, strength, and compensatory strategies(Davids et al., 2019; Fritz & Lusardi, 2009). Step length and step time are among determinants of mature gait (Sutherland, 1997), characterize neural control in CP (Bulea et al., 2017), and directly correlate with function (O'Sullivan et al., 2021). Asymmetry in step length and step time further provides insight into unequal limb contribution and impaired coordination, which are prevalent even in bilateral CP and are associated with reduced gait efficiency and increased energetic cost (Bulea et al., 2017;

Patterson et al., 2008).

Human gait reflects the behavior of a highly nonlinear dynamical system shaped by interactions among mechanical structure and neuromuscular control (West & Scafetta, 2003). Accordingly, responses of gait outcomes to intervention are not assumed to be linear or additive, and kinematic and spatiotemporal measures most directly related to the targeted surgical corrections were selected because they capture complementary aspects of gait quality and function, supporting this exploratory outcome validation analysis.

2.2. Methods

The following sections describe participant characteristics, data collection procedure, data processing steps, the derivation of kinematic gait outcome measures, and statistical methods used to analyze them.

2.2.1. Participants

Participants were 67 children with CP (GMFCS I–III; 46 male, 21 female; median age = 6.3 (IQR:5.3-9.9); mass 26.9 ± 13.2 kg), including 17 with hemiplegia, 48 with diplegia, and 1 with quadriplegia. Participants were retrospectively assigned to one of three SEMLS groups based on the surgical protocol received: 1) TDR-B — bilateral soft-tissue procedures (Achilles tendon lengthening, distal hamstring lengthening, and rectus femoris transfer) (n = 14); 2) TDFR-B — the above soft-tissue procedures combined with bilateral femoral derotational osteotomy (FDO) (n = 29); 3) TDFR-U — the same soft-tissue procedures combined with unilateral FDO (n = 24).

2.2.2. Data Collection

Gait data were collected between 1995 and 2017 using two motion-analysis systems. The first system

was a Kestrel 10-camera digital motion-capture system (Motion Analysis Corp., USA) with two KISTLER force plates (Switzerland). Marker placement followed the Helen Hayes marker set, and data were captured and processed in real time using *Cortex* and *OrthoTrak* software.

The second system was a Vicon motion-capture setup (Vicon 370; Oxford Metrics, Oxford, UK) with seven CCD cameras sampling at 60 Hz and two AMTI force plates (MA, USA). Reflective markers (25 mm) were applied using the Plug-in Gait model. Some datasets included full-body marker sets, but only lower-extremity data were analyzed to maximize participant inclusion.

Participants walked barefoot along a 9-m walkway, taking approximately 9 ± 4 strides per trial. On average, 3 ± 1 complete force-plate strikes (one foot fully isolated on a single force plate) were recorded per participant.

2.2.3. Data Processing

Marker trajectories data was pre-processed and gap-filled using Vicon Nexus (Version 2.18). Inverse dynamics analyses were performed in Visual3D (HAS-Motion, Version 2024.03.3) using six-degree-of-freedom segment models defined from a static calibration trial; if unavailable, a frame near mid-stance approximating quiet standing was used for model scaling.

Kinematic marker trajectories were low-pass filtered using zero-lag, fourth-order Butterworth filters. Cutoff frequencies were determined using residual analysis (Winter, 2009). A participant-specific approach was adopted for cutoff selection to account for inter-individual variability and the sensitivity of kinematic and kinetic outcomes to filtering choices, consistent with prior recommendations against using a single cutoff frequency across participants(Fazlali et al., 2020; Kristianslund et al., 2012). Residual analysis was conducted using marker trajectories and ground reaction force data from each participant's

trials. Participant-level outcomes were summarized using the median across trials to reduce the influence of outlier trials and residual high-frequency noise. Participant-specific cutoff frequencies were constrained to a data-driven range with a lower bound of 5.5 Hz and an upper bound of 10 Hz and were applied consistently within each participant.

These filtered signals were then used to build a 7-segement lower-extremity model. From the model the joint angles were calculated in Visual 3D as the orientation of distal segment in relation to the proximal segment using the XYZ Cardan sequence in each stride (Hamill et al., 2013). Gait events were first identified using the algorithm described by Zeni et al.(Zeni et al., 2008), which detects events based on the relative positions of the heel and toe markers with respect to the pelvis, and were subsequently verified by visual inspection.

2.2.4. Outcome Measures

As mentioned, the kinematic outcomes examined in this study were grouped into two categories: the Gait Deviation Index (GDI) as a global measure of gait pathology, and spatiotemporal measures encompassing the remaining discrete features, including walking velocity, step length, step time, and asymmetry indices. Details of outcome computation are provided below.

Gait Deviation Index

The Gait Deviation Index (GDI) provides a global measure of overall gait pathology by summarizing deviations in multi-joint kinematic waveforms relative to typically developing gait using a reduced-dimensionality representation of joint-angle patterns across the gait cycle (Schwartz & Rozumalski, 2008). A score of 100 reflects typical gait, with each 10-point decrease corresponding to approximately one standard deviation increase in gait pathology. The typically developing reference dataset made

publicly available by Schwartz and Rozumalski was used for GDI computation in the present study.

Lower-extremity joint angles at the hip, knee, and ankle in all three anatomical planes were extracted and time-normalized across the gait cycle to generate the kinematic waveforms required for GDI calculation. Joint-angle trajectories were first averaged across trials within each limb. Limb-specific GDI values were then computed and averaged across the right and left limbs to obtain a single participant-level GDI value.

Spatiotemporal Measures

Walking speed (m/s), step length (m), step time (s), and double-limb support (DLS) time were calculated directly in Visual3D from heel-strike and toe-off gait events. Gait events were identified using the Zeni et al. method (Zeni et al., 2008), with all detected events subsequently verified visually. To enable comparison across participants of different body sizes, spatiotemporal parameters were rendered dimensionless using normalization based on each participant's leg length (L_0) (Hof, 1996). Normalized walking speed was calculated as $v/\sqrt{gL_0}$, where g denotes gravitational acceleration. Step time was made dimensionless by normalization to $\sqrt{L_0/g}$, and step length was normalized to leg length. Double-limb support duration expressed as a percentage of stride time (DLS) was defined as the percentage of the gait cycle during which both feet were simultaneously in ground contact.

Right-left asymmetry in normalized step time ($\overline{sL}$) and normalized step time ($\overline{st}$), were computed based on the standard symmetry index proposed by Robbinson et al. (Robinson et al., 1987):

$$\text{AI (\%)} = \frac{|\text{Right - Left}|}{0.5 \times (\text{Right + Left})} \times 100$$

such that larger values of right–left asymmetry index of normalized step length ($\text{AI}_{\overline{sL}}$), and right–left

asymmetry index of normalized step time ($\overline{AI}_{st}$) indicate greater right–left differences regardless of direction. Discrete outcomes were summarized at the participant level by averaging across limbs to support evaluation of overall gait behavior within each SEMLS context, applied consistently across participants.

2.2.5. Statistical Analysis

A detailed description of the statistical methods is provided in Appendix A. Gait outcomes were analyzed using ordinary least squared (OLS) regression models that included Group, Time (pre vs. post), and their interaction, with normalized walking speed, time since surgery (months), age, mass, and sex included as covariates. Linearity of continuous predictors was assessed using spline-expanded OLS models; when nonlinearities were detected, the relevant spline terms were retained. Homogeneity of slopes across groups was evaluated through Group × covariate interactions, with group-specific slopes modeled when these terms were significant.

Due to the unequal size of the groups exacerbating the effect of heteroscedasticity (Box, 1954), the initial OLS model structure arrived at from the previous steps was refit using generalized least squares (GLS) with alternative variance structures (varIdent, varExp, varPower, varComb). Based on the procedure proposed by Pinheiro & Bates (Pinheiro & Bates, 2000), Akaike Information Criterion (AIC) (Akaike, 1998) was used to compare the fit of the models with different variance structures. The final model with the least AIC was selected for the subsequent analyses. Complete model coefficients and diagnostic plots for all outcomes are provided in Appendix B.

Estimated marginal means (EMMs) for each Group × Time combination were obtained from the final

model. Within-group pre–post changes (Post–Pre) were estimated using model-based contrasts, and between-group differences in change (differences in differences; DID) were derived from the Group × Time interaction. Sidak-adjusted confidence intervals and *p*-values were used for all pairwise DID comparisons (Šidák, 1967).

Effect sizes were expressed as Cohen's *d*: paired-samples *d* for within-group changes and independent-samples *d* for DID effects, with Hedges' small-sample correction applied to between-group comparisons. All analyses were performed in R (Version 4.5.1)(R Core Team, 2025) using the nlme, emmeans, and sandwich packages. P-values for pre–post changes and difference-in-differences comparisons were adjusted for family-wise error using the Holm method (Holm, 1979) across seven outcome comparisons.

To assess whether asymmetry measures were sensitive to surgical laterality rather than specific procedure subtype, we additionally tested pre–post change using a binary unilateral versus bilateral grouping via a Time × Laterality interaction.

2.3. Results

In the following sections, we first report associations between gait outcomes and model predictors, including participant anthropometry and demographics, walking speed, and time since surgery, and baseline asymmetry within patient groups defined by topographical involvement (hemiplegia vs diplegia). We then present within-group changes following surgery, followed by between-group differences in surgery-related changes.

2.3.1. Predictor Associations with Outcome and Baseline Asymmetry Correlations

Model coefficients and full diagnostic results for all outcomes are presented in Appendix B. Table 2.1. shows the association of predictors with outcomes. Time since surgery was a significant predictor of several kinematic outcomes. It was positively associated with GDI, step time asymmetry, normalized step length, and negatively with DLS. The association between time since surgery and normalized step time differed by group, with TDFR-U and TDR-B showing more positive associations than the reference TDFR-B group. The effect of Time (pre vs. post) on GDI varied by group. Relative to TDFR-B, the time effect in TDR-B was smaller and trivial in magnitude ($|d| = 0.17$). Overall, Time was a significant positive predictor of GDI (large effect) and DLS (small effect). Sex was a significant predictor of GDI, with females showing a trivial positive association.

Normalized speed was significantly associated with both DLS and GDI. Higher walking speeds were associated with shorter DLS (small effect, $|d| = 0.43$) and greater GDI (trivial effect, $|d| = 0.18$). Age was significantly associated with GDI and DLS. Older participants exhibited lower GDI (trivial effect) and shorter DLS (small effect). The association between age and R–L asymmetry in step time differed by group, with more positive age-related associations observed in TDR-B and TDFR-U relative to TDFR-B. Participant mass was strongly associated with normalized speed (very large effect) and step length (large effect) and positively associated with R–L asymmetry in step length (small effect). The relationship between mass and step-length asymmetry was group dependent, with more negative associations observed in TDFR-U and TDR-B compared with TDFR-B.

Table 2.1: Summary of predictor–outcome associations. Filled circles (●) indicate statistically significant positive associations and hollow circles (○) indicate statistically significant negative associations; Blank cells indicate non-significant effects. (–) denotes predictors excluded to avoid mechanistic correlations.

Predictor	GDI	Normalized Speed	Normalized Step Length	Double Limb Support Time	Normalized Step Time	Step Length Asymmetry	Step Time Asymmetry
Group (main effect)	●	●	●	●	●	○	●
Time (Post vs Pre)	●			●			
Time since surgery (months)	●		●	○	●		●
Normalized Speed	●			○			
Age	○			○			●
Mass	●	○	○			○	
Sex	●						

Baseline Asymmetry Correlations: At baseline, step-time asymmetry was greater in participants with hemiplegia (median [IQR]: 15.9 [5.45–28.3]) than in those with diplegia (median [IQR]: 7.44 [3.46–11.7]; Wilcoxon rank-sum test, W = 4304, $p < 0.001$). In contrast, step-length asymmetry was not different across participants with hemiplegia (median [IQR]: 7.05 [4.11–10.8]) than in those with diplegia (median [IQR]: 8.19 [3.32–16.9] at baseline; Wilcoxon rank-sum test, $p > 0.05$). Model predicting $AI_{\bar{st}}$ from surgery laterality and Time (pre- vs. post-), step-time asymmetry differed between unilateral and bilateral group overall (main effect of laterality, p = .003, see Appendix B Table B.6.7). However, no evidence was found that pre–post changes in $AI_{\bar{st}}$ differed between unilateral and bilateral procedures (Time × Laterality, p = .13). A significant Laterality × Age interaction indicated that age-related associations with asymmetry differed by laterality status (Table B.6.7). In a similar surgery laterality model, step length asymmetry was associated with normalized walking speed, lower asymmetry observed at higher speeds, and with time since surgery (Table B.5.7). No main effects of laterality, Time (pre- vs. post-surgery), mass, sex, or age were observed. We found no evidence of differences in pre–

post change in step length asymmetry between unilateral and bilateral procedures.

2.3.2. Within-Group Changes Following Surgery

As shown in Table 2.2, across all three surgical groups, GDI increased significantly from pre- to post-surgery (all $p \leq .003$), with moderate to large effect sizes. The magnitude of change was largest in TDFR-B, followed by TDR-B and TDFR-U.

In spatiotemporal outcomes, pre–post changes were generally small and did not reach statistical significance. Normalized walking speed ($\overline{v_{L_0}}$) and step length ($\overline{sL}$) showed no significant changes in any group.

Table 2.2: Estimated Changes in Kinematic Gait Outcomes Following Single-Event Multi-Level Surgery Across Three Surgical Protocols. Uncorrected p-values are reported. Holm correction across seven outcomes yielded identical statistical significance conclusions.

	TDR-B				TDFR-B				TDFR-U			
Outcome	Pre(M±SE)	Post(M±SE)	*p*	|d|	Pre(M±SE)	Post(M±SE)	*p*	|d|	Pre(M±SE)	Post(M±SE)	*p*	|d|
GDI	68.22 ± 2.41	76.24 ± 1.62	< .001*	0.99	58.60 ± 2.19	73.83 ± 1.19	< .001*	1.41	64.16 ± 3.45	75.09 ± 2.00	0.003*	0.62
$\overline{v_{L_0}}$	0.98 ± 0.09	1.02 ± 0.09	0.750	0.09	0.98 ± 0.06	1.12 ± 0.06	0.057	0.35	1.17 ± 0.04	1.24 ± 0.05	0.215	0.25
$\overline{sL}$	0.71 ± 0.04	0.69 ± 0.04	0.788	0.07	0.72 ± 0.03	0.73 ± 0.02	0.555	0.11	0.80 ± 0.02	0.82 ± 0.02	0.532	0.13
$\overline{st}$	0.80 ± 0.06	0.70 ± 0.05	0.051	0.52	0.70 ± 0.03	0.66 ± 0.02	0.273	0.20	0.66 ± 0.01	0.64 ± 0.01	0.236	0.24
DLS	28.18 ± 1.62	28.26 ± 1.65	0.968	0.01	22.08 ± 0.84	25.94 ± 1.02	0.001*	0.59	22.96 ± 0.86	25.02 ± 1.01	0.099	0.34
$AI_{\overline{sL}}$	2.19 ± 4.67	4.86 ± 4.64	0.648	0.12	15.09 ± 2.53	10.80 ± 2.28	0.102	0.30	7.16 ± 3.97	5.03 ± 4.13	0.680	0.08
$AI_{\overline{st}}$	7.32 ± 1.08	8.37 ± 1.15	0.382	0.23	6.98 ± 1.17	8.58 ± 1.45	0.345	0.18	15.52 ± 2.34	13.13 ± 1.85	0.401	0.17

Note. Pre = before surgery; Post = after surgery. Values are model-estimated means (M) with standard errors (SE).
p values are from model. d = Cohen's d. * $p < 0.05$.

Table.2.3: Between-Group Differences in Estimated Changes of Kinematic Gait Outcomes Following Surgery. Uncorrected *p*-values shown; see Table 2.4 for the changes in statistical significance following Holm correction.

	(TDR - B) - (TDFR - B)				(TDFR - U) - (TDFR - B)				(TDFR - U) - (TDR - B)			
Outcome	Δ	95% CI	*p*	|d|	Δ	95% CI	*p*	|d|	Δ	95% CI	*p*	|d|
GDI	-7.22	[-13.98, -0.45]	0.032*	0.81	-4.31	[-14.11, 5.50]	0.649	0.28	2.91	[-7.16, 12.98]	0.868	0.23
$\overline{v_{L_0}}$	-0.10	[-0.44, 0.23]	0.840	0.24	-0.07	[-0.29, 0.15]	0.807	0.22	0.03	[-0.28, 0.35]	0.994	0.08
$\overline{sL}$	-0.03	[-0.16, 0.10]	0.928	0.17	0.00	[-0.09, 0.09]	1.000	0.00	0.03	[-0.10, 0.16]	0.927	0.18
$\overline{st}$	-0.06	[-0.20, 0.08]	0.648	0.34	0.01	[-0.07, 0.10]	0.965	0.11	0.07	[-0.05, 0.19]	0.364	0.49
DLS	-3.78	[-9.57, 2.01]	0.316	0.50	-1.81	[-5.85, 2.24]	0.637	0.29	1.97	[-3.84, 7.79]	0.802	0.27
$AI_{\overline{sL}}$	6.95	[-8.21, 22.11]	0.617	0.35	2.16	[-11.47, 15.78]	0.975	0.10	-4.80	[-23.30, 13.71]	0.900	0.20
$AI_{\overline{st}}$	-0.55	[-5.53, 4.43]	0.991	0.08	-4.00	[-11.92, 3.92]	0.540	0.33	-3.45	[-10.79, 3.90]	0.599	0.37

Note. Δ = estimated between-group difference. *p* values are from model. d = Cohen's d. Significance: * $p < 0.05$

Table 2.4: Holm-Adjusted *p*-values for Between-Group Differences in Pre–Post Change (Difference-in-Differences) in Kinetic Gait Outcomes

contrast	outcome	*p* value	*p* Holm
(TDR-B) - (TDFR-B)	GDI	0.032	0.227

Note: Holm adjustment for multiple comparisons was applied across seven outcomes.

Double-limb support (DLS) increased significantly only in the TDFR-B group showing a large effect size (Cohen's d = 0.59, p = .001), whereas changes in the other groups were not statistically significant. Normalized stance time ($\overline{st}$) showed a near-significant reduction in TDR-B (p = .051) but did not reach significance in any group. Neither step-length asymmetry ($AI_{\overline{sL}}$) nor step-time asymmetry ($AI_{\overline{st}}$) demonstrated significant pre–post changes in any group, with effect sizes remaining small.

2.3.3. Between-Group Differences in Pre–Post Changes Following Surgery

Between-group comparisons of pre–post changes are summarized in Table 2.3; changes in statistical significance following Holm correction are shown in Table 2.4. No statistically significant differences in change were observed among the three surgical protocols for any kinematic gait outcome.

2.4. Discussion

In this exploratory validation analysis, kinematic and spatiotemporal outcomes demonstrated heterogeneous postoperative responses across surgical groups, consistent with the known heterogeneity of the CP population and variability in gait adaptation following multilevel orthopedic intervention (Lamberts et al., 2016; McGinley et al., 2012). Within-group analyses revealed significant postoperative improvements in GDI across all surgical groups, with larger effect sizes observed in the bilateral SEMLS groups (TDR-B and TDFR-B). These findings support the sensitivity of GDI to postoperative changes in global kinematic patterns and are consistent with its role as a composite indicator of overall gait pathology (Massaad et al., 2014; McMulkin & MacWilliams, 2015).

Smaller effect sizes in groups with higher baseline GDI align with prior observations that less-abnormal gait patterns exhibit reduced detectability of change on composite indices such as the GDI (Rutz et al., 2013). Importantly, this should not be interpreted as lack of surgical benefit but rather as a measurement characteristic of the GDI, which reflects global deviation from typical gait. Prior work has shown that substantial sagittal-plane kinematic changes may occur with minimal corresponding change in GDI, particularly when changes are multidirectional or symmetric about typical gait patterns (Barton et al., 2015; Rose et al., 2010). On the other hand, SEMLS studies report significant GDI responsiveness, consistent with our postoperative findings. This indicates GDI primarily reflects coherent global gait modification rather than gradual or multidirectional kinematic evolution (Cimolin et al., 2011a; Thomason et al., 2013).

Despite clear within-group improvements, between-group comparisons revealed no statistically significant differences, indicating that while GDI its postoperative responsiveness, inter-individual variability and overlapping change distributions limit its ability to discriminate between surgical approaches. Several covariates were significantly associated with GDI, providing insight into factors shaping postoperative gait behavior. GDI demonstrated a negative association with age, reflecting age-dependent responsiveness, consistent with reports of greater functional gains in younger children vs maintenance in older individuals (Chang et al., 2020; Hanson et al., 2025). GDI was positively associated with normalized walking speed and time since surgery, supporting its sensitivity to gait performance and recovery progression. In contrast to prior reports of a linear negative association between body mass and GDI (Malt et al., 2016),, the present analysis identified a non-linear relationship, suggesting that mass influences global gait pathology in a non-monotonic manner that may reflect interacting effects of growth, strength, and energetic demand.

Double-limb support time (DLS) increased significantly only in the bilateral FDO group (TDFR-B), with no significant changes observed in the soft-tissue–only (TDR-B) or unilateral FDO (TDFR-U) groups. Between-group contrasts showed wide confidence intervals, indicating substantial variability. The absence

of change in the bilateral soft-tissue group suggests that surgical extent and recovery demands, rather than bilaterality alone, influence DLS behavior. This interpretation is supported by the negative associations of DLS with walking speed, age, and time since surgery, consistent with developmental maturation and prior reports of inverse speed–DLS relationships (Hausdorff et al., 1999; Williams & Martin, 2019).

Other spatiotemporal measures, including normalized walking speed, step length, step time, and asymmetry metrics, demonstrated small effect sizes and nonsignificant changes both within and between groups, consistent with population heterogeneity and prior reports of variable post-SEMLS responses (Lamberts et al., 2016). Normalized walking speed was nonlinearly and negatively associated with mass, aligning with evidence of disproportionate strength–mass relationships in children with CP (Davids et al., 2015).

At baseline, step-time asymmetry was greater in participants with hemiplegia than diplegia, consistent with more pronounced inter-limb differences in hemiplegic gait (Böhm & Döderlein, 2012; Koller et al., 2023), supporting the construct validity of $AI_{\overline{st}}$. No baseline difference was observed for $AI_{\overline{sL}}$, suggesting limited sensitivity of this metric to diagnostic laterality. These asymmetry indices exhibited distinct patterns of association. $AI_{\overline{st}}$ differed between unilateral and bilateral SEMLS groups and demonstrated laterality-dependent age effects, indicating sensitivity to laterality and developmental factors, but did not show differential pre–post-surgical change. In contrast, $AI_{\overline{sL}}$ showed no laterality-dependent effects and was primarily associated with walking speed and time since surgery, indicating sensitivity to gait dynamics and recovery progression rather than laterality-specific correction.

Collectively, these findings indicate that kinematic and spatiotemporal measures reflect individualized gait adaptations rather than uniform group-level responses to specific surgical configurations. GDI emerged as a sensitive indicator of global postoperative gait modification, whereas spatiotemporal measures

demonstrated greater heterogeneity and limited between-group discrimination. Together, this pattern supports the use of these outcomes for characterizing overall gait adaptation and variability following SEMLS rather than for distinguishing between surgical approaches.

2.5. Limitations

This study has several limitations. Sample sizes varied across groups. Follow-up intervals differed, and only short- to mid-term postoperative outcomes were examined. Despite these limitations, the magnitude of observed changes in kinematic outcomes within FDO-inclusive groups suggests that these measures are sensitive to system-level perturbations and capable of capturing detectable changes following intervention, supporting their evaluation in a validation-oriented framework.

Several limitations should be considered when interpreting these findings. The heterogeneity of surgical procedures performed within SEMLS groups may have contributed to variability in gait outcomes, limiting the ability to attribute observed changes to specific surgical components. In addition, this exploratory analysis was designed to validate the behavior of gait metrics rather than to assess the comparative efficacy of surgical approaches, and causal inferences should therefore be avoided. Group-level summaries may also mask meaningful individual gait adaptations, particularly given the diversity of baseline gait patterns and postoperative motor strategies in children with cerebral palsy.

2.6. Conclusion

In summary, this exploratory validation analysis demonstrated that kinematic and spatiotemporal gait measures are responsive to postoperative change in ambulatory children with cerebral palsy, while exhibiting substantial inter-individual variability. Metrics such as the GDI captured global modifications in gait pathology following surgery but showed limited ability to distinguish between surgical configurations at the group level after adjustment for multiple comparisons. These findings support the use of kinematic and

spatiotemporal outcomes for characterizing postoperative gait behavior and variability, rather than for inferring differential surgical efficacy. Future work integrating these measures with kinetic and subject-specific modeling approaches may further clarify the mechanisms underlying heterogeneous gait adaptations following SEMLS.

Chapter 3: Gait Task-Related Joint Kinetics and Energetics

3.1. Introduction

Cerebral palsy (CP) is the most common cause of motor disability in childhood, affecting 2.7–3.4 per 1000 live births(McIntyre et al., 2022), and is associated with a high medical burden (Whitney et al., 2019). CP is an umbrella term for disorders of posture and movement caused by non-progressive lesions in the developing brain (Smithers-Sheedy et al., 2014). The neurological etiology of cerebral palsy varies in location, timing, and severity, contributing substantially to clinical heterogeneity (Metz et al., 2022). One manifestation of this heterogeneity is variation in motor subtype, with spastic cerebral palsy being the most common presentation (Novak et al., 2025). Spasticity has been associated with structural and functional muscle adaptations, such as increased stiffness and weakness, which are thought to contribute to the shortened muscle–tendon units frequently observed in cerebral palsy (Lieber et al., 2004). Over time, neuromuscular impairments and shortened muscle–tendon units contribute to joint contractures and progressive skeletal deformities during growth (Kerr Graham & Selber, 2003). "Lever-arm dysfunction" describes musculoskeletal deformities that alter the moment arms of forces driving movement, resulting in impaired function (Rethlefsen & Kay, 2013; Theologis, 2013). Lever-arm dysfunction contributes to progressive impairment of functional mobility in cerebral palsy and underlies the orthopedic surgical approach to functional improvement (Bell et al., 2002; Gage et al., 2009a).

In ambulatory individuals with cerebral palsy, the orthopedic approach to improving gait aims to correct dysfunctional moment arms in order to restore sagittal-plane balance across the hip, knee, and ankle (Kerr Graham & Selber, 2003; Silver et al., 1985). Single-event multilevel surgery (SEMLS), which addresses musculoskeletal deformities at multiple anatomical levels within a single surgical session, has become the standard surgical approach for ambulatory children with CP, as it reduces repeated hospitalizations and recovery periods while minimizing residual imbalances associated with staged procedures (Gage et al.,

2009b; Saraph et al., 2002; Schwartz et al., 2004; Zwick et al., 2001).

Pathological gait patterns in CP have been characterized based on recurring kinematic and kinetic features (Gage & Novacheck, 2001; Winters et al., 1987). For example, toe-walking gait is commonly associated with a characteristic "double-bump" ankle plantarflexion moment, reflecting impaired ankle dorsiflexion and reduced power generation during stance(Alvarez et al., 2007; Novacheck & Gage, 2007). These established kinetic signatures underscore the potential clinical relevance of kinetic variables for assessing surgical targets and postoperative gait behavior.

Instrumented gait analysis (IGA) is therefore widely used to support surgical planning and outcome evaluation in CP; however, consensus remains limited regarding which outcomes best capture clinically meaningful changes following intervention. Although IGA contributes to surgical decision- CP (Cook et al., 2003; DeLuca et al., 1997; Lofterød et al., 2007; Wren et al., 2011b), agreement on outcome selection for surgical indication and postoperative evaluation is lacking (Baker et al., 2016; Cook et al., 2003; DeLuca et al., 1997; Narayanan, 2007), and its use in postoperative rehabilitation remains limited (Hulleck et al., 2022).

Clinical heterogeneity in CP further complicates interpretation of gait outcomes, obscuring consistent postoperative patterns and yielding variable responses across individuals and procedures(Damiano, 2014; Lamberts et al., 2016; McGinley et al., 2012). This variability challenges group-level interpretation and can reduce clinical confidence in gait metrics, particularly when observed changes are difficult to relate to functional performance or treatment goals (Van Ooteghem et al., 2020; Wren et al., 2020). Kinematic measures are the most commonly used gait outcomes in clinical practice and are closely related to observable gait patterns (Gómez-Pérez et al., 2019) and the primary metrics reaching consensus in recent outcome-selection efforts (McCarthy et al., 2020), despite offering limited insight into underlying mechanical demands.

Accordingly, the present study focuses on gait-task–relevant kinetic outcomes that are biomechanically

grounded, clinically interpretable, and sensitive to postoperative change within defined SEMLS contexts. Three standard SEMLS protocols were examined to provide structured clinical frameworks for evaluating the behavior of selected kinetic measures.

Achilles tendon lengthening (TAL) is commonly performed to address equinus deformity and has been associated with improvements in ankle dorsiflexion and sagittal-plane ankle moments. However, reported effects on ankle push-off mechanics remain inconsistent, likely reflecting heterogeneity in surgical technique and dosage as well as differences in baseline gait pathology, including true versus apparent equinus (Davids et al., 2011; Dreher et al., 2012; Horsch et al., 2024; Rose et al., 1993; Tylkowski et al., 2009). Accordingly, ankle positive work during late stance (W_{LSt}^{Ank+}) was selected as a kinetic outcome, as it reflects both the magnitude and timing of plantarflexor contribution to forward propulsion and is sensitive to changes in ankle push-off mechanics (Delp et al., 1995; Dreher et al., 2012; Zelik & Adamczyk, 2016).

Distal hamstring lengthening (DHL) aims to correct crouch gait characterized by excessive knee flexion during the stance by targeting hamstring contracture. Prior studies have reported reductions in knee flexion following DHL (Laracca et al., 2014; Park et al., 2009). Improvements in crouch gait, reduces the demand on quadriceps to support the limb against (Novacheck & Gage, 2007). Accordingly, knee extensor impulse during the stance phase (J_{St}^{KneExt}) was selected as a kinetic outcome associated with DHL and crouch gait improvement.

Femoral derotational osteotomy (FDO) addresses in-toeing gait pattern associated with excessive femoral internal rotation. It has been reported to alter hip muscle moment arms (Kainz et al., 2023)as well as hip kinematics and kinetics during gait (Boyer et al., 2021; Cimolin et al., 2011b). Individuals with cerebral palsy have also been shown to exhibit proximal compensatory strategies, manifested by increased hip power generation (Cimolin et al., 2011b) and a reduced ratio of ankle to hip peak power compared with typically

developing controls and between affected and less-affected limbs (Ishihara & Higuchi, 2014; Olney et al., 1990; Riad et al., 2008). Accordingly, the ratio of ankle-to-hip peak propulsive power ($R_{p^+}^{A/H}$) was selected as a kinetic outcome, as it characterizes inter-joint power distribution and reflects proximal–distal power balance during gait.

Rectus femoris transfer (RFT) is performed to address stiff-knee gait, which is characterized by insufficient knee flexion during swing and impaired foot clearance (Lee et al., 2014; Õunpuu et al., 2015; Thawrani et al., 2012). The procedure aims to reduce inappropriate rectus femoris activity as a knee extensor while preserving its role as a hip flexor (Fox et al., 2009). Prior work has suggested that reductions in rectus femoris activity during pre-swing may have a greater influence on improvements in stiff-knee gait than changes occurring during swing phase itself (Reinbolt et al., 2008). Accordingly, hip flexor impulse during the pre-swing phase ($J_{\mathrm{PreSw}}^{HipFlx}$) was selected as a kinetic outcome to reflect changes in rectus femoris activity and associated improvements in stiff-knee gait mechanics.

Children with cerebral palsy exhibit greater metabolic energy expenditure during walking than typically developing peers (Campbell & Ball, 1978; Norman et al., 2004), which has been associated with reduced walking efficiency and increased fatigue. Energetic efficiency has been shown to correlate with clinical measures of motor function (Kerr et al., 2008). Work-based energetic metrics derived from joint mechanics are associated with metabolic energy expenditure (Marconi et al., 2014; van de Walle et al., 2012), and are elevated in cerebral palsy gait relative to typical development (van den Hecke et al., 2007). Accordingly, the sum of lower-body net joint work was selected as a surrogate measure of energetic demand relevant to walking efficiency and fatigue in cerebral palsy gait.

Because human gait reflects the behavior of a highly nonlinear dynamical system (West & Scafetta, 2003), responses of derived outcomes are interpreted as system-level behavior rather than proportional effects.

Accordingly, the outcomes described above were selected based on their direct mechanical relevance to the targeted surgical corrections as the focus of this exploratory analysis of gait-task–relevant kinetic measures, evaluated for coherent behavior across distinct SEMLS contexts to improve interpretability and clinical utility.

3.2. Methods

The following describes the study participants, data collection and processing procedures. The derivation of gait-related kinetic and work-based energetic outcomes follows. The section concludes with a description of the statistical methods used for analysis.

3.2.1. Participants

Participants were 67 children with CP (GMFCS I–III; 46 male, 21 female; median age = 6.3 (IQR:5.3-9.9)8 ± 3.9 years; mass 26.9 ± 13.2 kg), including 17 with hemiplegia, 48 with diplegia, and 1 with quadriplegia. Participants were retrospectively assigned to one of three SEMLS groups based on the surgical protocol received: 1) TDR-B — bilateral soft-tissue procedures (TAL, distal hamstring lengthening, and rectus femoris transfer) (n = 14); 2) TDFR-B — the above soft-tissue procedures combined with bilateral femoral derotational osteotomy (FDO) (n = 29); 3) TDFR-U — the same soft-tissue procedures combined with unilateral FDO (n = 24).

3.2.2. Data Collection

Gait data were collected between 1995 and 2017 using two motion-analysis systems. The first system was a Kestrel 10-camera digital motion-capture system (Motion Analysis Corp., USA) with two KISTLER force plates (Switzerland). Marker placement followed the Helen Hayes marker set, and data were captured and processed in real time using *Cortex* and *OrthoTrak* software.

The second system was a Vicon motion-capture setup (Vicon 370; Oxford Metrics, Oxford, UK) with seven CCD cameras sampling at 60 Hz and two AMTI force plates (MA, USA). Reflective markers (25 mm) were applied using the Plug-in Gait model. Some datasets included full-body marker sets, but only lower-extremity data were analyzed to maximize participant inclusion.

Participants walked barefoot along a 9-m walkway, taking approximately 9 ± 4 strides per trial. On average, 3 ± 1 complete force-plate strikes (one foot fully isolated on a single force plate) were recorded per participant.

3.2.3. Data Processing

Kinematic marker trajectories were low-pass filtered using zero-lag, fourth-order Butterworth filters. Cutoff frequencies were determined using residual analysis (Winter, 2009). A participant-specific approach was adopted for cutoff selection to account for inter-individual variability and the sensitivity of kinematic and kinetic outcomes to filtering choices, consistent with prior recommendations against using a single cutoff frequency across participants (Fazlali et al., 2020; Kristianslund et al., 2012). Residual analysis was conducted using marker trajectories and ground reaction force data from each participant's trials. Participant-level outcomes were summarized using the median across trials to reduce the influence of outlier trials and residual high-frequency noise. Participant-specific cutoff frequencies were constrained to a data-driven range with a lower bound of 5.5 Hz and an upper bound of 10 Hz and were applied consistently within each participant.

Marker trajectories were low-pass filtered at 6 Hz. These filtered signals were then used to build a 7-segement lower-extremity model. From the model the joint angles were calculated in Visual 3D as the orientation of distal segment in relation to the proximal segment using the XYZ Cardan sequence in each stride (Hamill et al., 2013). Gait events were first identified using the algorithm described by Zeni et al. (Zeni et al., 2008), which detects events based on the relative positions of the heel and toe markers with respect to

the pelvis, and were subsequently verified by visual inspection. Joint moments and powers were calculated using Visual 3D based on the iterative Newton-Euler inverse dynamics algorithm (Selbie et al., 2014) using the ground reaction forces in valid kinetic steps. A step was considered kinetically valid if only one foot of the participant was in contact with the force plate. Joint moment impulse and work were calculated as the integral of moments and powers (Winter, 2009).

3.2.4. Outcome Measures

The calculation of gait-related joint kinetics mechanistically linked to the SEMLS protocols under study, as well as the derivation of a work-based energetic outcome, is described below.

Gait Task-Related Joint Kinetics

Ankle positive work in late stance (W_{LSt}^{Ank+}) was defined as

$$W_{LSt}^{Ank+} = \int_{t=HR}^{TO} P^{Ank+}(t).dt$$

,

where the P^{Ank+} denotes the positive ankle joint power, which was integrated in the late stance; late stance was defined as the interval from heel-rise to toe-off (Whittle, 2007). Heel rise gait event was identified using a derivative- and threshold-based approach applied to the vertical heel marker trajectory. The first derivative of the vertical displacement signal was computed, and heel rise was defined as the first time point at which the derivative exceeded a threshold based on the signal's variability, defined as one standard deviation of the derivative during early stance, consistent with kinematic threshold-based gait event detection approaches reported previously (Zeni et al., 2008).

Knee extensor impulse during the stance phase (J_{St}^{KneExt}) was computed as

$$J_{St}^{KneExt} = \int_{t=HS}^{TO} M^{KneExt}(t).dt$$

, where the M^{KneExt} denotes the knee extensor moment, which was integrated over the stance phase, i.e., from heel strike to toe-off.

Hip flexor moment impulse in the pre-swing phase (J_{PreSw}^{HipFlx}) was calculated as

$$J_{PreSw}^{HipFlx} = \int_{t=CHS}^{TO} M^{HipFlx}(t).dt$$

, where M^{HipFlx} denotes the hip flexor moment, which was integrated over the pre-swing phase. Pre-swing was defined as the interval from contralateral heel strike to ipsilateral toe-off (Whittle, 2007).

Ratio of ankle to hip peak propulsive power ($R_{p^+}^{A/H}$) was calculated using

$$R_{p^+}^{A/H} = \frac{P_{\max}^{Ank+}}{P_{\max}^{Hip+}}$$

, as the ratio of the maximum ankle power to the maximum hip joint power within late stance (after heel-rise).

Work-Based Energetics

Sum of lower body net joint work (W_{tot}^{LB}) was calculated was

$$W_{tot}^{LB} = \sum_{j\in\{ankle,knee,hip\}} \int_{t=HS}^{TO} (P_j^+(t) + |P_j^-(t)|).dt$$

where P_j^+, P_j^- denote the positive and negative power of joint j, which was integrated over the stance

phase from heel strike to toe-off, and summed up across ankle, knee and hip joints.

Outcome were summarized at the participant level by averaging across limbs to support evaluation of overall gait behavior within each SEMLS context, applied consistently across participants.

3.2.5. Statistical Analysis

A detailed description of the statistical methods is provided in Appendix A. Gait outcomes were analyzed using ordinary least squared (OLS) regression models that included Group, Time (pre vs. post), and their interaction, with normalized walking speed, time since surgery (months), age, mass, and sex included as covariates. Linearity of continuous predictors was assessed using spline-expanded OLS models; when nonlinearities were detected, the relevant spline terms were retained. Homogeneity of slopes across groups was evaluated through Group × covariate interactions, with group-specific slopes modeled when these terms were significant.

Due to the unequal size of the groups exacerbating the effect of heteroscedasticity (Box, 1954), the initial OLS model structure arrived at from the previous steps was refit using generalized least squares (GLS) with alternative variance structures (varIdent, varExp, varPower, varComb). Based on the procedure proposed by Pinheiro & Bates (Pinheiro & Bates, 2000), Akaike Information Criterion (AIC) (Akaike, 1998) was used to compare the fit of the models with different variance structures. The final model with the least AIC was selected for the subsequent analyses. Complete model coefficients and diagnostic plots for all outcomes are provided in Appendix B.

Estimated marginal means (EMMs) for each Group × Time combination were obtained from the final model. Within-group pre–post changes (Post–Pre) were estimated using model-based contrasts, and between-group differences in change (differences in differences; DID) were derived from the Group × Time interaction. Sidak-adjusted confidence intervals and *p*-values were used for all pairwise DID comparisons

(Šidák, 1967).

Effect sizes were expressed as Cohen's *d*: paired-samples *d* for within-group changes and independent-samples *d* for DID effects, with Hedges' small-sample correction applied to between-group comparisons. All analyses were performed in R (Version 4.5.1)(R Core Team, 2025) using the nlme, emmeans, and sandwich packages. P-values for pre–post changes and difference-in-differences comparisons were adjusted for family-wise error using the Holm method (Holm, 1979) across seven outcome comparisons.

3.3. Results

In the following sections, we first report associations between gait outcomes and model predictors, including participant anthropometry, demographics, walking speed, and time since surgery. We then present within-group changes following surgery, followed by between-group differences in surgery-related changes.

3.3.1. Predictor Associations

As indicated in the summary Table 3.1 and detailed in the tables of model coefficients in Appendix C, outcomes were correlated with several predictors.

Ankle positive work in late stance (W_{LSt}^{Ank+}) did not show a significant pre–post change in the reference group (TDFR-B) (standardized $\beta = -0.32$, $p = .266$), indicating no detectable effect of surgery over the follow-up period for this outcome. No significant main effects of SEMLS group were observed for either the TDR-B group (standardized $\beta = 0.08$, $p = .759$; trivial effect) or the TDFR-U group (standardized $\beta = -0.13$, $p = .491$; trivial effect). Several covariates were significantly associated with the W_{LSt}^{Ank+}. Normalized walking speed showed a positive association (standardized $\beta = 0.10$, $p < .001$; trivial effect size), and time since surgery was also positively associated with W_{LSt}^{Ank+} (standardized $\beta = 0.12$, $p < .001$; trivial effect size). Body mass demonstrated a small negative association (standardized $\beta = -0.16$, $p = .038$; trivial effect size). Age

showed a positive trend that did not reach statistical significance (standardized β = 0.07, p = .070), while sex was not significantly associated with W_{LSt}^{Ank+} (p = .488). No significant Group × TimePost interactions were observed for either the TDR-B group (standardized β = −0.47, p = .838) or the TDFR-U group (standardized β = 0.13, p = .456), indicating similar pre–post patterns across SEMLS groups.

Knee extensor moment impulse in stance phase (J_{St}^{KneExt}) showed a significant main effect of SEMLS group. Relative to the reference group (TDFR-B), the TDR-B group exhibited higher values (standardized β = 0.93, p = .041), representing a large effect size, whereas the TDFR-U group showed lower values (standardized β = −0.50, p = .020), corresponding to a moderate effect size. No significant main effects were observed for time post-surgery, normalized walking speed, time since surgery, age, body mass, or sex (all p > .10), with all associated effects trivial in magnitude. A significant Group × TimePost interaction was observed for the TDR-B group (standardized β = −1.08, p = .023), indicating a differential pre–post change relative to the reference group with a large effect size. No significant interaction was observed for the TDFR-U group (standardized β = −0.01, p = .934).

In the model predicting hip flexor impulse in pre-swing phase ($J_{\mathrm{PreSw}}^{HipFlx}$), relative to the reference SEMLS group TDFR-B, the TDR-B group showed greater hip flexor impulse in pre-swing phase values (β = −1.62, p = .011; large effect), with no difference observed for TDFR-U. Age was indirectly associated with $J_{\mathrm{PreSw}}^{HipFlx}$ (β = 0.93, p < .001; large effect), with significant Group × Age interactions indicating attenuation of this effect in both TDR-B and TDFR-U groups. No significant main effects of time, speed, mass, or sex were observed, and no clear Group × TimePost interactions were detected.

Ratio of ankle to hip peak propulsive power ($R_{p^+}^{A/H}$) increased significantly from pre- to post-surgery in the reference group (TDFR-B) (standardized β = 0.63, p = .026), corresponding to a moderate effect size.

Time since surgery also showed a significant nonlinear association with $R_{p^+}^{A/H}$, as indicated by the first spline component (standardized β = 2.45, p = .014; large effect size). No significant main effects were observed for SEMLS group membership or demographic covariates, and no significant Group × TimePost interactions were detected (all p > .75), indicating similar pre–post changes across SEMLS groups.

Sum of lower body net joint work (W_{tot}^{LB}) showed a significant main effect of time post-surgery, with lower values observed at follow-up relative to baseline in the reference group (TDFR-B), corresponding to a trivial standardized effect size (β = −0.04, p = .005). A significant main effect of SEMLS group was observed for the TDFR-U group, which exhibited lower W_{tot}^{LB} values compared with the reference group, although the standardized effect size was trivial (β = −0.05, p = .021). The corresponding group difference for the TDR-B group did not reach statistical significance (p = .069; β = −0.06). Several covariates were significantly associated with W_{tot}^{LB}, including normalized walking speed (p < .001; β = 0.02), time since surgery (p = .001; β ≈ 0.00), body mass (p = .033; β = 0.06), and sex, with lower W_{tot}^{LB} observed in females (p = .015; β ≈ 0.00). All covariate effects were trivial in magnitude. No significant main effect of age was observed (p = .619). No significant Group × TimePost interactions were detected for either the TDR-B or TDFR-U groups (both p > .14), indicating similar pre–post changes across SEMLS groups. A significant Group × Mass interaction was observed for the TDFR-U group (p = .032; β = −0.05), with a similar trend observed for the TDR-B group (p = .052; β = −0.04), suggesting modest group-dependent differences in the association between body mass and the outcome.

Table 3.1: Summary of predictor–outcome associations. Filled circles (●), and hollow circles (○) indicate statistically significant direct and indirect associations, respectively; Blank cells indicate non-significant effects.

Predictor	Ankle Positive Work in Late Stance	Knee Extensor Impulse in Stance	Hip Flexor Impulse in Pre-Swing	Ratio of Ankle to Hip Peak Power	Sum of Lower-body Joints Net Work
Group (main effect)		○	●		○
Time (Post vs Pre)		○		●	○
Time since surgery (months)	●			●	○
Normalized Speed	●				●
Age			○		
Mass	○				●
Sex					●

3.3.2. Within-Group Changes Following Surgery

Results of within-group comparisons with uncorrected p-values shown in Table 3.2; Table 3.4 shows the results whose statistical significance changed following Holm correction for multiple comparison across the seven kinetic outcomes (including the two kinetic outcomes in chapter 4). Reported inferences are based on the corrected p-values. In the TDR-B group, significant pre–post reductions were observed in W_{LSt}^{Ank+}, J_{St}^{KneExt}, and W_{tot}^{LB}. No significant change was detected in $R_{p^+}^{A/H}$ in this soft-tissue-only SEMLS group. The TDFR-B group exhibited a more selective pattern of responsiveness. Significant pre–post changes were observed for W_{tot}^{LB}, which decreased postoperatively. No significant pre–post changes were observed in W_{LSt}^{Ank+}, J_{St}^{KneExt}, $R_{p^+}^{A/H}$, or W_{tot}^{LB} in this group. In the TDFR-U group, no significant pre–post reduction was observed after adjusting for multiple outcome comparisons (Table 3.2 and Table 3.4).

Table 3.2: Estimated Changes in Kinetic Gait Outcomes Following Single-Event Multi-Level Surgery Across Three Surgical Protocols. Uncorrected *p*-values shown; see Table 3.4 for Holm-corrected results used for inference.

	TDR-B				TDFR-B				TDFR-U			
Outcome	Pre(M±SE)	Post(M±SE)	*p*	|d|	Pre(M±SE)	Post(M±SE)	*p*	|d|	Pre(M±SE)	Post(M±SE)	*p*	|d|
W_{LSt}^{Ank+}	0.39 ± 0.03	0.23 ± 0.01	< .001*	1.74	0.43 ± 0.12	0.29 ± 0.05	0.263	0.21	0.35 ± 0.03	0.30 ± 0.02	0.240	0.24
J_{St}^{KneExt}	0.71 ± 0.13	0.33 ± 0.05	0.005*	0.78	0.42 ± 0.05	0.38 ± 0.04	0.527	0.12	0.29 ± 0.03	0.25 ± 0.03	0.436	0.16
J_{PreSw}^{HipFlx}	-0.19 ± 0.04	-0.11 ± 0.01	0.035*	0.59	-0.09 ± 0.01	-0.08 ± 0.01	0.429	0.15	-0.08 ± 0.00	-0.09 ± 0.01	0.216	0.26
$R_{p^+}^{A/H}$	1.61 ± 0.31	1.99 ± 0.26	0.215	0.35	1.38 ± 0.18	1.87 ± 0.18	0.026*	0.43	1.82 ± 0.23	2.21 ± 0.20	0.115	0.33
W_{tot}^{LB}	1.97 ± 0.40	0.87 ± 0.09	0.006*	0.76	4.06 ± 1.06	3.11 ± 0.83	0.004*	0.54	1.57 ± 0.16	1.16 ± 0.11	0.029*	0.46

Note. Pre = before surgery; Post = after surgery. Values are model-estimated means (M) with standard errors (SE).
p values are from model. d = Cohen's d. * $p < 0.05$.

Table 3.3: Between-Group Differences in Estimated Changes of Kinetic Gait Outcomes Following Single-Event Multi-Level Surgery. Uncorrected *p*-values shown; see Table 3.5 for Holm-corrected results used for inference.

	(TDR - B) - (TDFR - B)				(TDFR - U) - (TDFR - B)				(TDFR - U) - (TDR - B)			
Outcome	Δ	95% CI	*p*	|d|	Δ	95% CI	*p*	|d|	Δ	95% CI	*p*	|d|
W_{LSt}^{Ank+}	-0.03	[-0.34, 0.28]	0.996	0.07	0.10	[-0.22, 0.41]	0.837	0.21	0.13	[0.02, 0.23]	0.018*	0.93
J_{St}^{KneExt}	-0.34	[-0.69, 0.01]	0.063	0.73	0.01	[-0.17, 0.18]	1.000	0.02	0.35	[0.01, 0.68]	0.041*	0.81
J_{PreSw}^{HipFlx}	0.07	[-0.02, 0.17]	0.182	0.61	-0.02	[-0.04, 0.01]	0.400	0.39	-0.09	[-0.18, 0.00]	0.062	0.78
$R_{p^+}^{A/H}$	-0.11	[-0.98, 0.77]	0.987	0.09	-0.10	[-0.83, 0.63]	0.983	0.09	0.01	[-0.88, 0.90]	1.000	0.01
W_{tot}^{LB}	-0.15	[-1.41, 1.11]	0.989	0.09	0.55	[-0.34, 1.44]	0.364	0.41	0.70	[-0.36, 1.76]	0.303	0.54

Note. Δ = estimated between-group difference. *p* values are from model. d = Cohen's d. Significance: * $p < 0.05$

Table 3.4: Holm-Adjusted *p*-Values for Within-Group Pre–Post Changes in Kinetic Gait Outcomes Following Single-Event Multilevel Surgery

Group	Outcome	*p* value	*p* Holm
TDR-B	$J_{\mathrm{Pre}Sw}^{HipFlx}$	0.035	0.104
TDFR-B	$R_{p^+}^{A/H}$	0.026	0.129
TDFR-U	W_{tot}^{LB}	0.029	0.143

Note: Holm adjustment for multiple comparisons was applied across seven outcomes.

Table 3.5**Error! Use the Home tab to apply 0 to the text that you want to appear here.**: Holm-Adjusted *p*-Values for Between-Group Differences in Pre–Post Change (Difference-in-Differences) in Kinetic Gait Outcomes.

Contrast	Outcome	*p* value	*p* Holm
(TDFR-U) - (TDR-B)	W_{LSt}^{Ank+}	0.018	0.123
(TDFR-U) - (TDR-B)	J_{St}^{KneExt}	0.041	0.165

Note: Holm adjustment for multiple comparisons was applied across seven outcomes.

3.3.3. Between-Group Differences in Pre–Post Changes Following Surgery

Analysis of between-group differences indicated that pre–post changes in kinetic outcomes did not differ across the surgical groups (Table 3.3 and 3.5). The between-group differences detected with raw p-values (Table 3.3) lost significance upon Holm adjustment for multiple outcome comparisons across seven kinetic variables (Table 3.5).

3.4. Discussion

The examined kinetic gait outcomes demonstrate measure-specific sensitivity to postoperative gait modification, and important limitations in their discriminative capacity across surgical treatment groups. Several outcomes showed statistically significant within-group changes in at least one SEMLS configuration, most prominently in the TDR-B group, with moderate-to-large standardized effect sizes. These patterns suggest that selected kinetic measures can detect alterations in joint-level mechanical demands following

surgery, supporting their responsiveness at the group level.

Between-group comparisons further reinforce this interpretation. While several contrasts yielded moderate to large effect sizes and nominal *p*-values below 0.05, none of these differences remained statistically significant following Holm correction for multiple comparisons. The loss of between-group significance after adjustment suggests that, although these kinetic outcomes may reflect meaningful biomechanical changes within specific groups, their ability to reliably differentiate surgical strategies is limited. This pattern is consistent with a validation framing in which outcomes demonstrate sensitivity to gait modification but lack sufficient specificity or signal-to-noise ratio to support strong claims of between-protocol differentiation. The lack of between-protocol differentiation is particularly pronounced in the context of multi-level surgical interventions where overlapping biomechanical effects and compensation strategies are expected.

Ankle positive work during late stance (W_{LSt}^{Ank+}) following TAL exhibited substantial inter-individual variability, with reductions in plantarflexor power observed in some participants but not consistently across the cohort (Delp et al., 1995; Dreher et al., 2012; Lin et al., 2000). Although FDO alters lower-limb geometry and may increase the plantarflexor lever arm (Gage, 1990), no statistically detectable between-group differences were observed, indicating limited group-level separation. Together, these findings suggest that ankle positive work reflects heterogeneous postoperative push-off responses rather than a uniform effect attributable to specific SEMLS protocol groupings.

The finding of W_{LSt}^{Ank+} being associated positively with normalized walking speed and negatively with body mass, is consistent with prior biomechanical models showing that ankle push-off influences center-of-mass mechanics primarily by accelerating the trailing limb and increasing its kinetic energy during late stance, with the relative contribution of this limb-level action scaling with total body mass (Dumas et al.,

2007; Zelik & Adamczyk, 2016). The observed association with time since surgery suggests W_{LSt}^{Ank+} that varies over the recovery period, consistent with ongoing adaptation following surgical intervention.

In parallel with W_{LSt}^{Ank+}, $R_{p^+}^{A/H}$ demonstrated a significant association with time since surgery, characterized by a nonlinear pattern. This behavior suggests that postoperative changes in the relative distribution of distal and proximal joint contributions evolve over the recover period rather than progress uniformly. In contrast, the isolated ankle component exhibited only a weak linear association with time, indicating limited sensitivity when considered independently.

Together, these findings indicate that postoperative adaptation may be more effectively captured by relative or coordination-based metrics than by single-joint measures alone. The nonlinear time course observed in the $R_{p^+}^{A/H}$ may reflect phases of postoperative adaptation that vary with surgical context and rehabilitation demands. Therefore in procedures involving FDO that are more invasive and typically require extended rehabilitation, this plausibly contributes to more gradual or nonuniform changes in gait mechanics.

Both $R_{p^+}^{A/H}$, and W_{tot}^{LB} demonstrated statistically significant pre–post changes and additional dependence on time since surgery, with reduced total work occurring alongside increased relative ankle contribution, suggesting coordinated postoperative adaptation at both global and relative work levels. From a validation perspective, this pattern supports the utility of ratio-based outcomes for capturing coordinated postoperative changes in gait mechanics that may not be evident from isolated joint-level measures.

In TDR-B reductions in W_{tot}^{LB} were observed concurrently with changes in mechanical work distribution, including increased relative ankle contribution ($R_{p^+}^{A/H}$) and reduced crouch-related sagittal posture indicated by J_{St}^{KneExt}. These patterns are consistent with established associations between distal power generation,

proximal demand, and gait energetics, and support the interpretation that kinetic and energetic measures capture overlapping mechanical constructs.

The direct associations observed between W_{tot}^{LB} and normalized walking speed and body mass, as well as their association with sex, are consistent with prior biomechanical studies demonstrating that joint-level work scales with walking speed, body size, and anthropometric factors during gait (Dumas et al., 2007; Hof, 1996; Winter, 2009).

TDR-B group had greater J_{St}^{KneExt} relative to the TDFR-B reference group and was the only outcome to demonstrate a statistically significant reduction following SEMLS. This pattern suggests sensitivity of knee extensor impulse to soft-tissue–only surgical context, and limited differentiation across protocols.

The indirect association between $J_{\mathrm{Pre}Sw}^{HipFlx}$ and age is consistent with established developmental patterns of gait, with younger children relying more on proximal joint contributions for limb advancement and forward progression, with a gradual shift toward greater distal contributions as gait matures (Sutherland, 1997). Using TDFR-B as the reference, hip flexor impulse during pre-swing was greater in the TDR-B group, with no difference observed between TDFR-B and TDFR-U. In the absence of broader between-group effects, this pattern suggests limited group-level differentiation, with hip flexor impulse reflecting sensitivity to specific procedural contexts rather than consistent separation across SEMLS protocols.

3.5. Limitations

Several limitations specific to the kinetic outcomes analyses should be acknowledged. First, the exploratory design and limited sample sizes within SEMLS protocol groups reduced power to detect subtle between-group differences, particularly for joint-specific kinetic outcomes. Consequently, the absence of

statistically detectable group × time effects should not be interpreted as evidence that kinetic adaptations are equivalent across surgical protocols.

Second, kinetic outcomes were derived from inverse dynamics and external joint moments and work, which reflect net joint-level mechanical behavior but do not resolve underlying muscle forces, co-contraction, or internal work. Additionally, direct measures of energy expenditure (e.g., metabolic gas exchange) were not available. Accordingly, interpretations are limited to observed joint-level mechanical patterns rather than specific neuromuscular or metabolic mechanisms.

Finally, walking speed, while accounted for analytically, remains an important contributor to kinetic variability. Residual speed-related influences may therefore contribute to heterogeneity in observed kinetic responses.

3.6. Conclusion

This chapter provides an exploratory evaluation of joint-level kinetic and work-based gait outcomes following Single-Event Multi-Level Surgery in children with cerebral palsy. The results demonstrate that selected kinetic measures exhibit distinct patterns of postoperative behavior, with relative and global work-based outcomes showing consistent sensitivity to postoperative change and temporal adaptation.

In particular, the ankle-to-hip contribution ratio and total joint work captured coordinated shifts in joint-level mechanics following surgery, reflected by statistically detectable pre–post changes and associations with time since surgery. These findings suggest that relative and global kinetic measures may be useful for characterizing postoperative reorganization of gait mechanics, even when isolated joint-level kinetics show limited or heterogeneous change.

At the same time, the limited between-group differentiation observed across kinetic outcomes highlights the influence of patient heterogeneity and underscores the importance of interpreting kinetic measures as

descriptors of outcome behavior rather than indicators of procedure-specific effectiveness. From a validation perspective, this chapter supports the complementary role of kinetic and work-based measures in postoperative gait assessment, particularly for capturing coordinated mechanical adaptations that may not be evident from kinematics alone.

Chapter 4: Knee Adduction Moment–Based Indicators of Joint Loading

4.1. Introduction

Cerebral palsy (CP) is the most common cause of motor disability in childhood, affecting 2.7–3.4 per 1000 live births(McIntyre et al., 2022), and is associated with a high medical burden (Whitney et al., 2019), as well as elevated risk and prevalence of osteoarthritis (OA) (French et al., 2019; O'Connell et al., 2019). CP is an umbrella term for disorders of posture and movement caused by non-progressive lesions in the developing brain (Smithers-Sheedy et al., 2014). The neurological etiology of cerebral palsy varies in location, timing, and severity, contributing substantially to clinical heterogeneity (Metz et al., 2022). One manifestation of this heterogeneity is variation in motor subtype, with spastic cerebral palsy being the most common presentation (Novak et al., 2025). Spasticity has been associated with structural and functional muscle adaptations, such as increased stiffness and weakness, which are thought to contribute to the shortened muscle–tendon units frequently observed in cerebral palsy (Lieber et al., 2004). Over time, neuromuscular impairments and shortened muscle–tendon units contribute to joint contractures and progressive skeletal deformities during growth (Kerr Graham & Selber, 2003). "Lever-arm dysfunction" describes musculoskeletal deformities that alter the moment arms of forces driving movement, resulting in impaired function (Rethlefsen & Kay, 2013; Theologis, 2013). Lever-arm dysfunction contributes to progressive impairment of functional mobility in cerebral palsy and underlies the orthopedic surgical approach to functional improvement (Bell et al., 2002; Gage et al., 2009a).

In ambulatory individuals, orthopedic surgery interventions aim to correct contractures and dysfunctional lever arms to improve gait and reduce pain (Himpens et al., 2013). Single-event multilevel surgery (SEMLS), which involves musculoskeletal corrections at multiple anatomical levels within a single surgical session, is the standard orthopedic surgical approach for ambulatory children with CP as it reduces the number of hospitalizations and recovery periods and minimizes the risk of residual imbalances associated with staged

procedures (Gage et al., 2009b; Saraph et al., 2002; Schwartz et al., 2004; Zwick et al., 2001).

Beyond short-term gait correction, long-term joint health is an important consideration in this population. Adults with cerebral palsy exhibit a higher prevalence of knee osteoarthritis, which is associated with increased pain, fatigue, functional limitations, and healthcare utilization (Murphy et al., 2016; Whitney et al., 2019). Reported odds ratios for knee osteoarthritis in adults with CP range from 1.4 to 3.3 compared with typically developing peers (French et al., 2019). These elevated odds of knee osteoarthritis highlight the need to understand the biomechanical pathways through which long-term joint loading may contribute to degenerative change in individuals with cerebral palsy.

The mechanical loading environment at the joint both influences and is influenced by biological processes that contribute to degenerative changes in articular cartilage (Andriacchi et al., 2004). Joint-level mechanics have been linked to the progression of degenerative joint disease (Bennell et al., 2011; Brisson et al., 2021; Davis et al., 2019). The knee adduction moment (KAM) is commonly interpreted as an indicator of greater medial relative to lateral knee compartment loading (Schipplein & Andriacchi, 1991). Given the higher incidence of osteoarthritis in the medial knee compartment (Stoddart et al., 2021; Wise et al., 2012), KAM-based metrics have therefore been widely used as surrogate indicators of osteoarthritis-related loading pathomechanics (Foroughi et al., 2009). Accordingly, peak KAM, reflecting maximum instantaneous frontal-plane loading, and KAM impulse (J_{KAM}), capturing cumulative loading over stance, were selected to characterize knee loading magnitude and duration during gait. Within the context of a highly nonlinear gait system(West & Scafetta, 2003), these complementary metrics are not assumed to respond proportionally to changes in posture or structural correction, but rather to reflect distinct aspects of system-level loading behavior. Both peak KAM and KAM impulse have been linked to cartilage loss and long-term joint health risk (Bennell et al., 2011). Beyond frontal-plane loading, additional kinetic and kinematic factors have been implicated in osteoarthritis onset and severity, including knee joint compressive (Ko et al., 2013; Thibault et

al., 2002) and sagittal-plane knee kinematics (Anan et al., 2024; Astephen et al., 2008).

In CP, knee joint compressive forces have been shown in modeling and cadaver studies to be elevated relative to typical gait (Perry et al., 1975; Steele et al., 2012). This is in part attributed to increased muscular demand, particularly on knee extensors that support the posture, as shown in musculoskeletal modeling studies of crouch gait (Steele et al., 2012). This increased muscular demand has also been documented in cadaver studies (Perry et al., 1975), as well as EMG activity during standing with the crouch gait's characteristic flexed knee (Hsu et al., 1993).

In this context, mechanical indicators of knee loading may interact differently with long-term joint health in the cerebral palsy population, where compensatory gait mechanisms are common (Gage et al., 2009b). Changes in frontal-plane knee loading occur alongside excessive sagittal-plane knee flexion, and these measures represent distinct mechanical constructs that may not respond similarly to changes in gait posture or surgical intervention. Examining cross-sectional associations between knee flexion angle and KAM-based loading metrics therefore provides a framework for evaluating whether commonly-used indicators of knee loading behave coherently with respect to sagittal posture. This construct-level perspective motivates the present investigation of frontal- and sagittal-plane knee loading metrics in children with cerebral palsy.

4.2. Methods

The following describes the study participants, data collection and processing procedures. Next the derivation of outcome measures, and statistical methods used for analysis are presented.

4.2.1. Participants

Participants were 67 children with CP (GMFCS I–III; 46 male, 21 female; median age = 6.3 (IQR:5.3-9.9)8 ± 3.9 years; mass 26.9 ± 13.2 kg), including 17 with hemiplegia, 48 with diplegia, and 1 with

quadriplegia. Participants were retrospectively assigned to one of three SEMLS groups based on the surgical protocol received: 1) TDR-B — bilateral soft-tissue procedures (Achilles tendon lengthening, distal hamstring lengthening, and rectus femoris transfer) ($n = 14$); 2) TDFR-B — the above soft-tissue procedures combined with bilateral femoral derotational osteotomy (FDO) ($n = 29$); 3) TDFR-U — the same soft-tissue procedures combined with unilateral FDO ($n = 24$).

4.2.2. Data Collection

Gait data were collected between 1995 and 2017 using two motion-analysis systems. The first system was a Kestrel 10-camera digital motion-capture system (Motion Analysis Corp., USA) with two KISTLER force plates (Switzerland). Marker placement followed the Helen Hayes marker set, and data were captured and processed in real time using *Cortex* and *OrthoTrak* software.

The second system was a Vicon motion-capture setup (Vicon 370; Oxford Metrics, Oxford, UK) with seven CCD cameras sampling at 60 Hz and two AMTI force plates (MA, USA). Reflective markers (25 mm) were applied using the Plug-in Gait model. Some datasets included full-body marker sets, but only lower-extremity data were analyzed to maximize participant inclusion.

Participants walked barefoot along a 9-m walkway, taking approximately 9 ± 4 strides per trial. On average, 3 ± 1 complete force-plate strikes (one foot fully isolated on a single force plate) were recorded per participant.

4.2.3. Data Processing

Kinematic marker trajectories were low-pass filtered using zero-lag, fourth-order Butterworth filters. Cutoff frequencies were determined using residual analysis (Winter, 2009). A participant-specific approach was adopted for cutoff selection to account for inter-individual variability and the sensitivity of kinematic and kinetic outcomes to filtering choices, consistent with prior recommendations against using a single cutoff

frequency across participants(Fazlali et al., 2020; Kristianslund et al., 2012). Residual analysis was conducted using marker trajectories and ground reaction force data from each participant's trials. Participant-level outcomes were summarized using the median across trials to reduce the influence of outlier trials and residual high-frequency noise. Participant-specific cutoff frequencies were constrained to a data-driven range with a lower bound of 5.5 Hz and an upper bound of 10 Hz and were applied consistently within each participant.

These filtered signals were then used to build a 7-segement lower-extremity model. From the model the joint angles were calculated in Visual 3D as the orientation of distal segment in relation to the proximal segment using the XYZ Cardan sequence in each stride (Hamill et al., 2013). Gait events were first identified using the algorithm described by Zeni et al.(Zeni et al., 2008), which detects events based on the relative positions of the heel and toe markers with respect to the pelvis, and were subsequently verified by visual inspection. Joint moments and powers were calculated using Visual 3D based on the iterative Newton-Euler inverse dynamics algorithm (Selbie et al., 2014) using the ground reaction forces in valid kinetic steps. A step was considered kinetically valid if only one foot of the participant was in contact with the force plate. Joint moment impulse and work were calculated as the integral of moments and powers (Winter, 2009).

4.2.4. Outcome Measures

Outcome measures consisted of KAM outcome and their corresponding sagittal knee kinematics. Their calculation is described below.

KAM metrics

KAM impulse was calculated as

$$J_{KAM} = \int_{t=HS}^{TO} M^{KAdd}(t).dt$$

,where M^{KAdd} denotes the knee adduction moment which was integrated over the stance phase, defined

by heel-strike and toe-off gait events, using Visual3D. Peak KAM was defined as the maximum knee adduction moment observed during the stance phase.

Sagittal knee kinematics

To examine construct-level relationships between KAM metrics and sagittal-plane knee kinematics, mean and peak knee flexion angles during the stance phase were extracted using Visual3D. All measures were averaged across the left and right limbs to provide a single overall indicator of gait function.

Outcome were summarized at the participant level by averaging across limbs to support evaluation of overall gait behavior within each SEMLS context, applied consistently across participants.

4.2.5. Statistical Analysis

A detailed description of the statistical methods is provided in Appendix A. Gait outcomes were analyzed using ordinary least squared (OLS) regression models that included Group, Time (pre vs. post), and their interaction, with normalized walking speed, time since surgery (months), age, mass, and sex included as covariates. Linearity of continuous predictors was assessed using spline-expanded OLS models; when nonlinearities were detected, the relevant spline terms were retained. Homogeneity of slopes across groups was evaluated through Group × covariate interactions, with group-specific slopes modeled when these terms were significant.

Due to the unequal size of the groups exacerbating the effect of heteroscedasticity (Box, 1954), the initial OLS model structure arrived at from the previous steps was refit using generalized least squares (GLS) with alternative variance structures (varIdent, varExp, varPower, varComb). Based on the procedure proposed by Pinheiro & Bates (Pinheiro & Bates, 2000), Akaike Information Criterion (AIC) (Akaike, 1998) was used to compare the fit of the models with different variance structures. The final model with the least AIC was selected for the subsequent analyses. Complete model coefficients and diagnostic plots

for all outcomes are provided in Appendix B.

Estimated marginal means (EMMs) for each Group × Time combination were obtained from the final model. Within-group pre–post changes (Post–Pre) were estimated using model-based contrasts, and between-group differences in change (differences in differences; DID) were derived from the Group × Time interaction. Sidak-adjusted confidence intervals and *p*-values were used for all pairwise DID comparisons (Šidák, 1967).

Effect sizes were expressed as Cohen's *d*: paired-samples *d* for within-group changes and independent-samples *d* for DID effects, with Hedges' small-sample correction applied to between-group comparisons. All analyses were performed in R (Version 4.5.1)(R Core Team, 2025) using the nlme, emmeans, and sandwich packages.P-values for pre–post changes and difference-in-differences comparisons were adjusted for family-wise error using the Holm method (Holm, 1979) across seven outcome comparisons.

Cross-sectional associations between sagittal-plane knee angle and frontal-plane knee loading

The two associations examined at baseline were between: (1) KAM impulse during the stance phase and mean knee flexion angle both during stance, and (2) Peak KAM and knee flexion angle at that instant. Associations were assessed using Spearman correlation and partial Spearman correlation controlling for walking speed and body mass, given their known influence on joint loading (Kean et al., 2012; Robbins & Maly, 2009).

4.3. Results

In the following sections, we first report cross-sectional correlations between knee sagittal kinematics and KAM metric, followed by associations between gait outcomes and model predictors, including participant anthropometry and demographics, walking speed, and time since surgery. We then present within-group changes following surgery, and between-group differences in surgery-related changes.

4.3.1. Cross-Sectional Associations Between Crouch Knee Posture and Outcomes

At baseline, greater knee flexion angle at the instant of peak knee adduction moment was associated with lower peak KAM after controlling for walking speed and body mass (partial Spearman $\rho = -0.238$, $p = 0.024$, $N = 92$). Similarly, greater mean knee flexion angle during stance was associated with lower knee adduction moment impulse when controlling for walking speed and body mass (partial Spearman $\rho = -0.225$, $p = 0.033$, $N = 92$).

4.3.2. Predictor Associations with Outcomes

A detailed set of model diagnostic figures and tables, including assumption checks and final model coefficients, is provided in Appendix D. Several predictors showed significant associations with peak KAM and KAM impulse, as summarized in Table 4.1. Normalized walking speed was directly associated with peak KAM ($\beta = 0.18$, $p = .035$). Time (pre- vs post-surgery) showed a significant indirect association with peak KAM ($\beta = -0.82$, $p = .002$). KAM impulse was negatively associated with age ($\beta = -2.8$, $p = .046$). KAM impulse also demonstrated main effect of SEMLS group membership, with TDR-B membership showing a significant indirect association ($\beta = -0.65$, $p = .022$).

Table 4.1: Summary of predictor–outcome associations. Filled circles (●) indicate statistically significant positive associations and hollow circles (○) indicate statistically significant negative associations; Blank cells indicate non-significant effects.

Predictor	KAM Peak	KAM Impulse
Group (main effect)		○
Time (Post vs Pre)	○	
Normalized Speed	●	
Age		○

4.3.3. Within-Group Changes Following Surgery

Peak KAM decreased following surgery (Table 4.2), with only the bilateral FDO group surviving the

FWER Holm adjustment (Table 4.3). KAM impulse demonstrated a significant reduction exclusively in the unilateral FDO group (Table 4.1), which also remained significant after correction for multiple comparisons. No other group-specific changes survived adjustment.

4.3.4. Between-Group Differences in Pre–Post Changes Following Surgery

No statistically significant differences were observed between surgical groups for either peak knee adduction moment (KAM) or KAM impulse in any pairwise comparison (Table 4.2). Effect sizes for between-group contrasts were small, and confidence intervals overlapped zero across all comparisons, indicating no evidence of differential group effects.

4.4. Discussion

Our observed negative association between knee flexion angle and KAM-based metrics is consistent with prior reports in individuals with knee osteoarthritis (Anan et al., 2024) and healthy older adults (Igura et al., 2025). In these populations, greater knee flexion during stance has been linked to altered shock-attenuation strategies, including increased knee extensor negative power and work, accompanied by reductions in knee adduction moment, as demonstrated in musculoskeletal modeling studies (Nagano et al., 2015).

In the present study, the dissociation between changes in sagittal-plane knee posture and KAM-based outcomes suggests that these measures capture complementary aspects of postoperative knee loading rather than redundant information. Mechanistically, this dissociation may reflect alterations in internal knee loading that are not fully captured by external frontal-plane moments alone.

This consideration is particularly relevant regarding FDO-inclusive procedures that alter joint geometry. Femoral geometry, directly targeted by FDO, has been shown to significantly impact joint contact forces(Kainz et al., 2023; Modenese et al., 2021); a mechanism that is not directly related to KAM. Furthermore, anteversion has been suggested to significantly change muscular co-contractions

Table 4.2: Estimated Changes in Knee Adduction Moment Gait Outcomes Following Single-Event Multi-Level Surgery Across Three Surgical Protocols. Uncorrected p-values shown; see Table 4.4 for Holm-corrected results used for inference.

	TDR-B				TDFR-B				TDFR-U			
Outcome	Pre(M±SE)	Post(M±SE)	*p*	|d|	Pre(M±SE)	Post(M±SE)	*p*	|d|	Pre(M±SE)	Post(M±SE)	*p*	|d|
Peak KAM	0.51 ± 0.09	0.27 ± 0.06	0.019*	0.65	0.72 ± 0.12	0.34 ± 0.05	0.002*	0.59	0.63 ± 0.09	0.37 ± 0.06	0.021*	0.48
J_{KAM}	0.08 ± 0.04	0.02 ± 0.03	0.137	0.41	0.18 ± 0.03	0.12 ± 0.02	0.074	0.34	0.21 ± 0.04	0.08 ± 0.03	0.007*	0.56

Table 4.3: Between-Group Differences in Estimated Changes of Knee Adduction Moment Gait Outcomes Following Single-Event Multi-Level Surgery

	(TDR - B) - (TDFR - B)				(TDFR - U) - (TDFR - B)				(TDFR - U) - (TDR - B)			
Outcome	Δ	95% CI	*p*	|d|	Δ	95% CI	*p*	|d|	Δ	95% CI	*p*	|d|
Peak KAM	0.14	[-0.24, 0.52]	0.764	0.29	0.12	[-0.26, 0.51]	0.835	0.21	-0.02	[-0.37, 0.34]	0.999	0.04
J_{KAM}	0.01	[-0.11, 0.14]	0.995	0.07	-0.06	[-0.20, 0.08]	0.664	0.28	-0.07	[-0.21, 0.07]	0.537	0.41

Note. Δ = estimated between-group difference. *p* values are from model. d = Cohen's d. Significance: * $p < 0.05$

Table 4.4: Holm-Adjusted *p*-Values for Within-Group Pre–Post Changes in Knee Adduction Moment Gait Outcomes Following Single-Event Multilevel Surgery

Group	outcome	*p* value	*p* holm
TDR-B	Peak KAM	0.019	0.075
TDFR-U	Peak KAM	0.021	0.127

Note: FWER Holm adjustment was done for seven kinetic outcome including those in Chapter 3.

(Kainz et al., 2023). Any postoperative changes in neuromuscular control and muscle activation patterns in children may further redistribute muscle-driven joint compression without proportional changes in external moments compression (Veerkamp et al., 2019). Consistent with this interpretation, the KAM impulse model demonstrated a significant difference between the soft-tissue–only TDR-B group and the FDO-inclusive TDFR-B group, whereas the unilateral FDO group (TDFR-U) did not differ significantly from bilateral FDO.

The significant effect of time post-surgery observed in the peak KAM model reflects a reduction in frontal-plane knee loading over the postoperative period. While KAM-based metrics and joint contact forces represent distinct loading constructs, prior musculoskeletal modeling studies have similarly reported reductions in estimated knee joint contact forces following SEMLS (Escalda et al., 2023; Van Rossom et al., 2020). This suggests directional consistency in the knee mechanical environments indexed by these measures and their relevance to long-term joint health (Kean et al., 2012; Thibault et al., 2002). Moderate correlations between KAM and medial knee contact force previously reported (Kutzner et al., 2013), highlight that these measures reflect related but non-identical aspects of knee loading.

Finally, with respect to covariate effects, peak KAM in the present study demonstrated sensitivity to normalized walking speed, consistent with prior reports of positive associations between KAM metrics and speed (Robbins & Maly, 2009). However, unlike their findings which suggested greater speed sensitivity of KAM impulse due to loading duration effects, the present results indicated stronger speed-

related effects on peak KAM than on impulse. This suggests that, in this cohort, speed-related changes in waveform magnitude and timing outweighed duration-driven effects. Additionally, the sensitivity of KAM impulse to age suggests that apparent speed-related differences may be partially mediated by developmental changes in gait mechanics.

4.5. Limitations

The present analysis relied on KAM as an external surrogate of frontal-plane knee loading and did not directly quantify internal knee joint contact forces or compartment-specific cartilage stresses. As a frontal-plane measure, KAM does not capture sagittal- or transverse-plane mechanics, muscle co-contraction, or multi-planar interactions that may contribute to overall knee joint loading. Consequently, changes in internal mechanical demand at the knee may occur without proportional changes in KAM-based metrics. This limitation is particularly relevant for procedures such as femoral derotation osteotomy, which alter femoral geometry and joint morphology and may redistribute muscle-driven joint loading without corresponding changes in external frontal-plane moments. In addition, postoperative changes in neuromuscular control may further modify internal loading patterns not reflected by KAM.

Although walking speed was accounted for analytically, residual speed-related effects may contribute to inter-individual variability in KAM responses. Heterogeneity in baseline alignment, neuromuscular control, and lever-arm dysfunction across participants may further obscure meaningful individual-level adaptations at the group level. Finally, the follow-up window reflects short- to mid-term postoperative gait adaptation and does not permit direct evaluation of long-term joint health outcomes. Accordingly, interpretations relating to KAM-based changes to long-term joint health should be viewed as inferential rather than predictive.

4.6. Conclusion

This chapter evaluated frontal-plane knee loading following SEMLS using KAM-based metrics across surgical protocols and postoperative recovery. The findings show that KAM peak and KAM impulse capture distinct aspects of knee loading and exhibit differential sensitivity to surgical context, walking speed, age, and time post-surgery, indicating that these measures are not interchangeable.

Postoperative changes in KAM were modest and protocol-dependent, with reductions observed in specific SEMLS groups. Notably, changes in KAM did not consistently align with changes in sagittal-plane knee kinematics, highlighting the complementary information provided by frontal-plane loading metrics beyond posture-based measures. This dissociation was particularly relevant for FDO-inclusive procedures, where alterations in femoral geometry and neuromuscular control may influence internal knee loading without proportional changes in external moments.

Overall, these results support a validation-oriented interpretation of KAM-based outcomes as context-sensitive indicators of frontal-plane knee loading rather than direct surrogates of internal joint contact forces or global gait improvement. Their value lies in contributing complementary information within an integrated gait assessment framework, reinforcing the need for outcome selection and interpretation that account for surgical context, recovery stage, and patient-specific variability.

Chapter 5: Integrated Synthesis, Clinical Implications, and Future Directions

5.1. Synthesis

The outcome-specific and SEMLS-context–dependent patterns observed across this exploratory investigation highlight the need for structured consensus in outcome selection for SEMLS research. The present findings demonstrate that commonly used gait metrics are not interchangeable: global indices, spatiotemporal asymmetry measures, joint kinetics, and frontal-plane knee loading metrics captured distinct aspects of postoperative adaptation. This heterogeneity indicates that outcome relevance depends on clinical intent, surgical context, and stage of recovery rather than on universal responsiveness. Consensus-based approaches, such as interdisciplinary Delphi methodologies, provide a systematic framework for aligning outcome selection with clinically meaningful constructs for specific patient groups and treatment goals (McCarthy et al., 2020). By demonstrating differential sensitivity and construct specificity across outcome domains, the present work provides empirical justification for the development of condition-specific, consensus-driven outcome sets in SEMLS research.

Across SEMLS groups, non-uniform pre–post-surgical changes further indicate that each outcome captures a distinct aspect of gait behavior within the context of multi-level interventions. While global gait indices summarize overall deviation from typical walking, joint-level kinetic and loading metrics quantify construct-specific mechanical demands that may change independently of global gait appearance. In the presence of substantial heterogeneity at the individual level and across postoperative recovery trajectories, such outcomes may exhibit limited sensitivity for differentiating surgical protocols, reinforcing the importance of context-aware interpretation.

5.1.1. Predictor Effects

Instrumented gait analysis has been reported to delay surgical recommendation to approximately eight to ten years of age, a developmental period during which gait maturation and stabilization are thought to occur (Molenaers, 2006; Norlin et al., 1981; Sutherland, 1997). Within this developmental window, the present findings indicate that developmental associations with gait outcomes are heterogeneous, outcome-specific, and dependent on surgical context rather than uniformly directional.

Across gait domains, developmental associations differed by biomechanical construct (Fig. 5.1 and 5.2). Global kinematic and temporal measures exhibited distinct developmental patterns, whereas kinetic and loading-related outcomes demonstrated variable—and in some cases nonlinear—developmental behavior. Proximal and distal joint kinetics, as well as frontal-plane knee loading metrics, showed developmental associations that were modified by SEMLS protocol, indicating that these outcomes do not follow a single developmental trajectory across surgical contexts. From a validation perspective, these findings underscore the importance of interpreting developmental associations as construct-specific behaviors rather than general indicators of gait maturity, optimization, or surgical timing.

Walking speed consistently influenced both kinematic and kinetic gait outcomes, although its effects varied by biomechanical construct (Fig. 5.1 and 5.2). Kinematic measures primarily reflected speed-related changes in overall gait pattern and temporal organization, whereas kinetic and work-based outcomes exhibited stronger associations with speed due to increased mechanical demands required for forward progression. Rather than indicating improvement or decline, speed-related associations reflect fundamental biomechanical scaling and coordination effects that shape both movement patterns and joint-level demands.

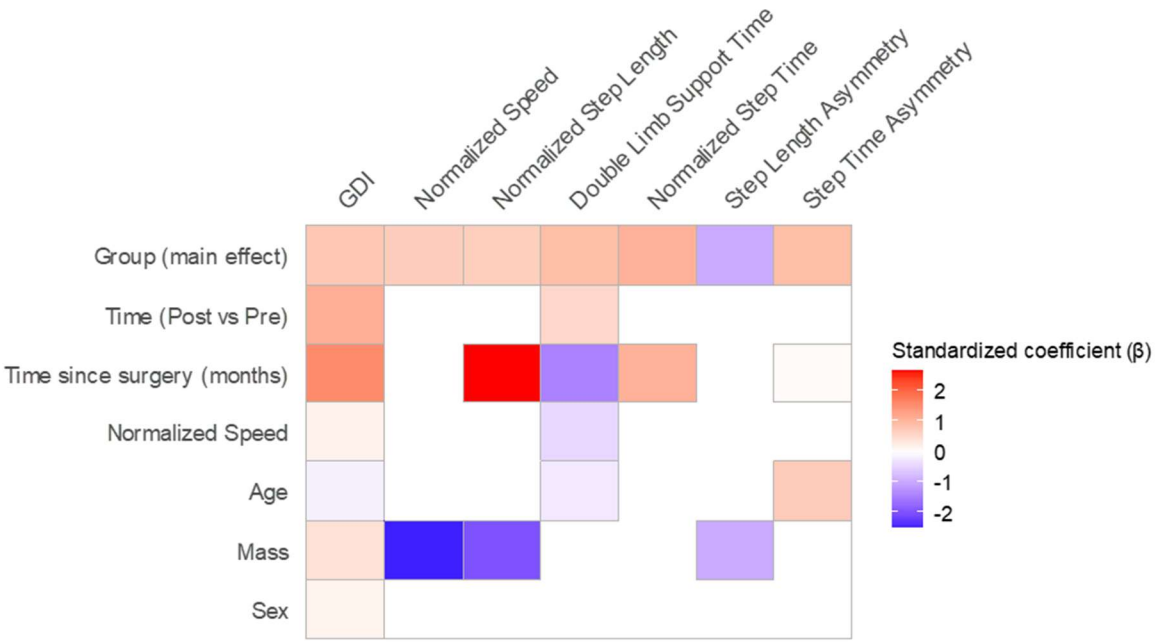


Figure 5.1: Summary of predictor effects across kinematic outcomes. Tiles represent standardized regression coefficients (β) from regression models, with color indicating direction and magnitude of association (red = positive, blue = negative).

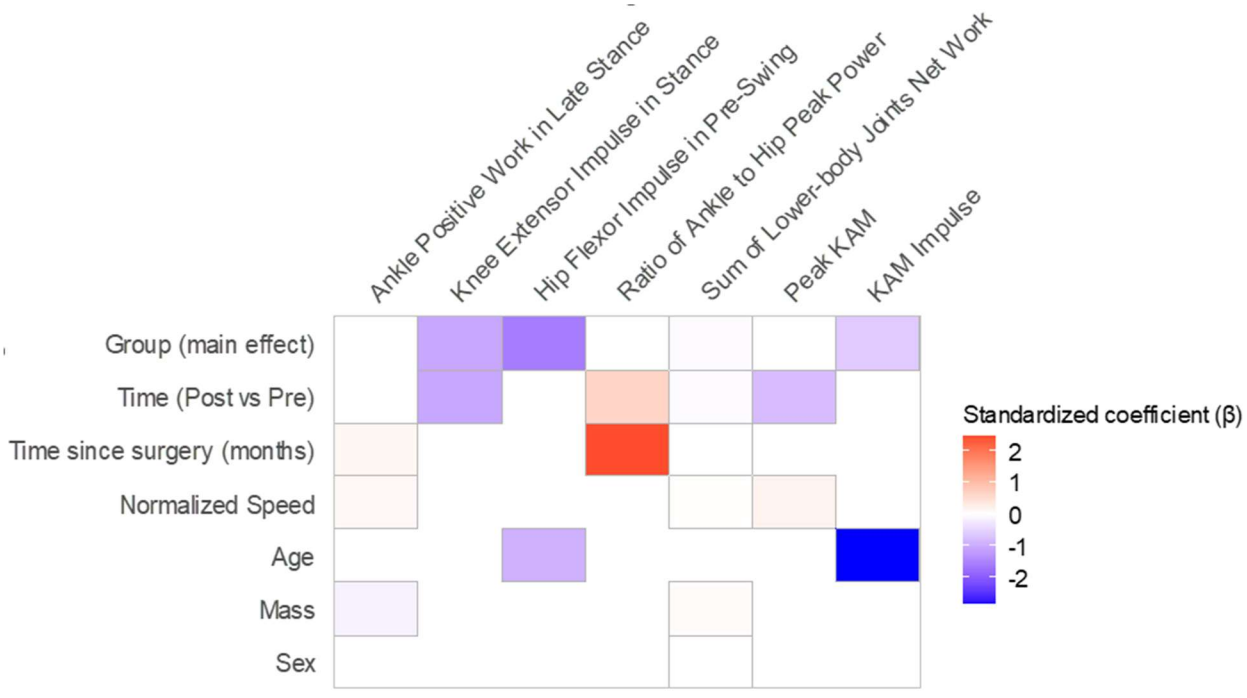


Figure 5.2: Summary of predictor effects across kinetic and frontal-plane knee loading outcomes. Tiles

represent standardized regression coefficients (β) from regression models, with color indicating direction and magnitude of association (red = positive, blue = negative).

5.1.2. Within-Group Ghanges and Between-Group Differences

Interpretation of postoperative change (Fig 5.3 and 5.4) is further complicated by the heterogeneous baseline gait profiles characteristic of children undergoing SEMLS. In such settings, approaches that normalize change relative to baseline values may introduce mathematical coupling and regression-to-the-mean effects (Barnett et al., 2005), particularly given the inherent measurement variability of gait analysis. To mitigate these issues, the present work avoids baseline-normalized change scores and instead accounts for baseline differences through covariate adjustment and subgroup-specific analyses. This approach allows pre–post patterns to be interpreted as indicators of outcome sensitivity rather than direct measures of treatment efficacy.

Many gait and joint loading metrics in cerebral palsy are expected to deteriorate with growth and continued exposure to abnormal loading(Bell et al., 2002; Johnson et al., 1997). Accordingly, the absence of statistically detectable change over the follow-up period should not necessarily be interpreted as a lack of effect (Gough et al., 2004; Rajagopal et al., 2018; Theologis et al., 2025). In line with this perspective, orthopedic surgery has been framed as aiming to maintain functional capacity rather than guarantee (Lynn et al., 2009). The concept of minimal clinically important difference (MCID) further contextualizes interpretation of change by emphasizing clinical relevance beyond statistical significance.

The MCID, defined as the magnitude of change required to reflect a perceptible improvement in function, helps translate objective gait metrics into clinically meaningful interpretation (Oeffinger et al., 2008). While group-level changes may not reach MCID thresholds, clinically meaningful improvements may still occur in individual patients. However, MCID thresholds for many biomechanical gait outcomes

remain inconsistently defined or unavailable, particularly in heterogeneous pediatric populations. In heterogeneous clinical populations such as CP children undergoing SEMLS, reliance on group mean changes may further obscure clinically meaningful individual responses, even when statistically significant effects are observed. Prior work has emphasized that interpretation of group-level gait outcomes must account for response variability and distributional effects rather than assuming uniform benefit across patients (Damiano, 2014).

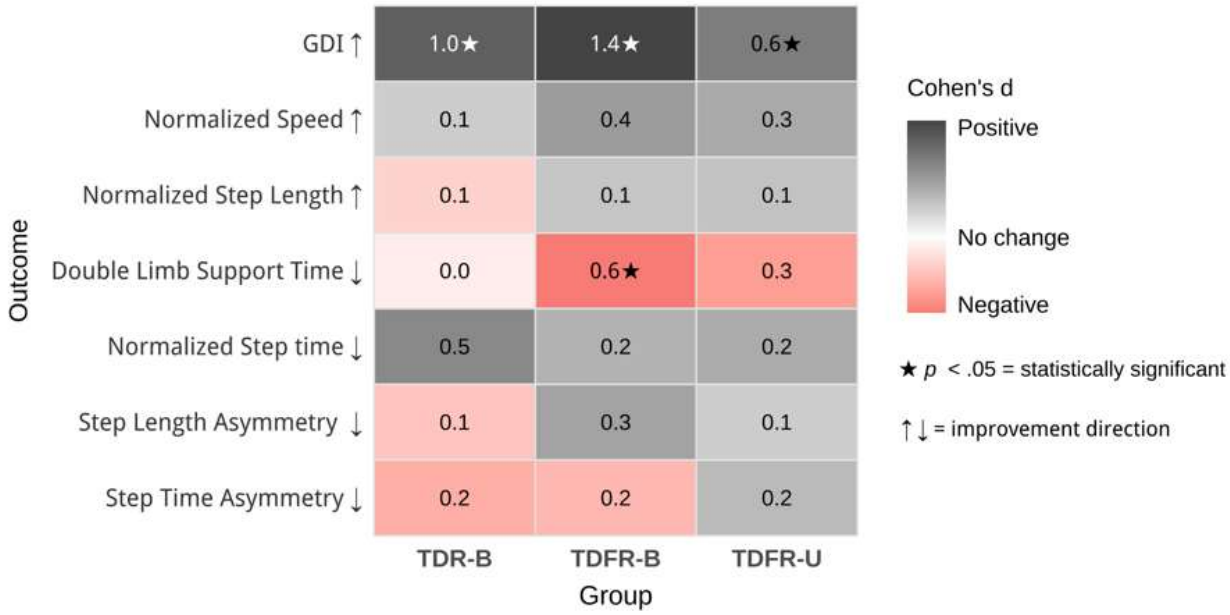


Figure 5.3: Magnitude and direction of pre–post-surgical changes in kinematic outcomes across SEMLS groups. Cells report Cohen's d effect sizes for within-group changes following surgery in the expected direction of improvement (↑/↓). Color indicates direction of change (gray = improvement, red = worsening, white = no change). Stars denote statistically significant changes ($p < .05$).

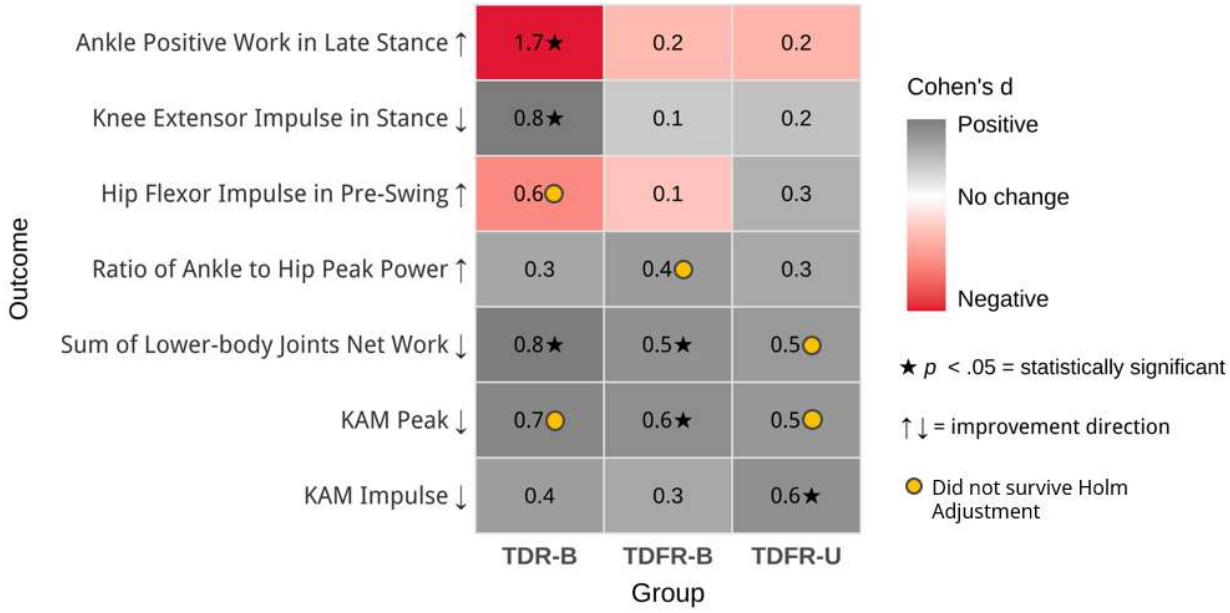


Figure 5.4: Magnitude and direction of pre–post-surgical changes in kinetic and knee loading outcomes across SEMLS groups. Cells report Cohen's d effect sizes for within-group changes following surgery in the expected direction of improvement (↑/↓). Color indicates direction of change (gray = improvement, red = worsening, white = no change). Stars denote statistically significant changes ($p < .05$), and yellow circles indicate effects that did not survive Holm correction. The figure highlights outcome-specific and protocol-dependent response patterns across SEMLS groups.

5.2. Clinical Implications

The clinical interpretability of gait outcomes is shaped by the complex relationship between biomechanical constructs (e.g., joint loading or muscular demand) and higher-level clinical constructs such as strength, pain, function, or participation (Baker et al., 2016; Steele & Schwartz, 2022). While biomechanical measures provide objective quantification of movement, sensitivity to change alone does not establish clinical importance. Exploratory analyses are therefore necessary to characterize how different outcome types behave across patient subgroups and interventions, providing an empirical basis for selecting outcomes aligned with specific clinical questions.

A unifying interpretation of the findings across chapters is that SEMLS should be viewed as an

enabling intervention rather than a discrete treatment endpoint. Long-term qualitative work further supports this interpretation, showing that despite sustained improvements in objective gait measures following SEMLS, adolescents report wide variation in how these changes translate to real-world functioning, independence, and coping strategies, underscoring the central role of postoperative rehabilitation and active engagement in shaping outcomes (Lehtonen et al., 2015). While surgery modifies musculoskeletal structure and lever-arm mechanics, postoperative gait outcomes reflect a prolonged period of rehabilitation and neuromuscular adaptation. Prior work has emphasized that SEMLS corrects structural constraints without directly normalizing motor control (Shuman et al., 2019), requiring extensive postoperative rehabilitation and motor relearning to translate biomechanical corrections into functional gait changes (Dreher et al., 2018; Õunpuu et al., 2015; Thomason et al., 2013). This framework helps explain the heterogeneous and outcome-specific patterns observed in the present study.

Recent clinical guidelines have upgraded the strength of evidence supporting instrumented gait analysis from weak to moderate, emphasizing its value as an objective assessment tool when interpreted in conjunction with clinical examination, patient-reported outcomes, and caregiver input, rather than as a prescriptive determinant of treatment in isolation(States et al., 2024). The considerations outlined above underscore that interpretation of postoperative change is highly outcome-dependent, context-sensitive, and patient-specific, reinforcing the need for structured, consensus-driven approaches to outcome selection in SEMLS research.

5.3. Future Directions

Future work should move beyond uniform outcome panels toward consensus-driven, context-specific selection of gait metrics tailored to surgical protocols, recovery phase, and patient characteristics.

Longitudinal designs with repeated post-operative assessments are needed to characterize recovery trajectories and to determine when kinetic and joint loading adaptations emerge relative to kinematic changes. Integrating instrumented gait analysis with patient-reported and functional outcomes will further support clinically meaningful interpretation, consistent with current guideline recommendations. Finally, developmentally informed modeling and prospective studies linking external loading metrics to long-term joint health may help refine the role of biomechanical outcomes in postoperative decision-making.

Appendices

Appendix A: Statistical Methods

A.1. Regression Model Analysis

For each gait outcome Y_{ij}, a generalized least-squares (GLS) model was fit, where participant i was measured at time point j (pre- or post-surgery). The model included surgical group, time, their interaction, and the covariates normalized walking speed v_{ij}, months since surgery t_{ij}, age at surgery a_{ij}, body mass m_{ij}, and sex s_{ij}. The model was:

$$Y_{ij} = \beta_0 + \beta_1\, Group_i + \beta_2 Time_j + \beta_3 \left(Group_i \times Time_j\right) + \beta_4 v_{ij} + \beta_5 t_{ij} + \beta_6 a_{ij} + \beta_7 m_{ij} + \beta_8 s_{ij} + \varepsilon_{ij}$$

All continuous covariates (walking speed, time since surgery (months), age, and mass) were mean-centered prior to modeling. Sex was kept as an uncentered factor.

Normalized walking speed v_i was excluded from the model when the outcome was normalized walking speed, normalized step length, or normalized step time, so that the effect of surgery could be estimated without confounding and without partially out the mechanistic influence of speed on step length and step time.

As detailed in the next sections, the linearity of each continuous covariate x effect was evaluated in an ordinary least squares (OLS) framework by comparing spline-expanded and linear specification using likelihood-ratio tests, consistent with recommended regression modeling practice(Fox, 2015b). Homogeneity of slopes across groups was then assessed in the linear model via tests of Group × x interactions. This fixed-effects structure was then carried forward to GLS modeling. Because alternative GLS variance structures are not generally nested, model selection among candidate variance–covariance

structures relied on Akaike's Information Criterion (AIC) rather than likelihood-ratio tests (Pinheiro and Bates, 2000; Burnham and Anderson, 2002; Zuur et al., 2009), and in the absence of 1-a strong prior, and 2-interest in finding a "true" model to justify BIC use instead(Konishi and Kitagawa, 2008).

A.1.1. Assumption Checks

Collinearity

All predictors exhibited acceptable collinearity levels, and no term approached thresholds typically used to indicate problematic variance inflation.

Multicollinearity was assessed using generalized variance inflation factors (GVIF) (Fox, 2015a). For multi-df terms, the adjusted measure GVIF1/(2 df) was used (Fox and Weisberg, 2011). Values were well below commonly used thresholds (e.g., 2--3), indicating that collinearity was not a concern. A summary of GVIF results is provided in Table A.1.

Linearity of Effects

To assess departures from linearity, each continuous covariate was evaluated using spline-expanded models with 2–4 degrees of freedom. For each covariate, models were compared sequentially—linear vs. 2-df spline, then (if needed) 3-df, and finally 4-df—using likelihood-ratio tests (anova(lm fit, lm spl))(Fox, 2015a). A significant improvement ($p < .05$) at any stage indicated evidence of nonlinearity. When a spline with a given degree of freedom was significant, higher-complexity splines were not tested, and that spline term was retained; otherwise, the linear term was used in the final model.

Homogeneity of Slopes (Effect Modification by Group)

For each continuous covariate x, a base GLS model was compared to a Group × x interaction model, using the same variance–covariance structure as the base fit. If the interaction produced a significantly better fit (likelihood-ratio test $p < .05$), the interaction term was retained for subsequent inference;

otherwise, common slopes were assumed across groups.

Table **Error! Use the Home tab to apply 0 to the text that you want to appear here.**.1: Adjusted variance inflation factors, $GVIF^{1/(2\cdot Df)}$.

Predictor	GVIF adj
Group	1.46
Time	1.55
v_{ij}	1.08
t_{ij}	1.06
a_{ij}	1.95
m_{ij}	1.99
s_{ij}	1.08
Group:Time	1.61

Note. Time = pre- vs. post-surgery. v_{ij} = normalized walking speed, t_{ij} = months since surgery, a_{ij} = age at surgery, m_{ij} = body mass, s_{ij} = sex.

Heteroscedasticity

Because unequal variances combined with unequal group sizes can invalidate standard OLS/ANOVA inference(Box, 1954), GLS models were used to accommodate residual het-eroscedasticity. Several variance–covariance structures were evaluated, including varIdent (group-specific residual variances), varExp (variance increasing or decreasing exponentially with a covariate), and varPower (variance proportional to fitted values raised to a power) (Aitkin, 1987; Pinheiro and Bates, 2000; Zuur et al., 2009). Following recommendations from Pinheiro and Bates (2000), combination structures (varComb) were also considered when both group-level and covariate-driven heterogeneity were plausible. These variance functions enable GLS to deliver efficient, unbiased parameter estimates under heteroscedasticity—conditions under which ordinary least squares does not yield valid inference.

Practically, the more flexible variance functions in GLS tend to absorb heteroscedasticity even when formal tests indicate only mild or equivocal departures from constant variance. Once a structured variance model is introduced, much of the apparent heterogeneity seen in residual plots is already accounted for by the model itself. Thus, the heteroscedasticity diagnostics presented in Appendices B to D serve primarily as descriptive confirmation of variance patterns rather than as strict decision rules.

Originally, models were fit using OLS unless significant heteroscedasticity was detected. However, because GLS yields valid inference under both homoscedastic and heteroscedastic conditions—and because OLS can be anticonservative or inefficient in the presence of unequal variances—GLS was ultimately applied uniformly across all outcomes. This provided a consistent inferential framework. The diagnostic figures are therefore included for transparency while the final models rely on the more general GLS framework.

A.1.2. Model Selection

Competing GLS variance structures were compared using Akaike's Information Criterion (AIC), which estimates the expected information loss and selects the model with the greatest predictive adequacy rather than the fewest parameters(Akaike, 1998; Burnham and Anderson, 2002). AIC is widely recommended for selecting among heteroscedastic variance functions in GLS models(Pinheiro and Bates, 2000; Zuur et al., 2009), where the goal is improved estimation under model misspecification rather than identification of a single "true" residual structure. By contrast, the Bayesian Information Criterion (BIC) imposes a heavier penalty on model complexity(Schwarz, 1978) and may favor overly simplistic variance structures, particularly in moderate sample sizes. For these reasons, AIC was the more appropriate criterion for the present analyses.

A.1.3. Model Results

Within-Group Changes

Within-group pre–post changes were estimated using marginal means adjusted for all other variables in the fitted using the emmeans package, which computes adjusted means and contrasts based on the model's fixed-effects structure and associated covariance estimates (Lenth and Piaskowski, 2017; Searle et al., 1980).

Effect Size Calculations

Paired-samples effect sizes for pre–post changes were calculated as:

where z is the model-based Wald statistic for the pre–post contrast and n is the sample size of the surgical group.

Between-Group Differences Pre–Post Differences (DID)

Adjusted marginal means and DID contrasts were computed using emmeans(Lenth & Piaskowski, 2017). Because these contrasts share the same model coefficients, they are correlated rather than independent(Bretz et al., 2016; Hsu, 1996). This correlation makes Bonferroni overly conservative(Hochberg & Tamhane, 1987), whereas the Sidak method remains valid but less conservative when contrasts are positively correlated (Šidák, 1967). Under the Sidak adjustment, the familywise error rate is controlled using

$$\alpha_{adj} = 1 - (1 - \alpha)^{1/m}$$

where m is the number of correlated contrasts being tested. However, because the design includes only three surgical groups, the resulting number of DID contrasts is small, and the Bonferroni and Sidak adjusted thresholds are numerically similar in practice, at $\alpha = 0.05$:

$$\alpha_{adj-Sidak} = 1 - (1 - 0.05)^{1/3} = 0.0169$$

, and

$$\alpha_{adj-Bonferroni} = 1 - 0.05 / 3 = 0.0166$$

Effect Size Calculations

Standardized DID contrasts were computed as independent-groups Cohen's d:

$$d = J\left(z\sqrt{\frac{1}{n_1}+\frac{1}{n_2}} \right)$$

where z is the DID contrast test statistic, n1 and n2 are group sample sizes, and

$$J = 1 - \frac{3}{4(df)-1}, \qquad df = n_1 + n_2 - 2$$

is the Hedges small-sample correction (Hedges, 1981).

A.1.4. Adjustment for Multiple Outcome Comparisons

Because multiple outcome variables were evaluated, control of the family-wise error rate (FWER) was required to limit the probability of making one or more Type I errors across the set of outcomes. We therefore applied the Holm sequential Bonferroni procedure(Holm, 1979) (Holm, 1979). The Holm method is a step-down approach in which the raw *p*-values are first ordered from smallest to largest and then compared sequentially to increasingly less stringent critical values (α/m, α/(m − 1), …, α), stopping when a comparison fails. This procedure provides strong control of the FWER while being uniformly more powerful than the classical Bonferroni correction. Importantly, unlike methods that assume independence among tests, the Holm adjustment remains valid under arbitrary dependence structures, which is appropriate for gait-related biomechanical outcomes that are inherently correlated across variables such as walking speed, step characteristics, joint kinetics, and joint contact forces(Hochberg & Tamhane, 1987). Holm-adjusted *p*-values were computed using *p*.adjust(method = "holm") in R.

The family for each Holm adjustment consisted of the set of outcome variables within a surgical group (e.g., seven kinematic outcomes in Chapter 2, and seven kinetic outcomes across Chapters 2 and 3).

$$p_{(i)} \leq \frac{i}{m} q$$

where $p(i)$ is the ith smallest p-value, m is the total number of tests (e.g., m = 7 kinematic gait outcomes analyzed), and q is the desired false discovery rate (0.05 in this analysis). Adjusted p-values were computed in R(R Core Team, 2025) using the `p.adjust` function with method = "holm".

Appendix B: Kinematic Models and Diagnostics

As described in Appendix A, regression assumptions were evaluated for each outcome. OLS and GLS models were fitted and compared using AIC to guide model selection. Diagnostic results and model comparison tables are presented, followed by coefficients from the selected models. .

B.1. GDI

B.1.1. Model Assumption Checks

Linearity of baseline effect (spline check)

Table 1 Goodness-of-Fit Comparison (AIC and ANOVA) of Linear and Spline Models Predicting GDI from SEMLS Group, Time (Pre- vs. Post- Surgery),and their Interaction

Term	Model	Df	AIC	ΔAIC	F	*p*	
All terms linear	Base	12	963.03				
Normalized Speed	Spline_df2	13	964.76	1.73	0.24	.622	
Normalized Speed	Spline_df3	14	965.47	2.44	0.70	.496	
Normalized Speed	Spline_df4	15	967.41	4.38	0.48	.694	
Time since surgery (months)	Spline_df2	13	965.02	1.99	0.01	.919	
Time since surgery (months)	Spline_df3	14	961.49	0.00	2.55	.083	
Time since surgery (months)	Spline_df4	15	959.94	0.00	2.80	.043	*
Age	Spline_df2	16	957.71	0.00	3.80	.054	
Age	Spline_df3	17	959.01	0.00	2.21	.115	
Age	Spline_df4	18	959.77	0.00	1.83	.146	
Body Mass	Spline_df2	16	957.02	0.00	4.44	.037	*

Note. ΔAIC = Difference in Akaike information criterion relative to the best-fitting model. Significance: *** $p < 0.001$, ** $p < 0.01$, * $p < 0.05$.

Homogeneity of slopes (Group × Baseline interaction test)

Table **Error! No text of specified style in document.**.2: Homogeneity-of-Slopes Test: AIC and ANOVA Results for Group–Predictor Interaction in the Group × Time Model Testing Pre-to-Post Change in GD

Term	AIC_Base	AIC_Int	ΔAIC	ANOVA p
Normalized Speed	957.02	958.62	1.61	.353
Age	957.02	957.79	0.77	.246
Sex (F)	957.02	960.99	3.98	.990
NS_4[Time since surgery (months)]	957.02	963.02	6.01	.390
NS_2[Body Mass]	957.02	954.90	0.00	.069

Note. AIC (Base) = model without the Group × Predictor interaction term; AIC (Int) = model with the interaction term. ΔAIC = difference relative to the Base model. $*p < .05$.

Normality, Homoscedasticity and variance structure comparison

Table **Error! No text of specified style in document.**.3: Tests of Normality and Homogeneity of Variance. Residual Diagnostics of LM Model Predicting GDI from SEMLS Group, Time (Pre-vs. Post-Surgery), and their Interaction

Metric	Shapiro-Wilk W	Breusch-Pagan $df(14)$	Levene $F(5, 124)$
Test Statistic	0.86	15.29	1.26
p	$< .001$ ***	.359	.287

Table **Error! No text of specified style in document.**B.2 Tests of Normality and Homogeneity of Variance. Residual Diagnostics of GLS Model Predicting GDI from SEMLS Group, Time (Pre-vs. Post-Surgery), and their Interaction

Metric	Shapiro-Wilk W	Levene F(5, 124)
Test Statistic	0.87	1.09
p	$< .001$ ***	.368

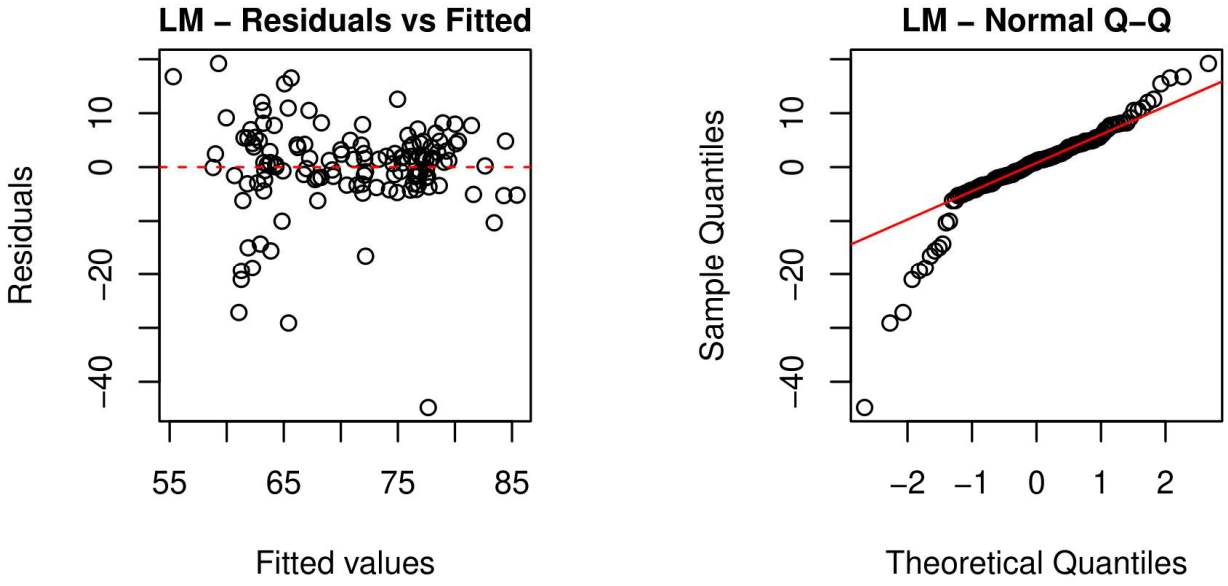


Figure B.1: Residuals–fitted and Q–Q plots showing evidence of acceptable homoscedasticity (left panel), and departures from normality (right, Q-Q plot) in the linear regression model predicting postoperative GDI.

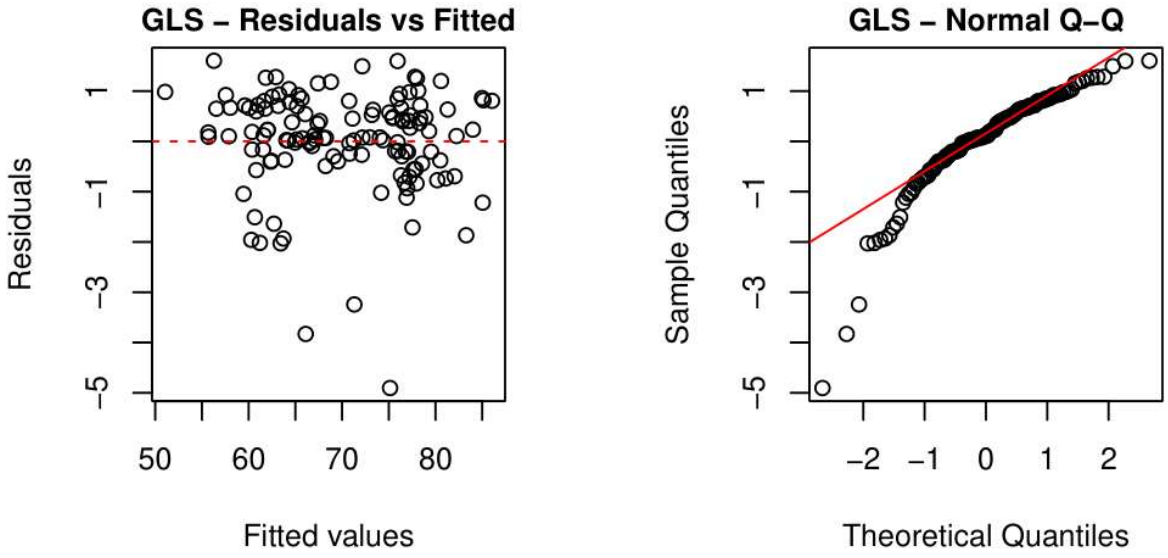


Figure B.2 Residuals–fitted and Q–Q plots showing evidence of acceptable homoscedasticity (left panel), and departures from normality (right, Q-Q plot) in the linear regression model predicting GDI.

B.1.2. Model Selection

Table 3 Model Comparison of Variance Structures when Predicting GDI from Group, Time, and Their Interaction

model	df	logLik	AIC	ΔAIC
combined variance	19	-441.76	921.52	0.00
exponential variance	17	-455.64	945.28	23.76
power variance	17	-455.68	945.36	23.84
group variance	18	-460.07	956.13	34.61
constant variance	16	-462.51	957.02	35.50

Model Coefficients

Table B.1.6: Regression Coefficients of Model Predicting GDI from SEMLS Group, Time, and Their Interaction, when Controlling for Other Covariates

Term	Estimate	CI	*p*	β
(Intercept)	55.73	[46.44, 65.03]	0.000	-1.56
GroupTDR-B	9.62	[4.50, 14.75]	0.000	0.76
GroupTDFR-U	5.56	[-1.86, 12.99]	0.145	0.41
TimePost	15.24	[11.30, 19.17]	0.000	1.09
Normalized Speed	6.43	[2.15, 10.72]	0.004	0.18
Age	-0.71	[-1.29, -0.13]	0.019	-0.16
sexF	3.04	[0.36, 5.73]	0.028	0.17
splines::ns(Time since surgery (months), df = 4)1	7.31	[-0.76, 15.37]	0.078	0.81
splines::ns(Time since surgery (months), df = 4)2	-14.04	[-29.46, 1.37]	0.077	-1.10
splines::ns(Time since surgery (months), df = 4)3	1.55	[-18.94, 22.04]	0.883	1.14
splines::ns(Time since surgery (months), df = 4)4	12.49	[3.88, 21.10]	0.005	1.54
splines::ns(Mass, df = 2)1	-3.24	[-14.51, 8.03]	0.575	-0.14
splines::ns(Mass, df = 2)2	19.62	[9.56, 29.69]	0.000	0.42
GroupTDR-B:TimePost	-7.22	[-12.77, -1.66]	0.012	-0.12
GroupTDFR-U:TimePost	-4.31	[-12.36, 3.75]	0.297	0.21

B.2. Normalized Walking Speed

B.2.1. Model Assumption Checks

Linearity of baseline effect (spline check)

Table **Error! No text of specified style in document.**.2.1 Goodness-of-Fit Comparison (AIC and ANOVA) of Linear and Spline Models Predicting Normalized Speed from SEMLS Group, Time (Pre- vs. Post- Surgery),and their Interaction

Term	Model	Df	AIC	ΔAIC	*F*	*p*
All terms linear	Base	11	33.94			
Time since surgery (months)	Spline_df2	12	33.47	0.00	2.29	.133
Time since surgery (months)	Spline_df3	13	35.33	1.39	1.20	.304
Time since surgery (months)	Spline_df4	14	34.79	0.85	1.58	.197
Age	Spline_df2	12	34.23	0.29	1.58	.211
Age	Spline_df3	13	35.35	1.41	1.19	.307
Age	Spline_df4	14	37.19	3.25	0.84	.476
Body Mass	**Spline_df2**	**12**	**28.28**	**0.00**	**7.24**	**.008 ****

Homogeneity of slopes (Group × Baseline interaction test)

Table 4.2.: Homogeneity-of-Slopes Test: AIC and ANOVA Results for Group–Predictor Interaction in the Group × Time Model Testing Pre-to-Post Change in Normalized Speed

Term	AIC_Base	AIC_Int	ΔAIC	ANOVA *p*
Time since surgery (months)	28.28	31.24	2.96	.626
Age	28.28	28.06	0.00	.149
Sex (F)	28.28	30.18	1.90	.388
NS_2[Body Mass]	28.28	31.39	3.11	.357

Note. AIC (Base) = model without the Group × Predictor interaction term; AIC (Int) = model with the interaction term. ΔAIC = difference relative to the Base model. *$p < .05$.

Normality, Homoscedasticity and variance structure comparison

Table **Error! No text of specified style in document.**.2.3:: Tests of Normality and Homogeneity of Variance. Residual Diagnostics of LM Model Predicting Normalized Speed from SEMLS Group, Time (Pre-vs. Post-Surgery), and their Interaction

Metric	Shapiro-Wilk W	Breusch-Pagan $df(10)$	Levene $F(5, 128)$
Test Statistic	0.99	9.66	2.49
p	.232	.471	.034 *

Table **Error! No text of specified style in document.**.2.4:: Tests of Normality and Homogeneity of Variance. Residual Diagnostics of GLS Model Predicting Normalized Speed from SEMLS Group, Time (Pre-vs. Post-Surgery), and their Interaction

Metric	Shapiro-Wilk W	Levene $F(5, 128)$
Test Statistic	0.99	0.21
P	.758	.958

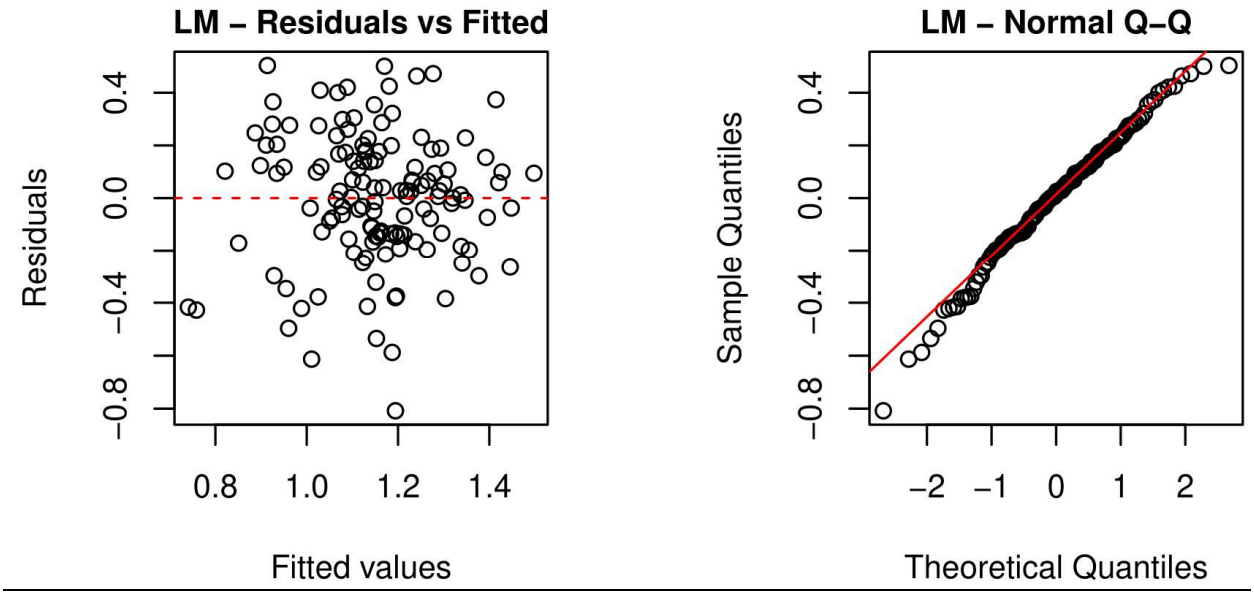


Figure B.2.1: Residuals–fitted and Q–Q plots showing sporadic condensed residuals, evidence of heteroskedasticity (left panel), and departures from normality (right, Q-Q plot) in the linear regression model predicting postoperative leg-length normalized walking speed

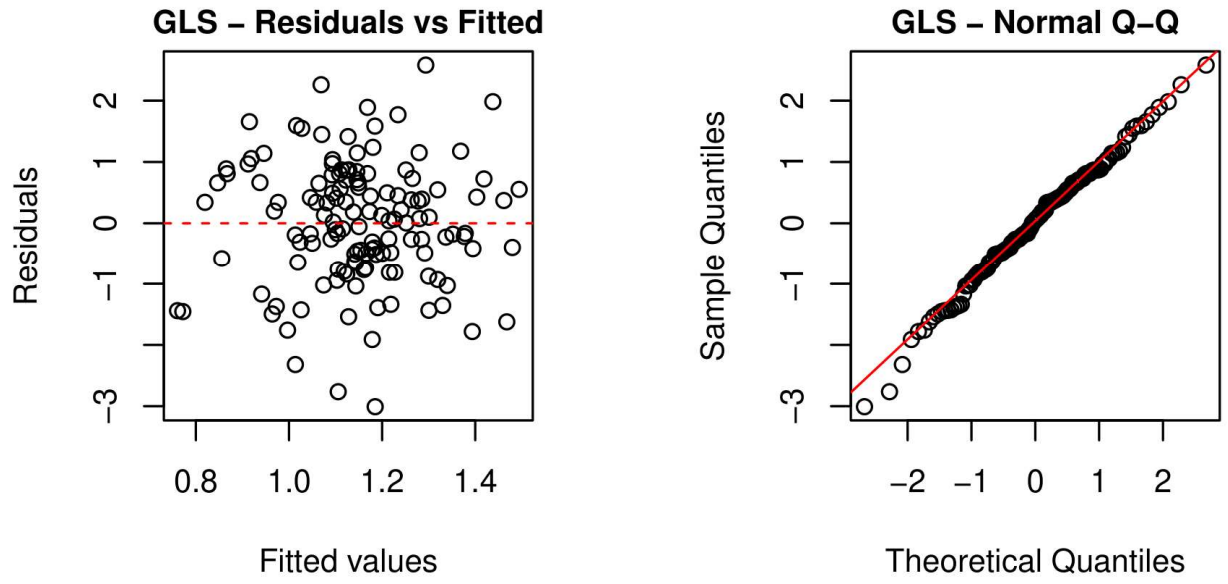


Figure B.2.2:Residuals–fitted and Q–Q plots showing evidence of heteroskedasticity (left panel), and departures from normality (right, Q-Q plot) in the linear regression model predicting postoperative leg-length normalized walking speed.

B.2.2. Model Selection

Table **Error! No text of specified style in document.**.2.5: Model Comparison of Variance Structures when Predicting Normalized Speed from Group, Time, and Their Interaction

model	df	logLik	AIC	ΔAIC
group variance	14	3.43	21.15	0.00
combined variance	15	3.88	22.24	1.09
exponential variance	13	1.12	23.75	2.61
power variance	13	1.04	23.93	2.78
constant variance	12	-2.14	28.28	7.13

Model Coefficients

Table **Error! No text of specified style in document.**.2.6: Regression Coefficients of GLS Model Predicting Normalized Speed from SEMLS Group, Time (Pre- vs. Post- Surgery), and their Interaction

Term	Estimate	CI	*p*	β
(Intercept)	1.24	[1.10, 1.37]	0.000	0.30
GroupTDR-B	0.01	[-0.19, 0.20]	0.960	0.02
GroupTDFR-U	0.20	[0.06, 0.33]	0.004	0.68
TimePost	0.14	[0.00, 0.29]	0.059	0.50
Time since surgery (months)	-0.01	[-0.02, 0.00]	0.283	-0.10
Age	0.00	[-0.02, 0.02]	0.736	-0.05
sexF	0.01	[-0.08, 0.10]	0.786	0.04
splines::ns(Mass, df = 2)1	-0.71	[-1.08, -0.33]	0.000	-2.48
splines::ns(Mass, df = 2)2	-0.13	[-0.49, 0.22]	0.463	-0.47
GroupTDR-B:TimePost	-0.10	[-0.38, 0.17]	0.459	-0.36
GroupTDFR-U:TimePost	-0.07	[-0.25, 0.11]	0.424	-0.26

B.3. Normalized Step Length

B.3.1. Model Assumption Checks

Linearity of baseline effect (spline check)

Table **Error! No text of specified style in document.**.3.1:6: Goodness-of-Fit Comparison (AIC and ANOVA) of Linear and Spline Models Predicting Normalized Step Length from SEMLS Group, Time (Pre- vs. Post-Surgery),and their Interaction

Term	Model	Df	AIC	ΔAIC	*F*	*p*	
All terms linear	Base	11	-192.54				
Time since surgery (months)	**Spline_df2**	**12**	**-198.11**	**0.00**	**7.15**	**.009**	**
Age	Spline_df2	13	-196.21	1.90	0.09	.759	
Age	Spline_df3	14	-194.22	3.89	0.05	.953	
Age	Spline_df4	15	-193.56	4.55	0.43	.729	
Body Mass	**Spline_df2**	**13**	**-201.20**	**0.00**	**4.73**	**.032**	*

Note. ΔAIC = Difference in Akaike information criterion relative to the best-fitting model. Significance: *** $p < 0.001$, ** $p < 0.01$, * $p < 0.05$.

Homogeneity of slopes (Group × Baseline interaction test)

Table **Error! No text of specified style in document.**.3.2:: Homogeneity-of-Slopes Test: AIC and ANOVA Results for Group–Predictor Interaction in the Group × Time Model Testing Pre-to-Post Change in Normalized Step Length

Term	AIC_Base	AIC_Int	ΔAIC	ANOVA *p*
Age	-201.20	-203.53	0.00	.059
Sex (F)	-201.20	-201.31	0.00	.159
NS_2[Time since surgery (months)]	-201.20	-194.57	6.64	.876
NS_2[Body Mass]	-201.20	-202.55	0.00	.081

Note. AIC (Base) = model without the Group × Predictor interaction term; AIC (Int) = model with the interaction term. ΔAIC = difference relative to the Base model. *$p < .05$.

Normality, Homoscedasticity and variance structure comparison

Table **Error! No text of specified style in document.**.3.3: : Tests of Normality and Homogeneity of Variance. Residual Diagnostics of LM Model Predicting Normalized Step Length from SEMLS Group, Time (Pre-vs. Post-Surgery), and their Interaction

Metric	Shapiro-Wilk W	Breusch-Pagan $df(11)$	Levene $F(5, 128)$
Test Statistic	0.99	11.12	1.90
p	.331	.434	.100

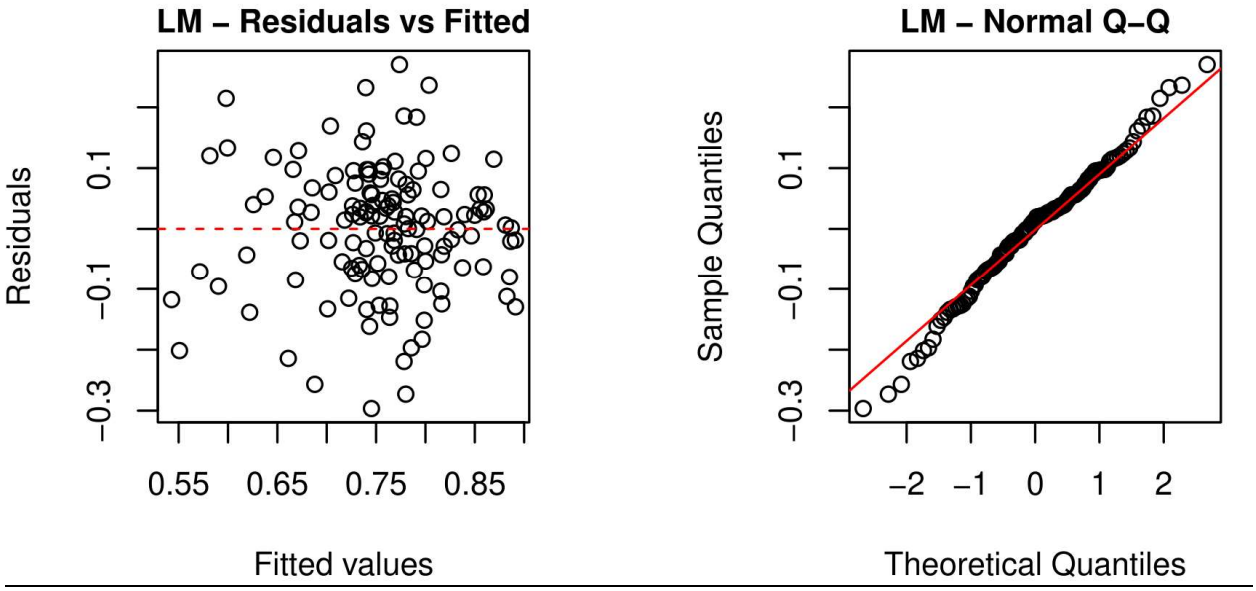


Figure B.3.1: Residuals spread increased slightly as fitted values grow, on a tight scale, indicating heteroscedasticity (left panel), and some deviations from normality (right panel).

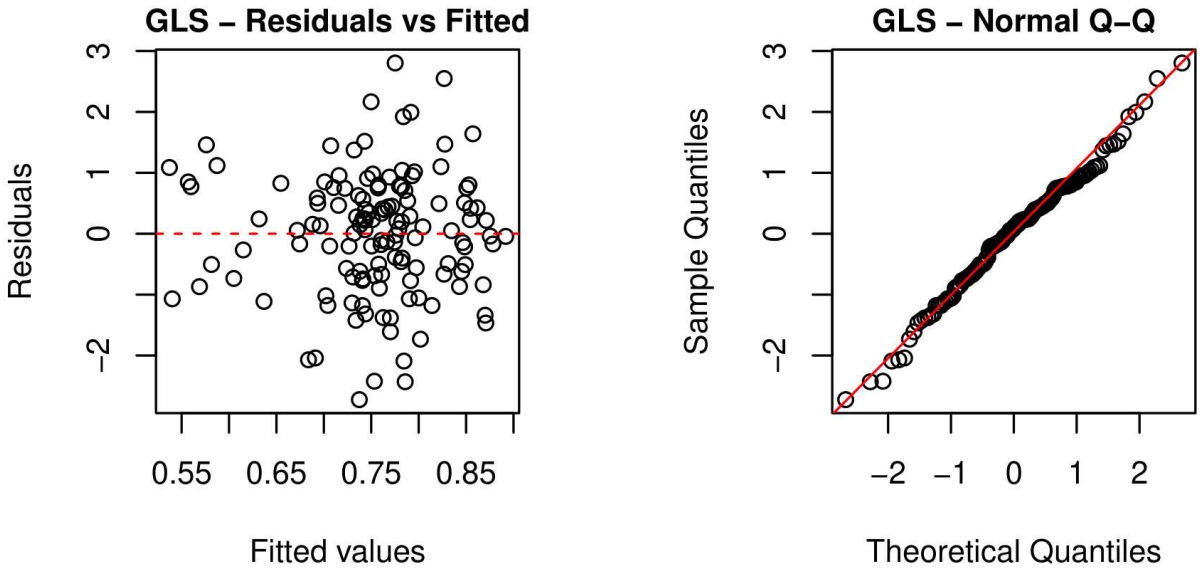


Figure B.3.2: GLS model with exponential variance structure residuals showed reduced patterns of heteroscedasticity (left panel), and minor deviations from normality (right panel)

Table **Error! No text of specified style in document.**.3.4:: Tests of Normality and Homogeneity of Variance. Residual Diagnostics of GLS Model Predicting Normalized Step Length from SEMLS Group, Time (Pre-vs. Post-Surgery), and their Interaction

Metric	Shapiro-Wilk *W*	Levene *F*(5, 128)
Test Statistic	0.99	0.76
p	.519	.580

.

B.3.2. Model Selection

Table **Error! No text of specified style in document.**.3.5:: Model Comparison of Variance Structures when Predicting Normalized Step Length from Group, Time, and Their Interaction

model	df	logLik	AIC	ΔAIC
exponential variance	14	116.93	-205.86	0.00
power variance	14	116.75	-205.50	0.36
group variance	15	117.05	-204.11	1.75
combined variance	16	118.01	-204.03	1.83
constant variance	13	113.60	-201.20	4.66

Model Coefficients

Table B.3.6: Regression Coefficients of Model Predicting Normalized Step Length from SEMLS Group, Time, and Their Interaction, when Controlling for Other Covariates

Term	Estimate	CI	*p*	β
(Intercept)	0.61	[0.43, 0.79]	0.000	-0.95
GroupTDR-B	-0.01	[-0.08, 0.07]	0.822	-0.09
GroupTDFR-U	0.09	[0.03, 0.14]	0.003	0.66
TimePost	0.02	[-0.04, 0.07]	0.556	0.13
Age	0.00	[-0.01, 0.01]	0.562	-0.09
sexF	-0.01	[-0.05, 0.03]	0.606	-0.08
splines::ns(Time since surgery (months), df = 2)1	0.39	[0.02, 0.77]	0.044	2.64
splines::ns(Time since surgery (months), df = 2)2	-0.03	[-0.20, 0.14]	0.759	-0.26
splines::ns(Mass, df = 2)1	-0.26	[-0.44, -0.08]	0.005	-1.98
splines::ns(Mass, df = 2)2	-0.12	[-0.30, 0.07]	0.222	-0.76
GroupTDR-B:TimePost	-0.03	[-0.14, 0.08]	0.585	-0.22
GroupTDFR-U:TimePost	0.00	[-0.08, 0.08]	1.000	-0.01

Note. All continuous predictors were mean-centered (mass [kg], age [yrs], normalized speed, baseline). Estimates are reported with 95% confidence intervals. Significance: *** $p < .001$, ** $p < .01$, * $p < .05$.

B.4. Normalized Step Time

B.4.1. Model Assumption Checks

Linearity of baseline effect (spline check)

Table **Error! No text of specified style in document.**.4.1:: Goodness-of-Fit Comparison (AIC and ANOVA) of Linear and Spline Models Predicting Normalized Step Time from SEMLS Group, Time (Pre- vs. Post- Surgery),and their Interaction

Term	Model	Df	AIC	ΔAIC	*F*	*p*	
All terms linear	Base	11	-99.54				
Time since surgery (months)	Spline_df2	12	-98.37	1.17	0.77	.383	
Time since surgery (months)	Spline_df3	13	-98.41	1.13	1.32	.271	
Time since surgery (months)	Spline_df4	14	-100.58	0.00	2.18	.094	
Age	**Spline_df2**	**12**	**-103.83**	**0.00**	**5.92**	**.016**	*****
Body Mass	Spline_df2	13	-104.56	0.00	2.51	.116	
Body Mass	Spline_df3	14	-105.61	0.00	2.67	.074	
Body Mass	Spline_df4	15	-105.55	0.00	2.37	.074	

Note. ΔAIC = Difference in Akaike information criterion relative to the best-fitting model. Significance: *** $p < 0.001$, ** $p < 0.01$, * $p < 0.05$.

Homogeneity of slopes (Group × Baseline interaction test)

Table **Error! No text of specified style in document.**.4.2:: Homogeneity-of-Slopes Test: AIC and ANOVA Results for Group–Predictor Interaction in the Group × Time Model Testing Pre-to-Post Change in Normalized Step Time

Term	AIC_Base	AIC_Int	ΔAIC	ANOVA *p*	
Time since surgery (months)	**-103.83**	**-140.60**	**0.00**	**< .001**	*******
Body Mass	-140.60	-138.47	2.13	.435	
Sex (F)	**-140.60**	**-152.71**	**0.00**	**< .001**	*******
NS_2[Age]	-152.71	-153.48	0.00	.108	

Note. AIC (Base) = model without the Group × Predictor interaction term; AIC (Int) = model with the interaction term. ΔAIC = difference relative to the Base model. *$p < .05$.

Normality, Homoscedasticity and variance structure comparison

Table **Error! No text of specified style in document.**.4.3:: Tests of Normality and Homogeneity of Variance. Residual Diagnostics of LM Model Predicting Normalized Step Time from SEMLS Group, Time (Pre-vs. Post-Surgery), and their Interaction

Metric	Shapiro-Wilk W	Breusch-Pagan $df(14)$	Levene $F(5, 128)$
Test Statistic	0.91	45.25	4.31
p	$< .001$ ***	$< .001$ ***	.001 **

Table **Error! No text of specified style in document.**.4.4.: Tests of Normality and Homogeneity of Variance. Residual Diagnostics of GLS Model Predicting Normalized Step Time from SEMLS Group, Time (Pre-vs. Post-Surgery), and their Interaction

Metric	Shapiro-Wilk W	Levene $F(5, 128)$
Test Statistic	0.93	0.62
p	$< .001$ ***	.686

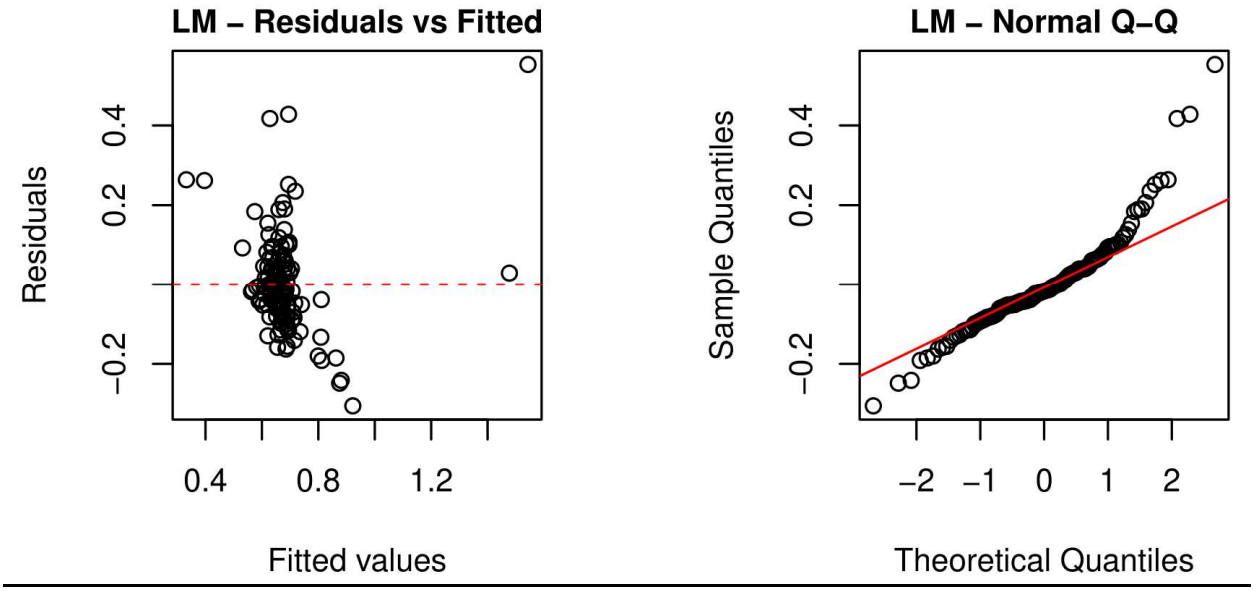


Figure B.4.1: Residual diagnostics plots of OLS model predicting normalized step time from SEMLS group, Time, and their Interaction.

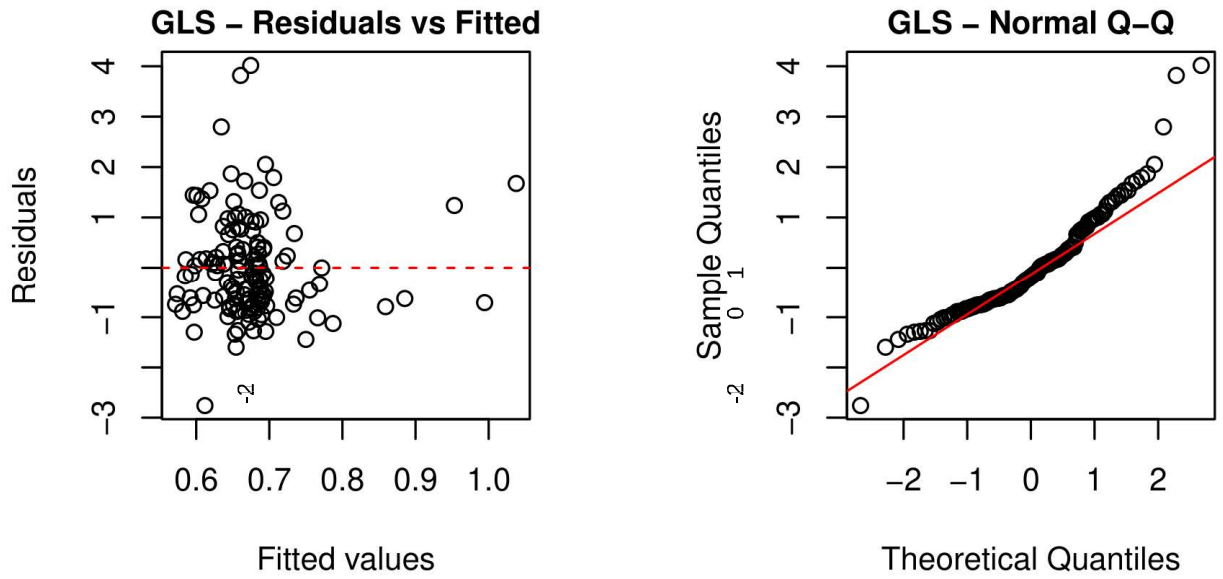


Figure B.4.2: Residuals–fitted and Q–Q plots showing evidence of heteroskedasticity (left panel), and departures from normality (right, Q-Q plot) in the linear regression model predicting normalized step time

B.4.2. Model Selection

Table **Error! No text of specified style in document.**.4.5: : Model Comparison of Variance Structures when Predicting Normalized Step Time from Group, Time, and Their Interaction

model	df	logLik	AIC	ΔAIC
combined variance	19	131.85	-225.69	0.00
power variance	17	126.58	-219.17	6.53
exponential variance	17	126.55	-219.10	6.59
group variance	18	118.26	-200.52	25.17
constant variance	16	92.35	-152.71	72.99

Model Coefficients

Table B.4.6: Regression Coefficients of Model Predicting Normalized Step Time from SEMLS Group, Time, and Their Interaction, when Controlling for Other Covariates

Term	Estimate	CI	*p*	β
(Intercept)	0.71	[0.65, 0.77]	0.000	0.17
GroupTDR-B	0.00	[-0.10, 0.10]	0.973	-0.16
GroupTDFR-U	-0.02	[-0.08, 0.04]	0.435	-0.28
TimePost	-0.03	[-0.09, 0.03]	0.276	-0.17
Time since surgery (months)	0.00	[-0.01, 0.00]	0.325	-0.06
Mass	0.00	[0.00, 0.00]	0.070	0.13
sexF	0.01	[-0.07, 0.08]	0.890	0.00
splines::ns(Age, df = 2)1	-0.02	[-0.17, 0.13]	0.778	-0.06
splines::ns(Age, df = 2)2	0.03	[-0.17, 0.23]	0.772	0.07
GroupTDR-B:TimePost	-0.06	[-0.17, 0.05]	0.296	-0.22
GroupTDFR-U:TimePost	0.01	[-0.05, 0.08]	0.675	0.14
GroupTDR-B:Time since surgery (months)	0.02	[0.00, 0.04]	0.043	1.06
GroupTDFR-U:Time since surgery (months)	0.02	[0.00, 0.03]	0.006	0.37
GroupTDR-B:sexF	0.20	[-0.03, 0.43]	0.093	1.36
GroupTDFR-U:sexF	-0.04	[-0.12, 0.05]	0.404	-0.05

B.5. Normalized Step Length Asymmetry

B.5.1. Model Assumption Checks

Linearity of baseline effect (spline check)

Table **Error! No text of specified style in document.**.5.1:: Goodness-of-Fit Comparison (AIC and ANOVA) of Linear and Spline Models Predicting Normalized Step Length Asymmetry from SEMLS Group, Time (Pre- vs. Post- Surgery),and their Interaction

Term	Model	Df	AIC	ΔAIC	*F*	*p*
All terms linear	Base	12	1110.70			
Normalized Speed	Spline_df2	13	1109.60	0.00	2.86	.093
Normalized Speed	Spline_df3	14	1110.47	0.00	1.94	.148
Normalized Speed	Spline_df4	15	1112.18	1.47	1.37	.254
Time since surgery (months)	Spline_df2	13	1110.96	0.25	1.60	.208
Time since surgery (months)	Spline_df3	14	1112.85	2.15	0.84	.433
Time since surgery (months)	Spline_df4	15	1114.45	3.75	0.68	.567
Age	Spline_df2	13	1111.16	0.46	1.41	.238
Age	**Spline_df3**	**14**	**1105.19**	**0.00**	**4.45**	**.014 ***
Body Mass	Spline_df2	15	1107.12	1.93	0.06	.806
Body Mass	Spline_df3	16	1106.37	1.19	1.26	.287
Body Mass	Spline_df4	17	1107.17	1.99	1.20	.315

Note. ΔAIC = Difference in Akaike information criterion relative to the best-fitting model. Significance: *** $p < 0.001$, ** $p < 0.01$, * $p < 0.05$.

Homogeneity of slopes (Group × Baseline interaction test)

Table **Error! No text of specified style in document.**.5.2: : Homogeneity-of-Slopes Test: AIC and ANOVA Results for Group–Predictor Interaction in the Group × Time Model Testing Pre-to-Post Change in Normalized Step Length Asymmetry

Term	AIC_Base	AIC_Int	ΔAIC	ANOVA *p*
Normalized Speed	1105.19	1108.11	2.92	.619
Time since surgery (months)	1105.19	1104.41	0.00	.120
Body Mass	**1105.19**	**1099.49**	**0.00**	**.014 ***
Sex (F)	1099.49	1101.09	1.60	.350
NS_3[Age]	1099.49	1100.46	0.97	.149

Note. AIC (Base) = model without the Group × Predictor interaction term; AIC (Int) = model with the interaction term. ΔAIC = difference relative to the Base model. *$p < .05$.

Normality, Homoscedasticity and variance structure comparison

Table **Error! No text of specified style in document.**.5.3:: Tests of Normality and Homogeneity of Variance. Residual Diagnostics of LM Model Predicting RL Asymmetry in Normalized Step Length from SEMLS Group, Time (Pre-vs. Post-Surgery), and their Interaction

Metric	Shapiro-Wilk W	Breusch-Pagan $df(14)$	Levene $F(5, 128)$
Test Statistic	0.84	25.45	0.46
p	$< .001$ ***	.030 *	.803

Table B.5.4: Tests of Normality and Homogeneity of Variance. Residual Diagnostics of GLS Model Predicting RL Asymmetry in Normalized Step Length from SEMLS Group, Time (Pre-vs. Post-Surgery), and their Interaction

Metric	Shapiro-Wilk W	Levene $F(5, 128)$
Test Statistic	0.90	0.70
p	$< .001$ ***	.624

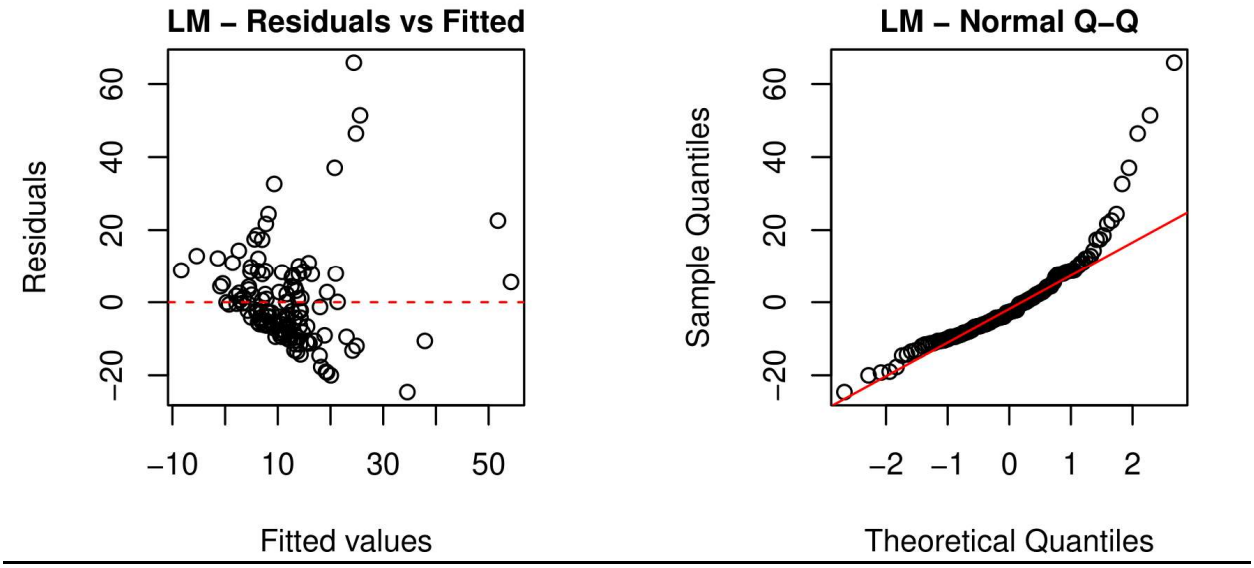


Figure B.5.1: Residual diagnostics for DID model predictting normalized step asymmetry show strong heteroskedasticity and pronounced right-tail deviations are evident, with several extreme positive residuals.

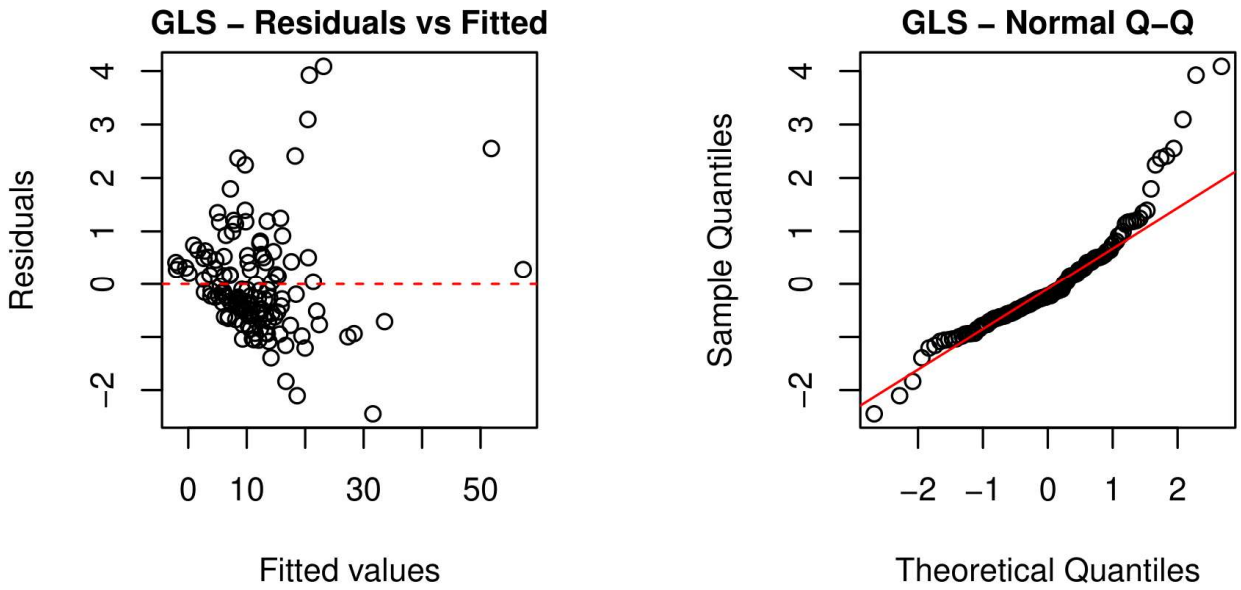


Figure B.5.2: Residuals show reduced heteroskedasticity relative to OLS but retain mild right-tailed skewness. The Q–Q plot indicates moderate deviation from normality in the upper tail, suggesting several large positive residuals.

B.5.2. Model Selection

Table **Error! No text of specified style in document.**.5.5:**Error! Use the Home tab to apply 0 to the text that you want to appear here.** Model Comparison of Variance Structures when Predicting RL Asymmetry in Normalized Step Length from Group, Time, and Their Interaction

model	df	logLik	AIC	ΔAIC
group variance	18	-525.34	1086.68	0.00
constant variance	16	-533.75	1099.49	12.81

Model Coefficients

Table B.5.6: Regression Coefficients of Model Predicting Step Length Asymmetry from SEMLS Group, Time, and Their Interaction, when Controlling for Other Covariates

Term	Estimate	CI	*p*	β
(Intercept)	27.22	[17.62, 36.81]	0.000	1.00
GroupTDR-B	-12.89	[-22.03, -3.76]	0.007	-0.83
GroupTDFR-U	-7.93	[-16.37, 0.52]	0.068	-0.51
TimePost	-4.29	[-9.42, 0.85]	0.104	-0.28

Term	Estimate	CI	*p*	β
Normalized Speed	-7.44	[-15.41, 0.52]	0.069	-0.14
Time since surgery (months)	-0.34	[-0.77, 0.10]	0.133	-0.10
Mass	0.65	[0.20, 1.10]	0.006	0.55
sexF	-2.62	[-7.50, 2.27]	0.296	-0.17
splines::ns(Age, df = 3)1	13.38	[-3.44, 30.20]	0.122	0.86
splines::ns(Age, df = 3)2	-3.54	[-29.59, 22.51]	0.791	-0.23
splines::ns(Age, df = 3)3	21.74	[-10.09, 53.58]	0.183	1.40
GroupTDR-B:TimePost	6.95	[-5.49, 19.40]	0.276	0.45
GroupTDFR-U:TimePost	2.16	[-9.03, 13.34]	0.706	0.14
GroupTDR-B:Mass	-1.13	[-1.67, -0.59]	0.000	-0.96
GroupTDFR-U:Mass	-0.51	[-0.99, -0.03]	0.038	-0.43

Laterality Effect Model

Table B.5.7: Regression Coefficients of Model Predicting Step Length Asymmetry from Surgery Laterality, Time, and Their Interaction, when Controlling for Other Covariates

Term	F.value	*p*.value
(Intercept)	57.78	<0.001
Laterality	0.01	0.931
Time	0.64	0.427
Normalized Speed	21.35	<0.001
Time since surgery (months)	4.79	0.031
Mass	1.08	0.300
sex	1.58	0.212
splines::ns(Age, df = 3)	1.77	0.156
Laterality:Time	0.01	0.924

Laterality:Mass	0.02	0.881

B.6. Step Time Asymmetry

B.6.1. Model Assumption Checks

Linearity of baseline effect (spline check)

Table **Error! No text of specified style in document.**.6.1: : Goodness-of-Fit Comparison (AIC and ANOVA) of Linear and Spline Models Predicting Step Time Asymmetry from SEMLS Group, Time (Pre- vs. Post- Surgery),and their Interaction

Term	Model	Df	AIC	ΔAIC	*F*	*p*
All terms linear	Base	12	965.69			
Normalized Speed	Spline_df2	13	967.34	1.64	0.33	.570
Normalized Speed	Spline_df3	14	968.07	2.38	0.74	.481
Normalized Speed	Spline_df4	15	969.95	4.25	0.52	.666
Time since surgery (months)	Spline_df2	13	964.61	0.00	2.84	.095
Time since surgery (months)	Spline_df3	14	965.85	0.16	1.76	.177
Time since surgery (months)	Spline_df4	15	967.85	2.15	1.16	.326
Age	Spline_df2	13	967.25	1.56	0.40	.528
Age	Spline_df3	14	968.70	3.01	0.45	.639
Age	Spline_df4	15	970.23	4.54	0.44	.725
Body Mass	Spline_df2	13	967.69	2.00	0.00	.977
Body Mass	Spline_df3	14	969.52	3.82	0.08	.923
Body Mass	Spline_df4	15	970.99	5.30	0.21	.889

Note. ΔAIC = Difference in Akaike information criterion relative to the best-fitting model. Significance: *** $p < 0.001$, ** $p < 0.01$, * $p < 0.05$.

Homogeneity of slopes (Group × Baseline interaction test)

Table **Error! No text of specified style in document.**.6.2: : Homogeneity-of-Slopes Test: AIC and ANOVA Results for Group–Predictor Interaction in the Group × Time Model Testing Pre-to-Post Change in RL Asymmetry in Normalized Step Time Asymmetry

Term	AIC_Base	AIC_Int	ΔAIC	ANOVA *p*
Normalized Speed	965.69	964.90	0.00	.115
Time since surgery (months)	965.69	965.67	0.00	.163
Age	**965.69**	**959.57**	**0.00**	**.010 ***
Body Mass	959.57	962.91	3.34	.747
Sex (F)	959.57	962.44	2.86	.603

Note. AIC (Base) = model without the Group × Predictor interaction term; AIC (Int) = model with the interaction term. ΔAIC = difference relative to the Base model. *$p < .05$.

Normality, Homoscedasticity and variance structure comparison

Table **Error! No text of specified style in document.**.6.3: : Tests of Normality and Homogeneity of Variance. Residual Diagnostics of LM Model Predicting Step Time Asymmetry from SEMLS Group, Time (Pre-vs. Post-Surgery), and their Interaction

Metric	Shapiro-Wilk W	Breusch-Pagan $df(12)$	Levene $F(5, 128)$
Test Statistic	0.93	22.96	2.89
p	$< .001$ ***	.028 *	.017 *

Table **Error! No text of specified style in document.**.6.:4 : Tests of Normality and Homogeneity of Variance. Residual Diagnostics of GLS Model Predicting Step Time Asymmetry from SEMLS Group, Time (Pre-vs. Post-Surgery), and their Interaction

Metric	Shapiro-Wilk W	Levene $F(5, 128)$
Test Statistic	0.93	0.25
p	$< .001$ ***	.941

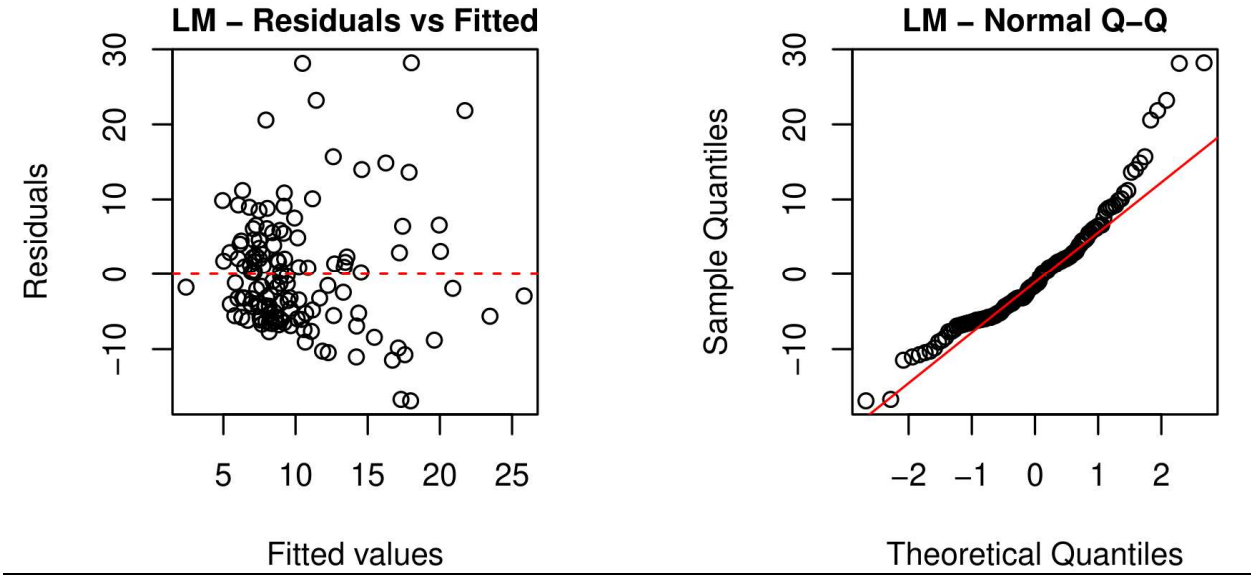


Figure B.6.1: Pronounced funnel shaped heteroscedastic residuals (left panel), non-normal distribution (right panel) in OLS model with nonlinear age term predicting step time asymmetry from group, time, and their interaction

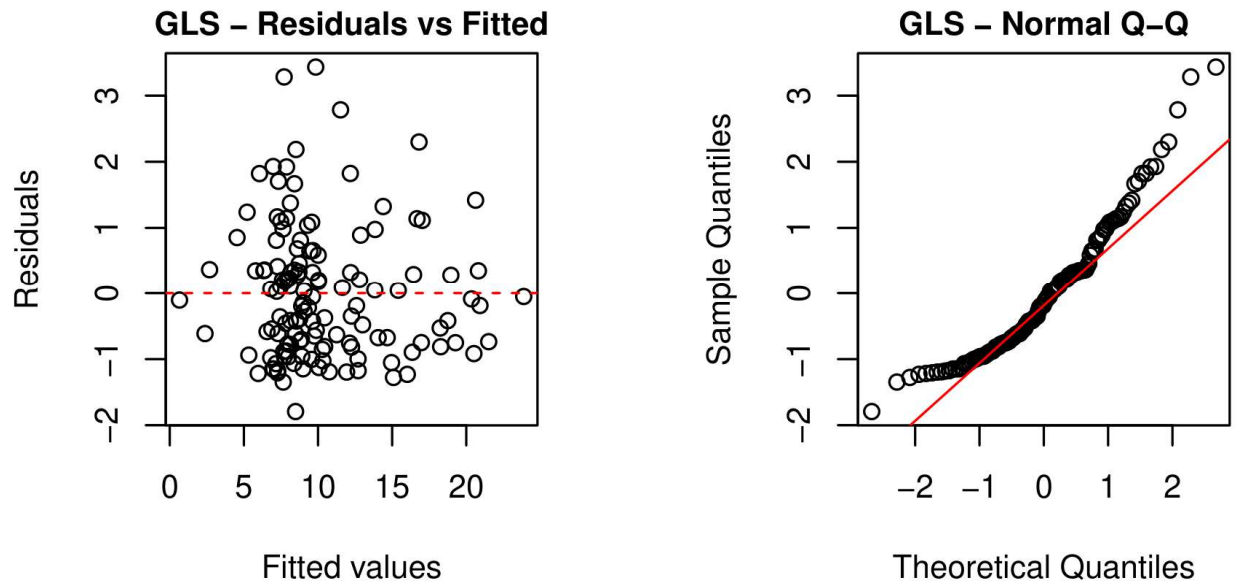


Figure B.6.2: Improved heteroskedasticity (left panel), and deviations from normality (right panel), when using a combination group-specific and exponential variance structures

B.6.2. Model Selection

Table **Error! No text of specified style in document.**.6.5: : Model Comparison of Variance Structures when Predicting Step Time Asymmetry from Group, Time, and Their Interaction

model	df	logLik	AIC	ΔAIC
combined variance	17	-448.24	930.48	0.00
power variance	15	-451.34	932.68	2.19
exponential variance	15	-453.65	937.31	6.82
group variance	16	-454.49	940.99	10.51
constant variance	14	-465.79	959.57	29.09

Model Coefficients

Table B.6.6: Regression Coefficients of Model Predicting Normalized Step Time Asymmetry from SEMLS Group, Time, and Their Interaction, when Controlling for Other Covariates

Term	Estimate	CI	*p*	β
(Intercept)	6.43	[4.40, 8.45]	0.000	-0.38
GroupTDR-B	0.34	[-2.48, 3.16]	0.813	0.09
GroupTDFR-U	8.54	[3.53, 13.55]	0.001	0.90
TimePost	1.60	[-1.72, 4.93]	0.347	0.11
Normalized Speed	-3.30	[-7.56, 0.97]	0.132	-0.10
Time since surgery (months)	0.47	[0.20, 0.73]	0.001	0.07
Age	-0.26	[-0.95, 0.43]	0.456	-0.02
Mass	-0.11	[-0.26, 0.04]	0.155	-0.17
sexF	1.11	[-1.75, 3.97]	0.449	-0.01
GroupTDR-B:TimePost	-0.55	[-4.64, 3.53]	0.792	-0.12
GroupTDFR-U:TimePost	-4.00	[-10.50, 2.50]	0.230	-0.28
GroupTDR-B:Age	0.53	[0.08, 0.98]	0.024	0.14
GroupTDFR-U:Age	1.45	[0.42, 2.48]	0.007	0.71

Laterality Effect Model

Table B.6.7: Regression Coefficients of Model Predicting Step Time Asymmetry from Surgery Laterality, Time, and Their Interaction, when Controlling for Other Covariates

Term	F.value	*p*.value
(Intercept)	131.23	<0.001
Time	0.77	0.381
Laterality	9.25	0.003
Normalized Speed	3.75	0.055
Time PostOp	0.14	0.710
Age	0.85	0.358
Mass	0.17	0.683
sex	0.00	1.000
Time:Laterality	2.31	0.131
Laterality:Age	6.62	0.011

B.7. Double-limb Support Time

B.7.1. Model Assumption Checks

Linearity of baseline effect (spline check)

Table **Error! No text of specified style in document.**.7.1: : Goodness-of-Fit Comparison (AIC and ANOVA) of Linear and Spline Models Predicting Double Limb Support Time from SEMLS Group, Time (Pre- vs. Post- Surgery),and their Interaction

Term	Model	Df	AIC	ΔAIC	*F*	*p*	
All terms linear	Base	12	838.24				
Normalized Speed	Spline_df2	13	836.87	0.00	3.11	.080	
Normalized Speed	Spline_df3	14	838.82	0.58	1.57	.213	
Normalized Speed	Spline_df4	15	840.82	2.57	1.04	.379	
Time since surgery (months)	Spline_df2	13	837.59	0.00	2.44	.121	
Time since surgery (months)	**Spline_df3**	**14**	**833.92**	**0.00**	**3.87**	**.023**	*****
Age	Spline_df2	15	835.92	2.00	0.00	.962	
Age	Spline_df3	16	837.88	3.96	0.02	.982	
Age	Spline_df4	17	839.27	5.34	0.19	.901	
Body Mass	Spline_df2	15	835.66	1.74	0.24	.627	
Body Mass	Spline_df3	16	835.82	1.89	0.94	.392	
Body Mass	Spline_df4	17	833.13	0.00	2.05	.111	

Note. ΔAIC = Difference in Akaike information criterion relative to the best-fitting model. Significance: *** $p < 0.001$, ** $p < 0.01$, * $p < 0.05$.

Homogeneity of slopes (Group × Baseline interaction test)

Table **Error! No text of specified style in document.**.7.2:: Homogeneity-of-Slopes Test: AIC and ANOVA Results for Group–Predictor Interaction in the Group × Time Model Testing Pre-to-Post Change in Double Limb Support Time

Term	AIC_Base	AIC_Int	ΔAIC	ANOVA p
Normalized Speed	833.92	835.08	1.16	.283
Age	833.92	836.14	2.22	.453
Body Mass	833.92	835.42	1.49	.328
Sex (F)	833.92	837.47	3.54	.817
NS_3[Time since surgery (months)]	833.92	836.81	2.89	.241

Note. AIC (Base) = model without the Group × Predictor interaction term; AIC (Int) = model with the interaction term. ΔAIC = difference relative to the Base model. *$p < .05$.

Normality, Homoscedasticity and variance structure comparison

Table B.7.3: Tests of Normality and Homogeneity of Variance. Residual Diagnostics of LM Model Predicting Double Limb Support Time from SEMLS Group, Time (Pre-vs. Post-Surgery), and their Interaction

Metric	Shapiro-Wilk W	Breusch-Pagan $df(12)$	Levene $F(5, 128)$
Test Statistic	0.97	33.89	1.19
p	.009 **	< .001 ***	.316

Table **Error! No text of specified style in document.**.7.4: : Tests of Normality and Homogeneity of Variance. Residual Diagnostics of GLS Model Predicting Double Limb Support Time from SEMLS Group, Time (Pre-vs. Post-Surgery), and their Interaction

Metric	Shapiro-Wilk W	Levene $F(5, 128)$
Test Statistic	0.98	2.39
p	.016 *	.041 *

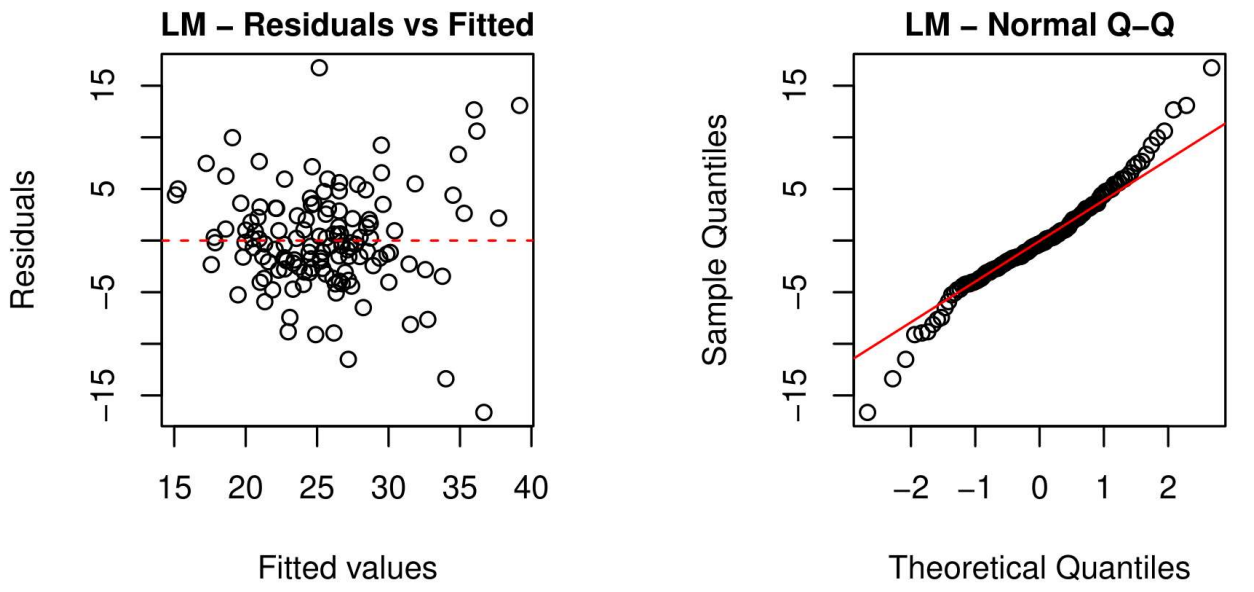
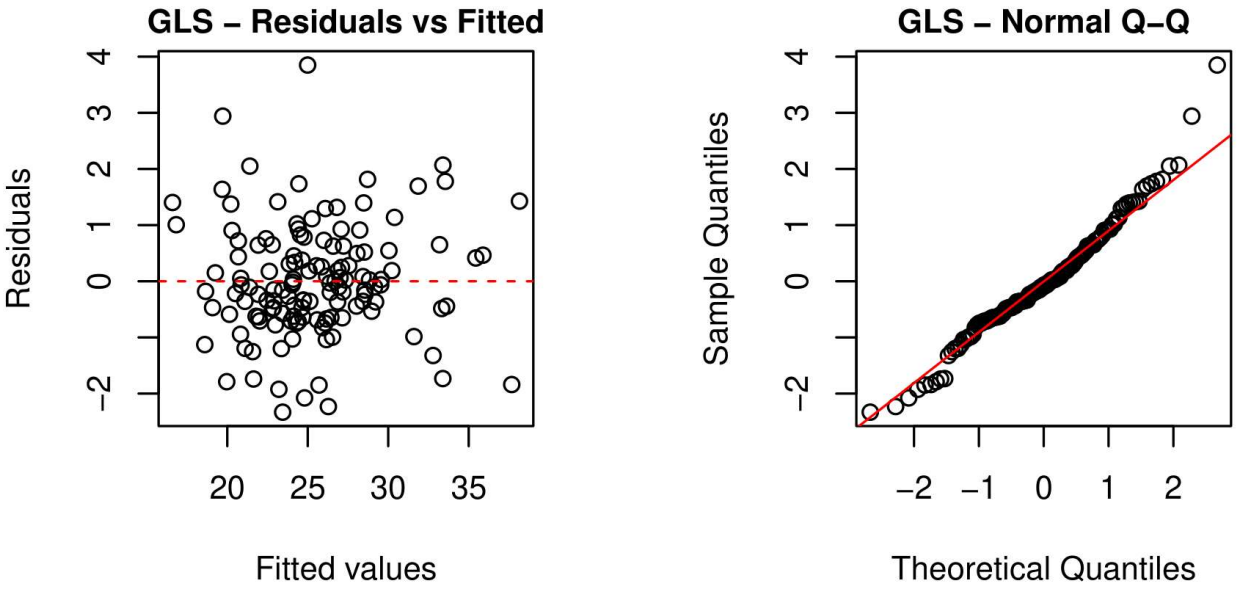


Figure B.7.1: OLS model's residuals show more spread with higher fitted values indicating heteroscedasticity (left panel), and deviation from normality (right panel)



Figuer B.7.2: The GLS model with exponential variance structure showed more uniform spread of residuals, reducing heteroscedasticity (left panel), and deviation from normality (right panel)

B.7.2. Model Selection

Table **Error! No text of specified style in document.**.7.5: : Model Comparison of Variance Structures when Predicting Double Limb Support Time from Group, Time, and Their Interaction

model	df	logLik	AIC	ΔAIC
exponential variance	15	-392.11	814.21	0.00
combined variance	17	-391.03	816.05	1.84
power variance	15	-393.17	816.35	2.13
group variance	16	-400.22	832.43	18.22
constant variance	14	-402.96	833.92	19.71

- Model Coefficients

Table B.7:6: Regression Coefficients of Model Predicting DLS from SEMLS Group, Time, and Their Interaction, when Controlling for Other Covariates

Term	Estimate	CI	*p*	β
(Intercept)	20.88	[12.98, 28.78]	0.000	-0.68
GroupTDR-B	6.10	[2.55, 9.65]	0.001	0.90
GroupTDFR-U	0.88	[-1.41, 3.17]	0.451	0.12
TimePost	3.87	[1.49, 6.24]	0.002	0.55
Normalized Speed	-10.86	[-14.22, -7.49]	0.000	-0.44
Age	-0.45	[-0.86, -0.04]	0.032	-0.25
Mass	0.10	[-0.02, 0.22]	0.093	0.19
sexF	-0.28	[-2.08, 1.53]	0.766	-0.04
splines::ns(Time since surgery (months), df = 3)1	-10.43	[-18.85, -2.01]	0.017	-1.43
splines::ns(Time since surgery (months), df = 3)2	6.13	[-9.02, 21.27]	0.430	0.89
splines::ns(Time since surgery (months), df = 3)3	5.41	[-4.31, 15.12]	0.277	0.81
GroupTDR-B:TimePost	-3.78	[-8.53, 0.97]	0.122	-0.56
GroupTDFR-U:TimePost	-1.81	[-5.13, 1.52]	0.289	-0.25

Appendix C: Joint Kinetics and Energetics Models and Diagnostics

C.1. Ankle Positive Work in Late Stance

C.1.1. Model Assumption Checks

Linearity of baseline effect (spline check)

Table C.7.1 Goodness-of-Fit Comparison (AIC and ANOVA) of Linear and Spline Models Predicting Ankle Positive Work In Late Stance from SEMLS Group, Time (Pre- vs. Post- Surgery),and their Interaction

Term	Model	df	AIC	ΔAIC	*F*	*p*
All terms linear	Base	12	5.32			
Normalized Speed	Spline_df2	13	7.26	1.94	0.06	.811
Normalized Speed	Spline_df3	14	9.08	3.76	0.11	.899
Normalized Speed	Spline_df4	15	10.52	5.20	0.24	.871
Time since surgery (months)	Spline_df2	13	5.78	0.46	1.39	.241
Time since surgery (months)	Spline_df3	14	7.55	2.22	0.80	.454
Time since surgery (months)	Spline_df4	15	9.53	4.21	0.53	.663
Age	Spline_df2	13	7.30	1.97	0.02	.879
Age	Spline_df3	14	9.07	3.75	0.11	.894
Age	Spline_df4	15	10.37	5.04	0.28	.838
Body Mass	Spline_df2	13	7.29	1.97	0.03	.864
Body Mass	Spline_df3	14	9.29	3.97	0.02	.985
Body Mass	Spline_df4	15	10.76	5.43	0.17	.918

Note. ΔAIC = Difference in Akaike information criterion relative to the best-fitting model. Significance: *** $p < 0.001$, ** $p < 0.01$, * $p < 0.05$.

Homogeneity of slopes (Group × Baseline interaction test)

Table C.1.3: Homogeneity-of-Slopes Test: AIC and ANOVA Results for Group–Predictor Interaction in the Group × Time Model Testing Pre-to-Post Change in Ankle Positive Work in Late Stance

Term	AIC_Base	AIC_Int	ΔAIC	ANOVA p
Normalized Speed	5.32	9.06	3.73	.889
Time since surgery (months)	5.32	8.03	2.71	.563
Age	5.32	9.19	3.87	.944
Body Mass	5.32	8.86	3.54	.814
Sex (F)	5.32	8.91	3.59	.832

Note. AIC (Base) = model without the Group × Predictor interaction term; AIC (Int) = model with the interaction term. ΔAIC = difference relative to the Base model. *$p < .05$.

Normality, Homoscedasticity and variance structure comparison

Table **Error! No text of specified style in document.**C.1:4: Tests of Normality and Homogeneity of Variance. Residual Diagnostics of LM Model Predicting Ratio of Ankle to Hip Peak Power from SEMLS Group, Time (Pre- vs. Post-Surgery), and their Interaction

Metric	Shapiro-Wilk W	Breusch-Pagan $df(13)$	Levene $F(5, 110)$
Test Statistic	0.95	5.17	0.23
p	$< .001$ ***	.971	.950

Table C.1:5: Tests of Normality and Homogeneity of Variance. Residual Diagnostics of GLS Model Predicting Ratio of Ankle to Hip Peak Power from SEMLS Group, Time (Pre-vs. Post-Surgery), and their Interaction

Metric	Shapiro-Wilk W	Levene $F(5, 110)$
Test Statistic	0.95	0.23
p	$< .001$ ***	.951

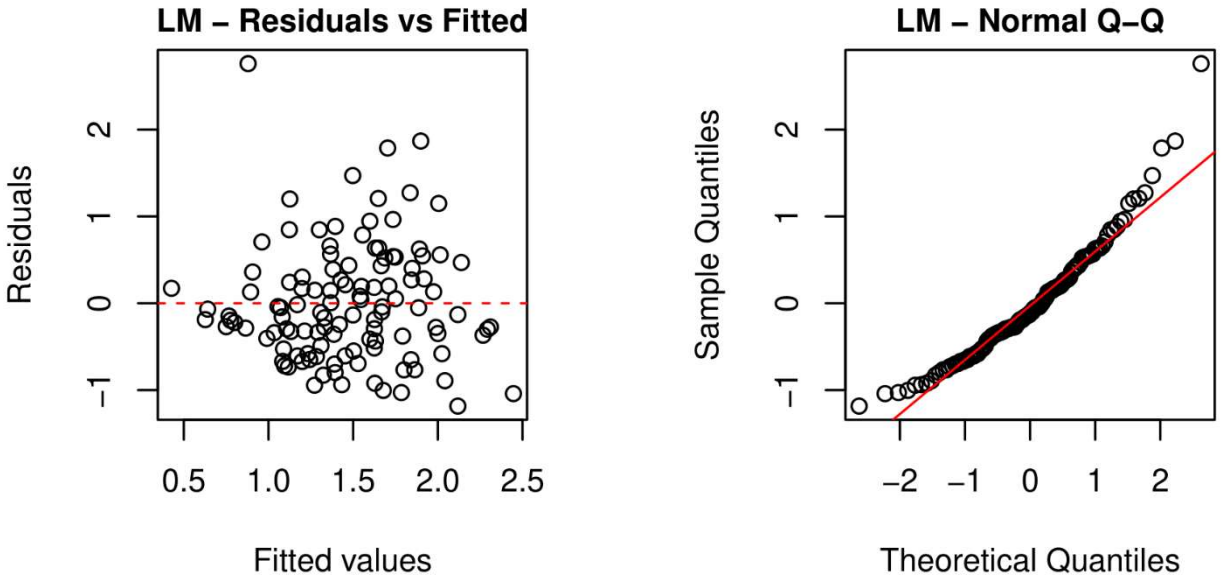


Figure C.1.1: Residuals of the OLS model showed non constant spread of residuals, i.e. heteroscedasticity, (left panel), and deviation from normality (right panel)

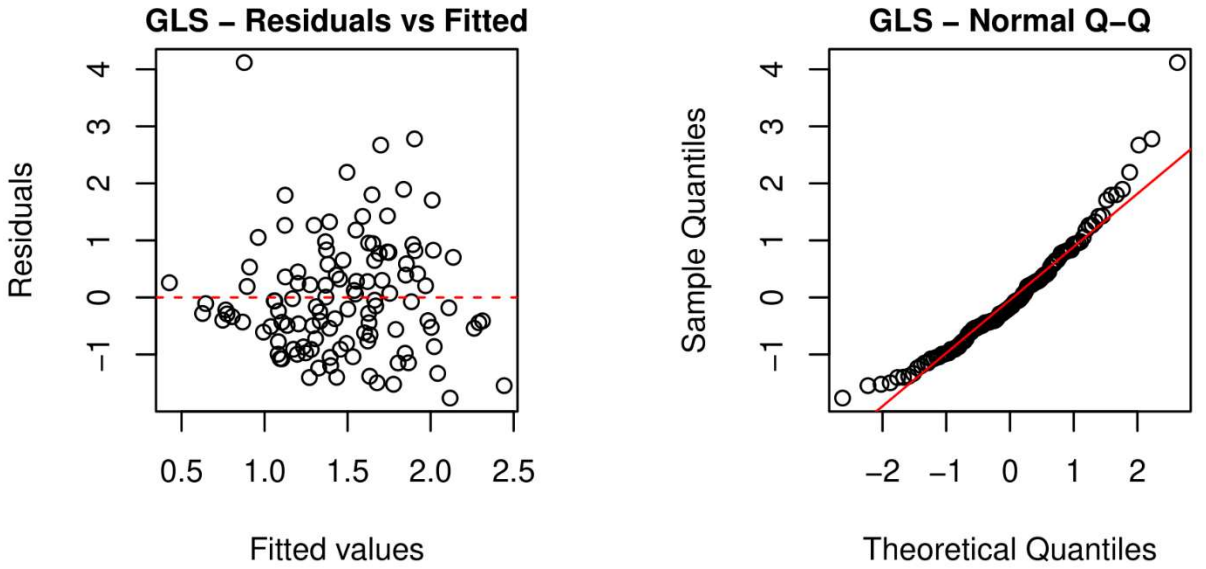


Figure C.1.2: Residuals of the GLS model showed more balanced spread of residual (left panel), and deviation from normality (right panel).

C.1.2. Model Selection

Table 8: Model Comparison of Variance Structures when Predicting Ankle Positive Work in Late Stance from Group, Time, and Their Interaction

model	df	logLik	AIC	ΔAIC
combined variance	15	48.81	-67.61	0.00
group variance	14	39.92	-51.85	15.76
constant variance	12	9.34	5.32	72.93

Model Coefficients

Table C.1.6: Regression Coefficients of Model Predicting Ankle Positive Work in Late Stance from SEMLS Group, Time, and Their Interaction, when Controlling for Other Covariates

Term	Estimate	CI	*p*	β
(Intercept)	0.42	[0.19, 0.65]	0.000	0.20
GroupTDR-B	-0.04	[-0.27, 0.20]	0.759	0.08
GroupTDFR-U	-0.08	[-0.32, 0.15]	0.491	-0.13
TimePost	-0.14	[-0.39, 0.11]	0.266	-0.32
Normalized Speed	0.13	[0.09, 0.18]	0.000	0.10
Time since surgery (months)	0.01	[0.00, 0.01]	0.000	0.12
Age	0.00	[0.00, 0.01]	0.070	0.07
Mass	0.00	[0.00, 0.00]	0.038	-0.16
sexF	0.01	[-0.02, 0.05]	0.488	0.02
GroupTDR-B:TimePost	-0.03	[-0.28, 0.23]	0.838	-0.47
GroupTDFR-U:TimePost	0.10	[-0.16, 0.36]	0.456	0.13

C.2. Knee Extensor Impulse in Stance Phase

C.2.1. Model Assumption Checks

Linearity of baseline effect (spline check)

Table C.2.1: Goodness-of-Fit Comparison (AIC and ANOVA) of Linear and Spline Models Predicting Knee Extensor Impulse in Stance from SEMLS Group, Time (Pre- vs. Post- Surgery),and their Interaction

Term	Model	Df	AIC	ΔAIC	*F*	*p*
All terms linear	Base	12	866.32			
Normalized Speed	Spline_df2	13	867.38	1.06	0.84	.360
Normalized Speed	Spline_df3	14	869.36	3.05	0.43	.655
Normalized Speed	Spline_df4	15	868.72	2.40	1.07	.364
Time since surgery (months)	Spline_df2	13	868.31	1.99	0.01	.921
Time since surgery (months)	Spline_df3	14	870.28	3.97	0.01	.985
Time since surgery (months)	Spline_df4	15	872.11	5.79	0.06	.980
Age	Spline_df2	13	867.89	1.57	0.38	.537
Age	Spline_df3	14	869.09	2.77	0.55	.580
Age	Spline_df4	15	870.52	4.20	0.53	.661
Body Mass	Spline_df2	13	868.26	1.95	0.05	.829
Body Mass	Spline_df3	14	869.97	3.65	0.16	.856
Body Mass	Spline_df4	15	872.10	5.78	0.06	.978

Note. ΔAIC = Difference in Akaike information criterion relative to the best-fitting model. Significance: *** $p < 0.001$, ** $p < 0.01$, * $p < 0.05$.

Homogeneity of slopes (Group × Baseline interaction test)

Table C.2.2: Homogeneity-of-Slopes Test: AIC and ANOVA Results for Group–Predictor Interaction in the Group × Time Model Testing Pre-to-Post Change in Knee Extensor Impulse in Stance

Term	AIC_Base	AIC_Int	ΔAIC	ANOVA p
Normalized Speed	866.32	870.11	3.80	.914
Time since surgery (months)	866.32	870.31	4.00	.998
Age	866.32	869.66	3.35	.748
Body Mass	866.32	869.92	3.60	.838
Sex (F)	866.32	869.82	3.50	.802

Note. AIC (Base) = model without the Group × Predictor interaction term; AIC (Int) = model with the interaction term. ΔAIC = difference relative to the Base model. *$p < .05$.

Normality, Homoscedasticity and variance structure comparison

Table **Error! No text of specified style in document.**C.2.3:: Tests of Normality and Homogeneity of Variance. Residual Diagnostics of LM Model Predicting Knee Extensor Impulse in Stance from SEMLS Group, Time (Pre-vs. Post-Surgery), and their Interaction

Metric	Shapiro-Wilk W	Breusch-Pagan $df(10)$	Levene $F(5, 110)$
Test Statistic	0.19	4.60	0.63
p	$< .001$ ***	.916	.676

Table **Error! No text of specified style in document.**C.2.4:: Tests of Normality and Homogeneity of Variance. Residual Diagnostics of GLS Model Predicting Knee Extensor Impulse in Stance from SEMLS Group, Time (Pre-vs. Post-Surgery), and their Interaction

Metric	Shapiro-Wilk W	Levene $F(5, 110)$
Test Statistic	0.71	3.64
p	$< .001$ ***	.004 **

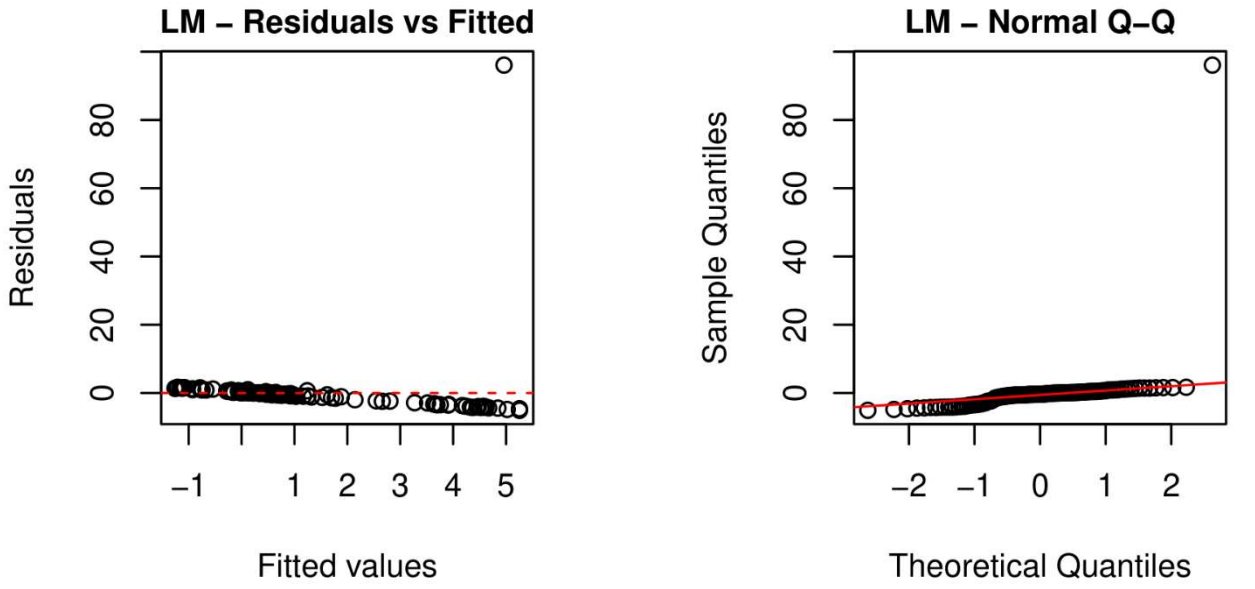


Figure C.2.1: Residuals diagnostics show heteroskedasticity (left panel), some deviation from normality at the tails in OLS model with 2df spline mass term and its group modification by group predicting knee extensor impulse during the stance phase from SEMLS group, time (pre-vs. post-surgery), and their interaction

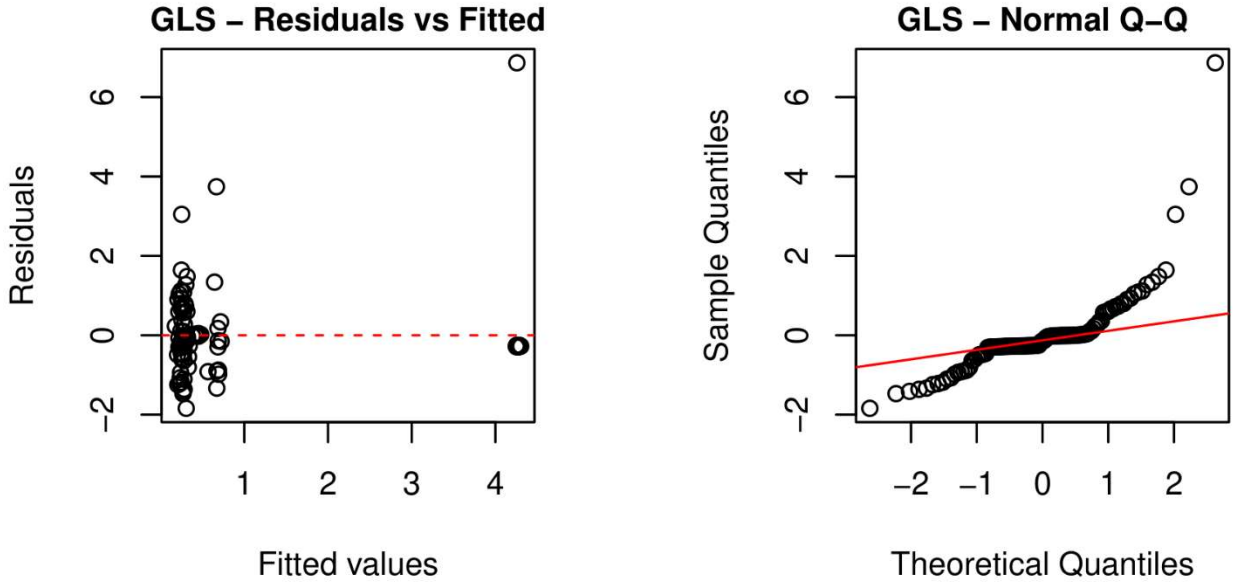


Figure C.2.2: Residuals diagnostics show improved heteroskedasticity (left panel), some deviation from normality at the tails in GLS model with power variance structure predicting knee extensor moment impulse during the stance phase from SEMLS group, time (pre-vs. post-surgery), and their interaction.

C.2.2. Model Selection

Model Comparisons

Table C.2.5: Model Comparison of Variance Structures when Predicting Knee Extensor Impulse in Stance from Group, Time, and Their Interaction

model	df	logLik	AIC	ΔAIC
group variance	14	-180.55	389.10	0.00
constant variance	12	-421.16	866.32	477.22

Model Coefficients

Table C.2.6: Regression Coefficients of Model Predicting Knee Extensor Moment Impulse in Stance Phase from SEMLS Group, Time, and Their Interaction, when Controlling for Other Covariates

Term	Estimate	CI	*p*	β
(Intercept)	0.41	[0.32, 0.50]	0.000	0.14
GroupTDR-B	0.29	[0.02, 0.56]	0.041	0.93
GroupTDFR-U	-0.14	[-0.25, -0.02]	0.020	-0.50
TimePost	-0.04	[-0.16, 0.08]	0.529	-0.16
Normalized Speed	-0.05	[-0.19, 0.09]	0.448	-0.08
Time since surgery (months)	0.01	[-0.01, 0.02]	0.375	0.06
Age	-0.01	[-0.02, 0.00]	0.115	-0.18
Mass	0.00	[0.00, 0.00]	0.886	0.02
sexF	0.03	[-0.04, 0.10]	0.354	0.12
GroupTDR-B:TimePost	-0.34	[-0.63, -0.05]	0.023	-1.08
GroupTDFR-U:TimePost	0.01	[-0.14, 0.15]	0.934	-0.01

C.3. Hip Flexor Moment Impulse in Pre-Swing

C.3.1. Model Assumption Checks

Linearity of baseline effect (spline check)

Table C.3.1: Goodness-of-Fit Comparison (AIC and ANOVA) of Linear and Spline Models Predicting Hip Flexor Impulse in Pre-Swing from SEMLS Group, Time (Pre- vs. Post- Surgery),and their Interaction

Term	Model	Df	AIC	ΔAIC	*F*	*p*
All terms linear	Base	12	-358.38			
Normalized Speed	Spline_df2	13	-357.70	0.69	1.18	.279
Normalized Speed	Spline_df3	14	-356.69	1.69	1.04	.358
Normalized Speed	Spline_df4	15	-355.93	2.45	1.06	.371
Time since surgery (months)	Spline_df2	13	-359.03	0.00	2.40	.124
Time since surgery (months)	Spline_df3	14	-358.32	0.06	1.78	.174
Time since surgery (months)	Spline_df4	15	-359.32	0.00	2.10	.105
Age	Spline_df2	13	-356.49	1.89	0.10	.755
Age	Spline_df3	14	-355.02	3.36	0.28	.753
Age	Spline_df4	15	-360.82	0.00	2.57	.059
Body Mass	Spline_df2	13	-356.98	1.40	0.54	.465
Body Mass	Spline_df3	14	-356.81	1.57	1.09	.340
Body Mass	Spline_df4	15	-358.81	0.00	1.94	.128

Note. ΔAIC = Difference in Akaike information criterion relative to the best-fitting model. Significance: *** $p < 0.001$, ** $p < 0.01$, * $p < 0.05$.

Homogeneity of slopes (Group × Baseline interaction test)

Table C.3.2:: Homogeneity-of-Slopes Test: AIC and ANOVA Results for Group–Predictor Interaction in the Group × Time Model Testing Pre-to-Post Change in Hip Flexor Impulse in Pre-Swing

Term	AIC_Base	AIC_Int	ΔAIC	ANOVA p
Normalized Speed	-358.38	-355.83	2.56	.527
Time since surgery (months)	-358.38	-356.09	2.29	.468
Age	**-358.38**	**-361.17**	**0.00**	**.049 ***
Body Mass	-361.17	-362.54	0.00	.097
Sex (F)	-361.17	-357.37	3.81	.920

Note. AIC (Base) = model without the Group × Predictor interaction term; AIC (Int) = model with the interaction term. ΔAIC = difference relative to the Base model. *$p < .05$.

Normality, Homoscedasticity and variance structure comparison

Table **Error! No text of specified style in document.**C.3.3:: Tests of Normality and Homogeneity of Variance. Residual Diagnostics of LM Model Predicting Hip Flexor Impulse in Pre-Swing from SEMLS Group, Time (Pre-vs. Post-Surgery), and their Interaction

Metric	Shapiro-Wilk W	Breusch-Pagan $df(12)$	Levene $F(5, 110)$
Test Statistic	0.93	37.30	5.65
p	$< .001$ ***	$< .001$ ***	$< .001$ ***

Table **Error! No text of specified style in document.**C.3.4:: Tests of Normality and Homogeneity of Variance. Residual Diagnostics of GLS Model Predicting Hip Flexor Impulse in Pre-Swing from SEMLS Group, Time (Pre-vs. Post-Surgery), and their Interaction

Metric	Shapiro-Wilk W	Levene $F(5, 110)$
Test Statistic	0.95	1.44
p	$< .001$ ***	.214

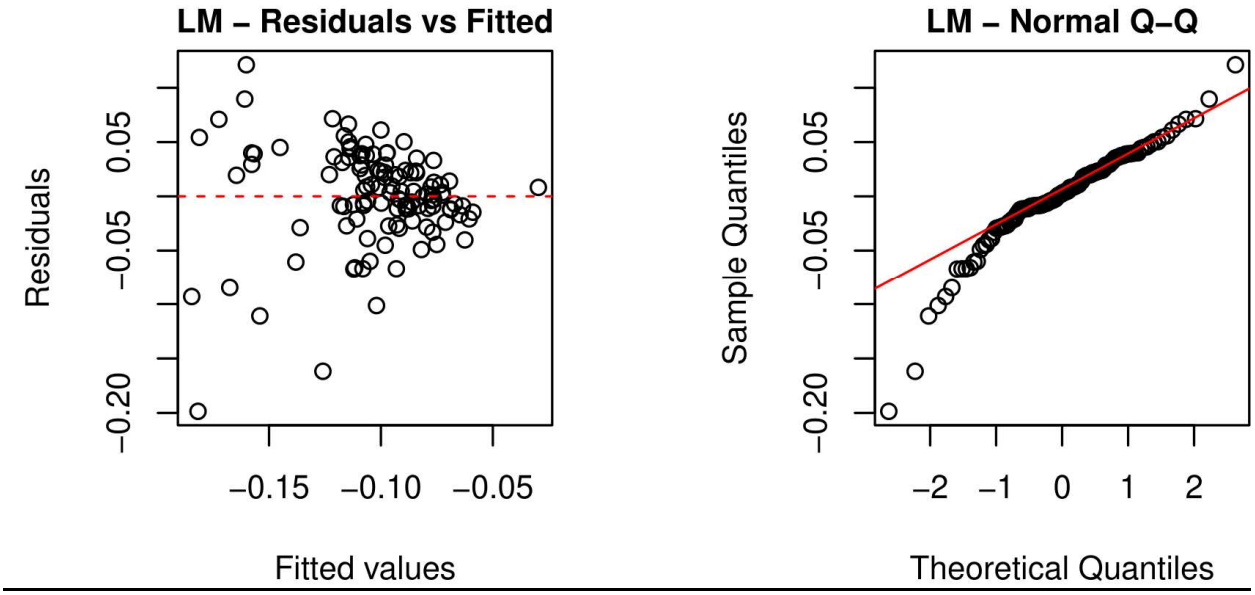


Figure C.3.1: OLS model with a combined variance structure showed heteroscedasticity (left panel), and deviations from normality

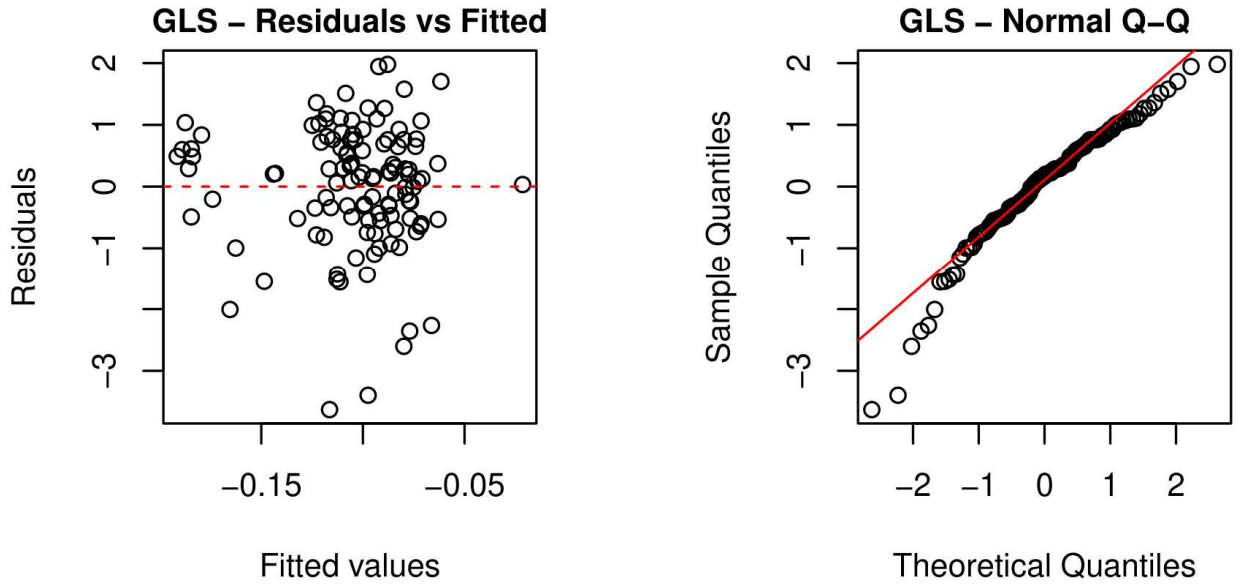


Figure C.3.2: GLS model with a combined variance structure showed decreased heteroscedasticity (left panel), and reduced deviations from normality (right panel)

C.3.2. Model Selection

Table **Error! No text of specified style in document.**C.3.5: : Model Comparison of Variance Structures when Predicting Hip Flexor Impulse in Pre-Swing from Group, Time, and Their Interaction

model	df	logLik	AIC	ΔAIC
power variance	15	231.42	-432.84	0.00
combined variance	17	232.97	-431.94	0.90
exponential variance	15	226.89	-423.77	9.07
group variance	16	219.27	-406.54	26.30
constant variance	14	194.59	-361.17	71.67

Model Coefficients

Table C.3.6: Regression Coefficients of Model Predicting Hip Flexor Moment Impulse in Pre-Swing Phase from SEMLS Group, Time, and Their Interaction, when Controlling for Other Covariates

Term	Estimate	CI	*p*	β
(Intercept)	-0.08	[-0.10, -0.07]	0.000	0.56
GroupTDR-B	-0.10	[-0.17, -0.02]	0.011	-1.62
GroupTDFR-U	0.01	[-0.01, 0.02]	0.361	-0.07
TimePost	0.01	[-0.01, 0.03]	0.431	-0.16
Normalized Speed	0.00	[-0.02, 0.02]	0.972	0.11
Time since surgery (months)	0.00	[0.00, 0.00]	0.202	-0.24
Age	0.02	[0.01, 0.02]	0.000	0.93
Mass	0.00	[0.00, 0.00]	0.072	0.14
sexF	-0.01	[-0.02, 0.01]	0.257	-0.20
GroupTDR-B:TimePost	0.07	[0.00, 0.15]	0.068	1.20
GroupTDFR-U:TimePost	-0.02	[-0.04, 0.01]	0.160	-0.16
GroupTDR-B:Age	-0.01	[-0.02, -0.01]	0.000	-0.96
GroupTDFR-U:Age	-0.01	[-0.02, -0.01]	0.000	-0.85

C.4. Sum of Lower Body Net Joint Work

C.4.1. Model Assumption Checks

Linearity of baseline effect (spline check)

Table **Error! No text of specified style in document.**C.4.1: Goodness-of-Fit Comparison (AIC and ANOVA) of Linear and Spline Models Predicting Sum of Lower-Body Joints Net Work from SEMLS Group, Time (Pre- vs. Post- Surgery),and their Interaction

Term	Model	Df	AIC	ΔAIC	*F*	*p*
All terms linear	Base	12	964.61			
Normalized Speed	Spline_df2	13	966.20	1.59	0.37	.545
Normalized Speed	Spline_df3	14	968.21	3.60	0.18	.837
Normalized Speed	Spline_df4	15	967.12	2.51	1.04	.379
Time since surgery (months)	Spline_df2	13	966.61	2.00	0.00	.986
Time since surgery (months)	Spline_df3	14	968.61	4.00	0.00	1.000
Time since surgery (months)	Spline_df4	15	970.40	5.78	0.06	.979
Age	Spline_df2	13	966.57	1.96	0.04	.849
Age	Spline_df3	14	967.33	2.72	0.57	.567
Age	Spline_df4	15	969.60	4.99	0.30	.827
Body Mass	Spline_df2	13	965.64	1.02	0.88	.351
Body Mass	Spline_df3	14	966.66	2.05	0.87	.421
Body Mass	Spline_df4	15	968.81	4.20	0.53	.661

Note. ΔAIC = Difference in Akaike information criterion relative to the best-fitting model. Significance: *** $p < 0.001$, ** $p < 0.01$, * $p < 0.05$.

Homogeneity of slopes (Group × Baseline interaction test)

Table C.4.2: Homogeneity-of-Slopes Test: AIC and ANOVA Results for Group–Predictor Interaction in the Group × Time Model Testing Pre-to-Post Change in Sum of Lower-Body Joints Net Work

Term	AIC_Base	AIC_Int	ΔAIC	ANOVA p
Normalized Speed	964.61	968.19	3.57	.828
Time since surgery (months)	964.61	968.60	3.99	.994
Age	964.61	968.28	3.67	.862
Body Mass	**964.61**	**960.13**	**0.00**	**.023 ***
Sex (F)	960.13	962.29	2.16	.448

Note. AIC (Base) = model without the Group × Predictor interaction term; AIC (Int) = model with the interaction term. ΔAIC = difference relative to the Base model. *$p < .05$.

Normality, Homoscedasticity and variance structure comparison

Table **Error! No text of specified style in document.**C.4.3: Tests of Normality and Homogeneity of Variance. Residual Diagnostics of LM Model Predicting Sum of Lower-Body Joints Net Work from SEMLS Group, Time (Pre-vs. Post-Surgery), and their Interaction

Metric	Shapiro-Wilk W	Breusch-Pagan $df(12)$	Levene $F(5, 110)$
Test Statistic	0.29	15.70	1.67
p	$< .001$ ***	.205	.148

Table C.4.4: Tests of Normality and Homogeneity of Variance. Residual Diagnostics of GLS Model Predicting Sum of Lower-Body Joints Net Work from SEMLS Group, Time (Pre-vs. Post-Surgery), and their Interaction

Metric	Shapiro-Wilk W	Levene $F(5, 110)$
Test Statistic	0.69	0.36
p	$< .001$ ***	.877

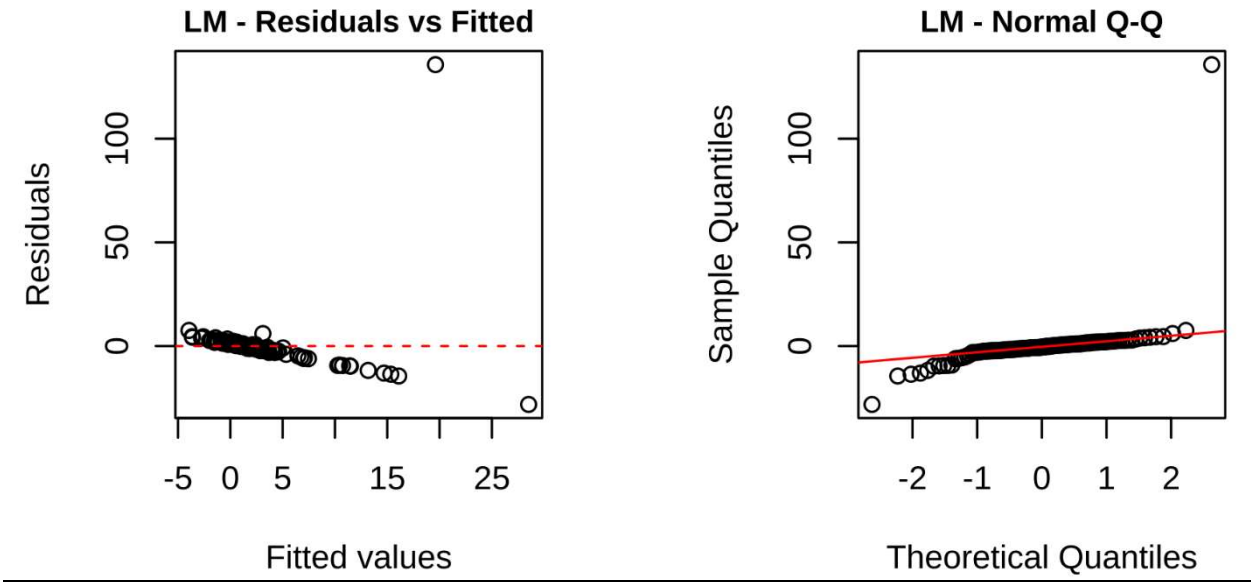
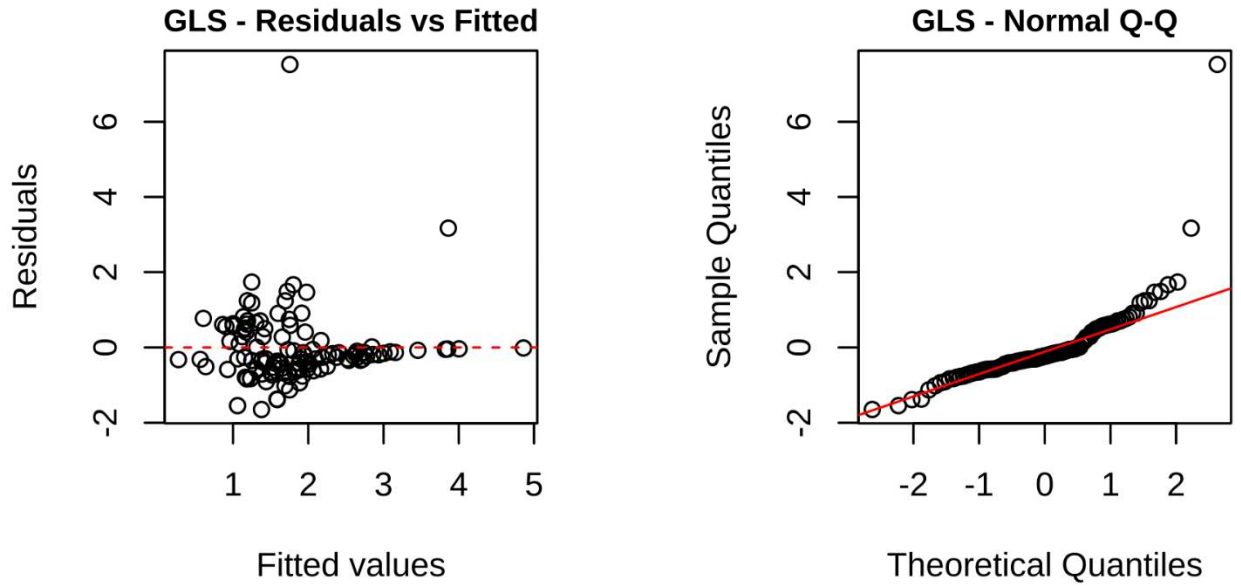


Figure C.4.1: Residuals–fitted and Q–Q plots showing heteroskedasticity (left panel), and departures from normality (right, Q-Q plot) in the linear regression model predicting sum of lower body net joint work



Residuals–fitted and Q–Q plots showing reduced heteroskedasticity (left panel), and departures from normality (right, Q-Q plot) in the GLS regression model predicting sum of lower body net joint work

C.4.2. Model Selection

Table C.4.5: Model Comparison of Variance Structures when Predicting Sum of Lower-Body Joints Net Work from Group, Time, and Their Interaction

model	df	logLik	AIC	ΔAIC
exponential variance	15	-180.30	390.60	0.00
combined variance	17	-209.26	452.51	61.92
group variance	16	-304.62	641.23	250.64
constant variance	14	-466.06	960.13	569.53

Model Coefficients

Table C.4.6: Regression Coefficients of Model Predicting Sum of Lower Body Net Joint Work from SEMLS Group, Time, and Their Interaction, when Controlling for Other Covariates

Term	Estimate	CI	*p*	β
(Intercept)	4.16	[2.05, 6.27]	0.000	-0.03
GroupTDR-B	-2.12	[-4.37, 0.14]	0.069	-0.06
GroupTDFR-U	-2.52	[-4.64, -0.41]	0.021	-0.05
TimePost	-0.95	[-1.60, -0.30]	0.005	-0.04
Normalized Speed	0.84	[0.42, 1.26]	0.000	0.02
Time since surgery (months)	-0.04	[-0.06, -0.02]	0.001	0.00
Age	0.01	[-0.04, 0.06]	0.619	-0.01
Mass	0.21	[0.02, 0.40]	0.033	0.06
sexF	-0.23	[-0.41, -0.05]	0.015	0.00
GroupTDR-B:TimePost	-0.15	[-1.18, 0.88]	0.776	0.01
GroupTDFR-U:TimePost	0.55	[-0.18, 1.28]	0.143	0.01
GroupTDR-B:Mass	-0.19	[-0.38, 0.00]	0.052	-0.04
GroupTDFR-U:Mass	-0.21	[-0.39, -0.02]	0.032	-0.05

C.5. Ratio Of Ankle To Hip Peak Propulsive Power

C.5.1. Model Assumption Checks

Linearity of baseline effect (spline check)

Table **Error! No text of specified style in document.**C.5.1: Goodness-of-Fit Comparison (AIC and ANOVA) of Linear and Spline Models Predicting Ratio of Ankle to Hip Peak Power from SEMLS Group, Time (Pre- vs. Post- Surgery),and their Interaction

Term	Model	Df	AIC	ΔAIC	*F*	*p*
All terms linear	Base	12	273.87			
Normalized Speed	Spline_df2	13	275.67	1.80	0.18	.672
Normalized Speed	Spline_df3	14	277.62	3.75	0.11	.894
Normalized Speed	Spline_df4	15	276.10	2.23	1.12	.344
Time since surgery (months)	**Spline_df2**	**13**	**270.34**	**0.00**	**5.08**	**.026 ***
Age	Spline_df2	14	272.00	1.65	0.31	.581
Age	**Spline_df3**	**15**	**266.53**	**0.00**	**3.55**	**.032 ***
Body Mass	Spline_df2	16	265.59	0.00	2.60	.110
Body Mass	Spline_df3	17	265.34	0.00	2.29	.107
Body Mass	Spline_df4	18	266.96	0.43	1.62	.189

Note. ΔAIC = Difference in Akaike information criterion relative to the best-fitting model. Significance: *** $p < 0.001$, ** $p < 0.01$, * $p < 0.05$.

Homogeneity of slopes (Group × Baseline interaction test)

Table **Error! No text of specified style in document.**C.5.2: Homogeneity-of-Slopes Test: AIC and ANOVA Results for Group–Predictor Interaction in the Group × Time Model Testing Pre-to-Post Change in Ratio of Ankle to Hip Peak Power

Term	AIC_Base	AIC_Int	ΔAIC	ANOVA *p*
Normalized Speed	266.53	268.47	1.94	.412
Body Mass	266.53	268.03	1.50	.340
Sex (F)	266.53	265.12	0.00	.097
NS_2[Time since surgery (months)]	266.53	269.79	3.26	.400
NS_3[Age]	266.53	274.97	8.44	.808

Note. AIC (Base) = model without the Group × Predictor interaction term; AIC (Int) = model with the interaction term. ΔAIC = difference relative to the Base model. *$p < .05$.

Normality, Homoscedasticity and variance structure comparison

Table C.5.3: Tests of Normality and Homogeneity of Variance. Residual Diagnostics of LM Model Predicting Ratio of Ankle to Hip Peak Power from SEMLS Group, Time (Pre-vs. Post-Surgery), and their Interaction

Metric	Shapiro-Wilk W	Breusch-Pagan $df(13)$	Levene $F(5, 110)$
Test Statistic	0.95	5.17	0.23
p	$< .001$ ***	.971	.950

C.5.2. Model Selection

Model Comparisons

Model Comparison of Variance Structures when Predicting Ratio of Ankle to Hip Peak Power from Group, Time, and Their Interaction

model	df	logLik	AIC	ΔAIC
constant variance	15	-118.28	266.55	0.00
power variance	16	-118.02	268.03	1.48
exponential variance	16	-118.05	268.10	1.55
group variance	17	-117.69	269.39	2.84
combined variance	18	-117.53	271.06	4.51

Model Coefficients

Table C.5.6: Regression Coefficients of GLS Model Predicting Ankle to Hip Peak Propulsive Power Generation Ratio from SEMLS Group, Time (Pre- vs. Post- Surgery), and their Interaction

Term	Estimate	CI	*p*	β
(Intercept)	-0.46	[-1.50, 0.59]	0.389	-2.47
GroupTDR-B	0.23	[-0.40, 0.86]	0.472	0.29
GroupTDFR-U	0.44	[-0.07, 0.95]	0.089	0.56
TimePost	0.49	[0.06, 0.92]	0.026	0.63
Normalized Speed	-0.37	[-0.95, 0.22]	0.218	-0.13
Mass	0.01	[-0.01, 0.03]	0.263	0.20
sexF	0.27	[-0.11, 0.65]	0.168	0.34
splines::ns(Time since surgery (months), df = 2)1	1.92	[0.40, 3.44]	0.014	2.45
splines::ns(Time since surgery (months), df = 2)2	-0.26	[-1.00, 0.48]	0.493	-0.33
splines::ns(Age, df = 3)1	-0.82	[-1.78, 0.14]	0.092	-1.05
splines::ns(Age, df = 3)2	0.66	[-1.06, 2.39]	0.447	0.85
splines::ns(Age, df = 3)3	-0.67	[-2.65, 1.31]	0.503	-0.86
GroupTDR-B:TimePost	-0.11	[-0.84, 0.63]	0.773	-0.14
GroupTDFR-U:TimePost	-0.10	[-0.73, 0.53]	0.755	-0.13

Appendix D: Knee Adduction Moment–Based Indicators of Joint Loading Models and Diagnostics

D.1. Peak KAM

D.1.1. Model Assumption Checks

Linearity of baseline effect (spline check)

Table **Error! No text of specified style in document.**: Goodness-of-Fit Comparison (AIC and ANOVA) of Linear and Spline Models Predicting Peak Kam from SEMLS Group, Time (Pre- vs. Post- Surgery),and their Interaction

Term	Model	Df	AIC	ΔAIC	*F*	*p*
All terms linear	Base	12	108.35			
Normalized Speed	Spline_df2	13	110.34	1.99	0.01	.925
Normalized Speed	Spline_df3	14	112.21	3.86	0.06	.938
Normalized Speed	Spline_df4	15	114.24	5.88	0.03	.992
Time since surgery (months)	Spline_df2	13	110.35	2.00	0.00	.965
Time since surgery (months)	Spline_df3	14	111.58	3.23	0.34	.710
Time since surgery (months)	Spline_df4	15	112.62	4.27	0.51	.676
Age	Spline_df2	13	108.87	0.52	1.33	.251
Age	Spline_df3	14	106.44	0.00	2.69	.073
Age	Spline_df4	15	107.05	0.00	2.21	.092
Body Mass	Spline_df2	13	106.56	0.00	3.46	.066
Body Mass	Spline_df3	14	108.55	0.20	1.71	.185
Body Mass	Spline_df4	15	109.58	1.23	1.43	.239

Note. ΔAIC = Difference in Akaike information criterion relative to the best-fitting model. Significance: *** $p < 0.001$, ** $p < 0.01$, * $p < 0.05$.

Homogeneity of slopes (Group × Baseline interaction test)

Table **Error! No text of specified style in document.**2: Homogeneity-of-Slopes Test: AIC and ANOVA Results for Group–Predictor Interaction in the Group × Time Model Testing Pre-to-Post Change in Peak KAM

Term	AIC_Base	AIC_Int	ΔAIC	ANOVA p
Normalized Speed	108.35	109.61	1.26	.296
Time since surgery (months)	108.35	112.21	3.86	.940
Age	108.35	106.47	0.00	.073
Body Mass	108.35	109.06	0.71	.232
Sex (F)	108.35	111.00	2.65	.549

Note. AIC (Base) = model without the Group × Predictor interaction term; AIC (Int) = model with the interaction term. ΔAIC = difference relative to the Base model. $*p < .05$.

Normality, Homoscedasticity and variance structure comparison

Table D.1.3: Tests of Normality and Homogeneity of Variance. Residual Diagnostics of LM Model Predicting Peak KAM from SEMLS Group, Time (Pre-vs. Post-Surgery), and their Interaction

Metric	Shapiro-Wilk W	Breusch-Pagan $df(10)$	Levene $F(5, 110)$
Test Statistic	0.79	7.96	2.38
p	$< .001$ ***	.633	.043 *

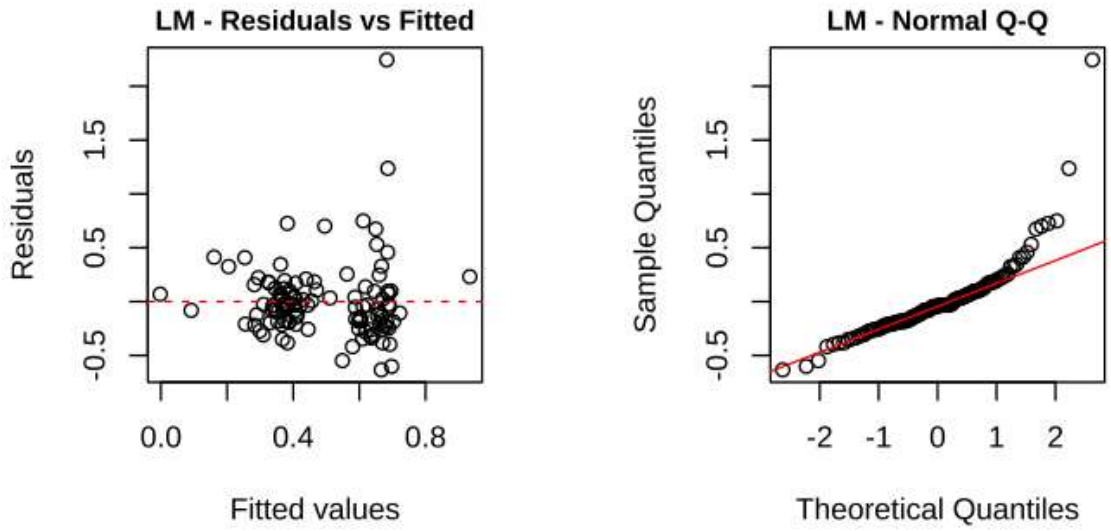


Figure D.1.1: Residuals versus fitted values (left) indicate no strong systematic pattern, suggesting an adequate linear mean structure, while the normal Q–Q plot (right) shows approximate normality with mild

deviation in the upper tail. Overall, these diagnostics support the appropriateness of the linear modeling assumptions for peak KAM

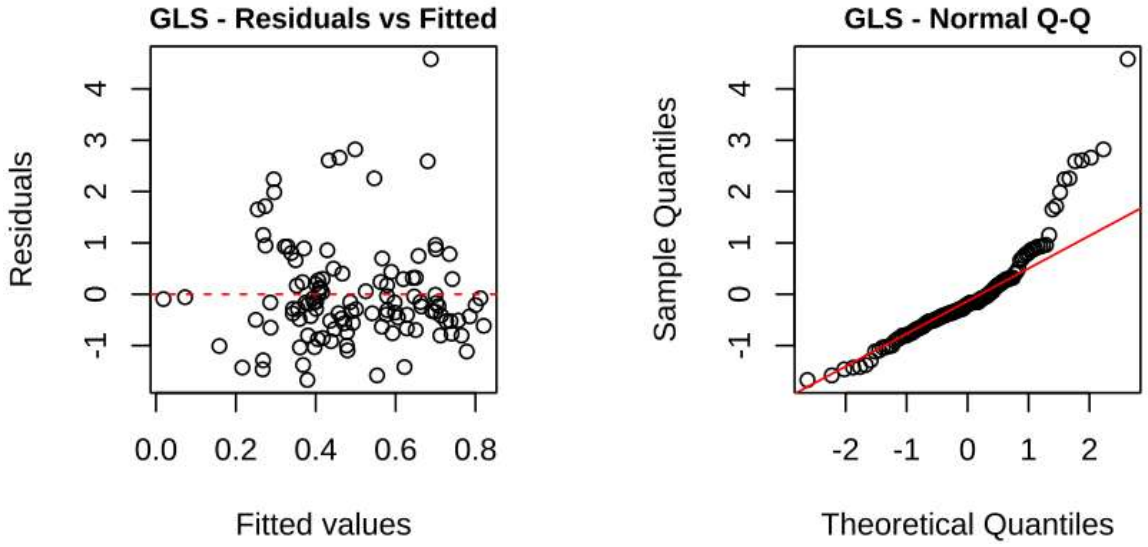


Figure D.1.2: Residuals versus fitted values (left) and normal Q–Q plot (right) are shown to assess model assumptions. The residuals exhibit no strong systematic structure across fitted values, and the Q–Q plot indicates approximate normality with mild upper-tail deviation.

D.1.2. Model Selection

Model Comparisons

Table D.1.5: Model Comparison of Variance Structures when Predicting Peak KAM from Group, Time, and Their Interaction

model	df	logLik	AIC	ΔAIC
exponential variance	13	-26.36	78.73	0.00
group variance	14	-34.95	97.90	19.17
constant variance	12	-42.18	108.35	29.62

Model Coefficients

Table D.1.6: Regression Coefficients of Model Predicting peak KAM from SEMLS Group, Time, and Their Interaction, when Controlling for Other Covariates

Term	Estimate	CI	*p*	β
(Intercept)	0.74	[0.51, 0.96]	0.000	0.45
GroupTDR-B	-0.21	[-0.49, 0.08]	0.153	-0.52
GroupTDFR-U	-0.09	[-0.38, 0.20]	0.542	-0.15
TimePost	-0.38	[-0.61, -0.14]	0.002	-0.82
Normalized Speed	0.23	[0.02, 0.44]	0.035	0.18
Time since surgery (months)	0.00	[-0.01, 0.01]	0.846	0.01
Age	-0.02	[-0.04, 0.00]	0.110	-0.22
Body Mass	0.01	[0.00, 0.01]	0.161	0.26
sexF	-0.05	[-0.17, 0.07]	0.388	0.01
GroupTDR-B:TimePost	0.14	[-0.17, 0.45]	0.384	0.40
GroupTDFR-U:TimePost	0.12	[-0.20, 0.44]	0.453	0.15

D.2. KAM Impulse

D.2.1. Model Assumption Checks

Linearity of baseline effect

Table D.2.1: Goodness-of-Fit Comparison (AIC and ANOVA) of Linear and Spline Models Predicting Kam Impulse from SEMLS Group, Time (Pre- vs. Post- Surgery),and their Interaction

Term	Model	Df	AIC	ΔAIC	*F*	*p*
All terms linear	Base	12	-110.56			
Normalized Speed	Spline_df2	13	-108.90	1.66	0.31	.581
Normalized Speed	Spline_df3	14	-106.89	3.66	0.15	.861
Normalized Speed	Spline_df4	15	-105.20	5.36	0.19	.904
Time since surgery (months)	Spline_df2	13	-108.56	2.00	0.00	.964
Time since surgery (months)	Spline_df3	14	-107.83	2.73	0.57	.569
Time since surgery (months)	Spline_df4	15	-106.10	4.45	0.46	.713
Age	Spline_df2	13	-109.24	1.31	0.62	.433
Age	**Spline_df3**	**14**	**-113.95**	**0.00**	**3.39**	**.038 ***
Body Mass	Spline_df2	15	-115.98	0.00	3.60	.060
Body Mass	Spline_df3	16	-114.19	0.00	1.88	.158
Body Mass	Spline_df4	17	-113.98	0.00	1.78	.156

Note. ΔAIC = Difference in Akaike information criterion relative to the best-fitting model. Significance: *** $p < 0.001$, ** $p < 0.01$, * $p < 0.05$

Homogeneity of slopes (Group × Baseline interaction test)

Table **Error! No text of specified style in document.**D.2.2: Homogeneity-of-Slopes Test: AIC and ANOVA Results for Group×Predictor Interaction in the Group × Time Model Testing Pre-to-Post Change in KAM Impulse

Term	AIC_Base	AIC_Int	ΔAIC	ANOVA p
Normalized Speed	-113.95	-114.63	0.00	.131
Time since surgery (months)	-113.95	-110.31	3.64	.856
Body Mass	-113.95	-113.48	0.47	.215
Sex (F)	-113.95	-110.14	3.81	.921
NS_3[Age]	-113.95	-111.82	2.13	.209

Note. AIC (Base) = model without the Group × Predictor interaction term; AIC (Int) = model with the interaction term. ΔAIC = difference relative to the Base model. *$p < .05$.

Normality, Homoscedasticity and variance structure comparison

Table **Error! No text of specified style in document.**D.2.3: Tests of Normality and Homogeneity of Variance. Residual Diagnostics of LM Model Predicting KAM Impulse from SEMLS Group, Time (Pre-vs. Post-Surgery), and their Interaction

Metric	Shapiro-Wilk W	Breusch-Pagan $df(12)$	Levene $F(5, 110)$
Test Statistic	0.94	15.04	2.30
p	$< .001$ ***	.239	.050

Table D.2.4: Tests of Normality and Homogeneity of Variance. Residual Diagnostics of GLS Model Predicting KAM Impulse from SEMLS Group, Time (Pre-vs. Post-Surgery), and their Interaction

Metric	Shapiro-Wilk W	Levene $F(5, 110)$
Test Statistic	0.95	1.80
p	$< .001$ ***	.118

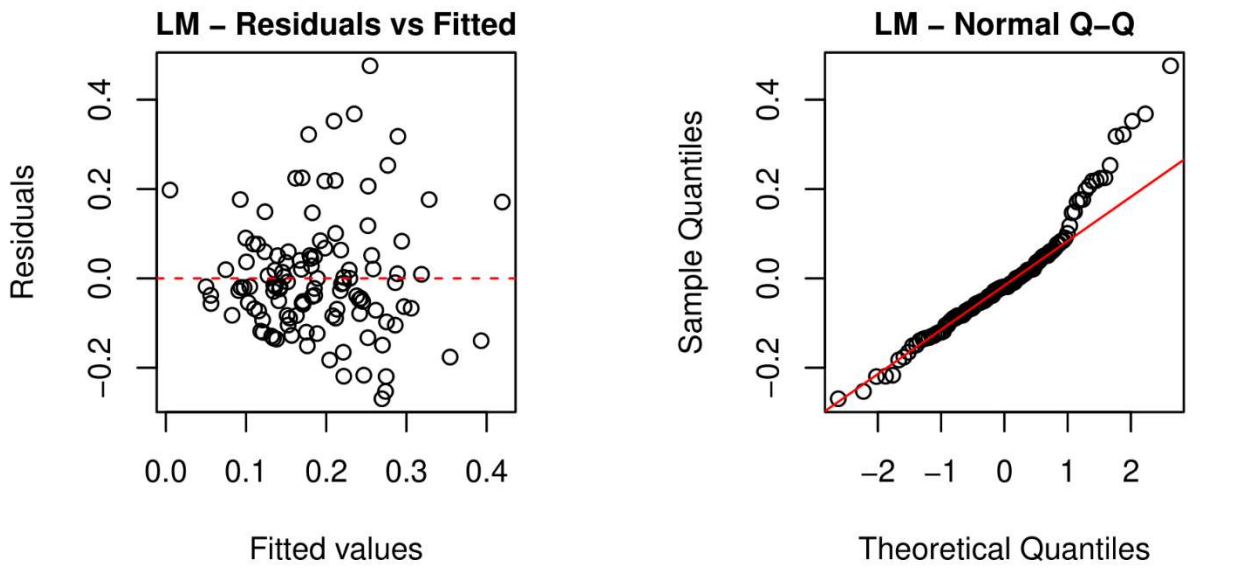


Figure D.2.1: Residuals versus fitted values show a relatively stable spread across fitted values, and the normal Q–Q plot indicates approximate normality with mild upper-tail deviation.

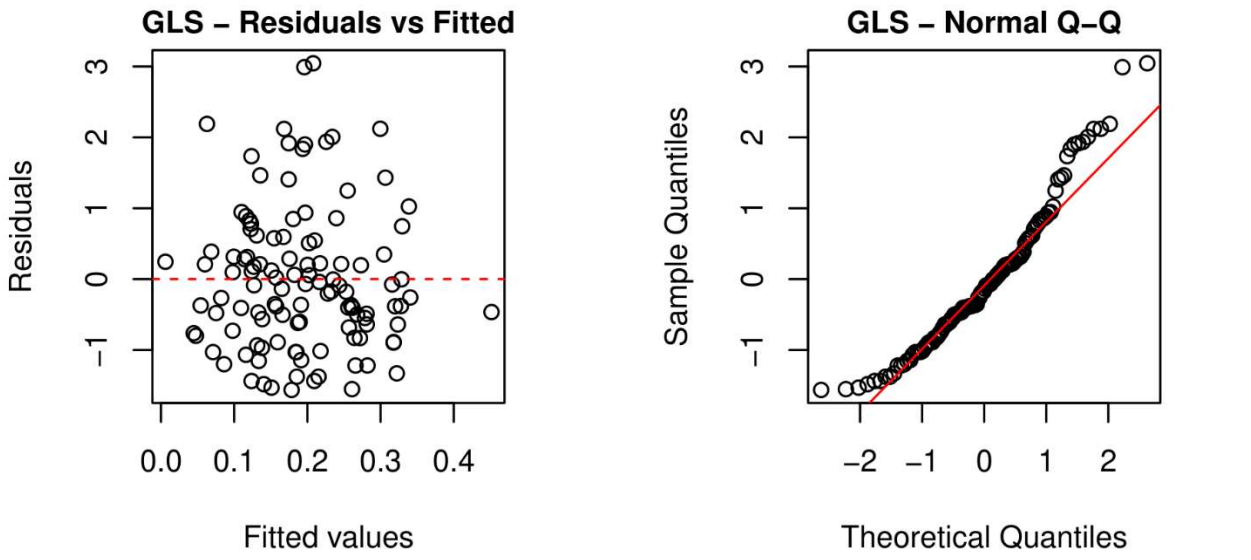


Figure D.2.2: Residuals versus fitted values show greater dispersion across fitted values, and the normal Q–Q plot indicates departures from normality in the upper tail.

D.2.2. Model Selection

Model Comparisons

Table D.2.5: Model Comparison of Variance Structures when Predicting KAM Impulse from Group, Time, and Their Interaction

model	df	logLik	AIC	ΔAIC
exponential variance	15	80.56	-131.13	0.00
constant variance	14	70.87	-113.75	17.38
group variance	16	71.03	-110.06	21.06

Model Coefficients

Table **Error! No text of specified style in document.**D.2.6:: Regression Coefficients of Model Predicting KAM Impulse from SEMLS Group, Time, and Their Interaction, when Controlling for Other Covariates

Term	Estimate	CI	*p*	β
(Intercept)	0.45	[0.32, 0.59]	0.000	1.53
GroupTDR-B	-0.11	[-0.20, -0.02]	0.022	-0.65
GroupTDFR-U	0.03	[-0.08, 0.13]	0.617	0.18
TimePost	-0.07	[-0.14, 0.01]	0.077	-0.40
Normalized Speed	0.04	[-0.05, 0.13]	0.394	0.06
Time since surgery (months)	0.01	[0.00, 0.01]	0.109	0.11
Body Mass	0.00	[0.00, 0.00]	0.511	0.14
sexF	-0.01	[-0.06, 0.04]	0.698	-0.03
splines::ns(Age, df = 3)1	0.08	[-0.07, 0.22]	0.297	0.26
splines::ns(Age, df = 3)2	-0.47	[-0.70, -0.23]	0.000	-2.88
splines::ns(Age, df = 3)3	-0.15	[-0.31, 0.02]	0.078	-0.99
GroupTDR-B:TimePost	0.01	[-0.09, 0.11]	0.827	0.11
GroupTDFR-U:TimePost	-0.06	[-0.18, 0.06]	0.307	-0.37

References

Adolfsen, S. E., Õunpuu, S., Bell, K. J., & DeLuca, P. A. (2007). Kinematic and kinetic outcomes after identical multilevel soft tissue surgery in children with cerebral palsy. *Journal of Pediatric Orthopaedics*, *27*(6), 658–667. https://doi.org/10.1097/BPO.0b013e3180dca114

Akaike, H. (1998). A New Look at the Statistical Model Identification. In E. Parzen, K. Tanabe, & G. Kitagawa (Eds.), *Selected Papers of Hirotugu Akaike* (pp. 215–222). Springer. https://doi.org/10.1007/978-1-4612-1694-0_16

Almoajil, H., Dawes, H., Hopewell, S., Toye, F., Jenkinson, C., & Theologis, T. (2020). Development of a core outcome set for lower limb orthopaedic surgical interventions in ambulant children and young people with cerebral palsy: A study protocol. *BMJ Open*, *10*(3), e034744. https://doi.org/10.1136/bmjopen-2019-034744

Almoajil, H., Theologis, T., Dawes, H., Pierce, J., Meaney, A., Baklouti, A., Poverini, L., Hopewell, S., & Toye, F. (2022). *Exploring the factors that influence stakeholders' expectations and subsequent perception of lower limb orthopaedic surgical outcomes for ambulant children with cerebral palsy-a qualitative study*. https://doi.org/10.1080/09638288.2021.2025272

Alvarez, C., De Vera, M., Beauchamp, R., Ward, V., & Black, A. (2007). Classification of idiopathic toe walking based on gait analysis: Development and application of the ITW severity classification. *Gait & Posture*, *26*(3), 428–435. https://doi.org/10.1016/j.gaitpost.2006.10.011

Amen, J., ElGebeily, M., El.Mikkawy, DaliaM. E., Yousry, A., & El-Sobky, T. (2018). Single-event multilevel surgery for crouching cerebral palsy children: Correlations with quality

of life and functional mobility. *Journal of Musculoskeletal Surgery and Research*, *2*(4), 148. https://doi.org/10.4103/jmsr.jmsr_48_18

Anan, M., Tokuda, K., Tanimoto, K., & Sawada, T. (2024). The relationship between knee flexion excursion and mechanical stress during gait in medial knee osteoarthritis. *Clinical Biomechanics*, *112*. https://doi.org/10.1016/j.clinbiomech.2024.106180

Andriacchi, T. P., Mündermann, A., Smith, R. L., Alexander, E. J., Dyrby, C. O., & Koo, S. (2004). A framework for the in vivo pathomechanics of osteoarthritis at the knee. *Annals of Biomedical Engineering*, *32*(3), 447–457. https://doi.org/10.1023/B:ABME.0000017541.82498.37

Arnold, A. S., Liu, M. Q., Schwartz, M. H., Õunpuu, S., & Delp, S. L. (2006). The role of estimating muscle-tendon lengths and velocities of the hamstrings in the evaluation and treatment of crouch gait. *Gait and Posture*, *23*(3), 273–281. https://doi.org/10.1016/j.gaitpost.2005.03.003

Asakawa, D. S., Blemker, S. S., Gold, G. E., & Delp, S. L. (2002). In vivo motion of the rectus femoris muscle after tendon transfer surgery. *Journal of Biomechanics*, *35*(8), 1029–1037. https://doi.org/10.1016/S0021-9290(02)00048-9

Astephen, J. L., Deluzio, K. J., Caldwell, G. E., & Dunbar, M. J. (2008). Biomechanical changes at the hip, knee, and ankle joints during gait are associated with knee osteoarthritis severity. *Journal of Orthopaedic Research*, *26*(3), 332–341. https://doi.org/10.1002/jor.20496

Badawi, N., Watson, L., Petterson, B., Blair, E., Slee, J., Haan, E., & Stanley, F. (1998). What constitutes cerebral palsy? *Developmental Medicine and Child Neurology*, *40*(8), 520–527. https://doi.org/10.1111/j.1469-8749.1998.tb15410.x

Baker, R., Esquenazi, A., Benedetti, M. G., & Desloovere, K. (2016). Gait analysis: Clinical facts. *European Journal of Physical and Rehabilitation Medicine*, *52*(4), 560–574.

Barnett, A. G., van der Pols, J. C., & Dobson, A. J. (2005). Regression to the mean: What it is and how to deal with it. *International Journal of Epidemiology*, *34*(1), 215–220. https://doi.org/10.1093/ije/dyh299

Barton, G. J., Hawken, M. B., Holmes, G., & Schwartz, M. H. (2015). A gait index may underestimate changes of gait: A comparison of the Movement Deviation Profile and the Gait Deviation Index. *Computer Methods in Biomechanics and Biomedical Engineering*, *18*(1), 57–63. https://doi.org/10.1080/10255842.2013.776549

Bell, K. J., Õunpuu, S., DeLuca, P. A., & Romness, M. J. (2002). Natural Progression of Gait in Children With Cerebral Palsy. *Journal of Pediatric Orthopaedics*, *22*(5), 677.

Bennell, K. L., Bowles, K.-A., Wang, Y., Cicuttini, F., Davies-Tuck, M., & Hinman, R. S. (2011). Higher dynamic medial knee load predicts greater cartilage loss over 12 months in medial knee osteoarthritis. *Annals of the Rheumatic Diseases*, *70*(10), 1770–1774. https://doi.org/10.1136/ard.2010.147082

Beveridge, B., Feltracco, D., Struyf, J., Strauss, E., Dang, S., Phelan, S., Wright, F. V., & Gibson, B. E. (2015). "You gotta try it all": Parents' Experiences with Robotic Gait Training for their Children with Cerebral Palsy. *Physical & Occupational Therapy In Pediatrics*, *35*(4), 327–341. https://doi.org/10.3109/01942638.2014.990547

Bjornson, K. F., Belza, B., Kartin, D., Logsdon, R., McLaughlin, J., & Thompson, E. A. (2008). The Relationship of Physical Activity to Health Status and Quality of Life in Cerebral Palsy. *Pediatric Physical Therapy : The Official Publication of the Section on Pediatrics*

of the American Physical Therapy Association, *20*(3), 247–253. https://doi.org/10.1097/PEP.0b013e318181a959

Bjornson, K. F., Zhou, C., Stevenson, R., & Christakis, D. A. (2013). Capacity to participation in cerebral palsy: Evidence of an indirect path via performance. *Archives of Physical Medicine and Rehabilitation*, *94*(12), 2365–2372. https://doi.org/10.1016/j.apmr.2013.06.020

Böhm, H., & Döderlein, L. (2012). Gait asymmetries in children with cerebral palsy: Do they deteriorate with running? *Gait and Posture*, *35*(2), 322–327. https://doi.org/10.1016/j.gaitpost.2011.10.003

Box, G. E. P. (1954). Some Theorems on Quadratic Forms Applied in the Study of Analysis of Variance Problems, I. Effect of Inequality of Variance in the One-Way Classification. *The Annals of Mathematical Statistics*, *25*(2), 290–302.

Boyer, E. R., Duffy, E. A., Walt, K., Muñoz Hamen, A., Healy, M. T., Schwartz, M. H., & Novacheck, T. F. (2021). Long-term functional outcomes after an external femoral derotation osteotomy in individuals with cerebral palsy. *Gait and Posture*, *87*(March), 184–191. https://doi.org/10.1016/j.gaitpost.2021.04.029

Bretz, F., Hothorn, T., & Westfall, P. (2016). *Multiple Comparisons Using R*. Chapman and Hall/CRC. https://doi.org/10.1201/9781420010909

Brisson, N. M., Gatti, A. A., Damm, P., Duda, G. N., & Maly, M. R. (2021). Association of Machine Learning–Based Predictions of Medial Knee Contact Force With Cartilage Loss Over 2.5 Years in Knee Osteoarthritis. *Arthritis & Rheumatology*, *73*(9), 1638–1645. https://doi.org/10.1002/art.41735

Bulea, T. C., Stanley, C. J., & Damiano, D. L. (2017). Part 2: Adaptation of gait kinematics in unilateral cerebral palsy demonstrates preserved independent neural control of each limb. *Frontiers in Human Neuroscience*, *11*(February), 1–12. https://doi.org/10.3389/fnhum.2017.00050

Campbell, J., & Ball, J. (1978). Energetics of walking in cerebral palsy. *The Orthopedic Clinics of North America*, *9*(2), 374–377.

Carollo, J. J., Henley, J., Krzak, J., Zucker-Levin, A., Long, J., Õunpuu, S., Pierce, W., Pierz, K., Schwabe, A. L., Stout, J. L., Whitaker, A. T., & Alderink, G. (2025). The Commission for Motion Laboratory Accreditation (CMLA): History, process, and peer-review to assure excellence in clinical motion analysis. *Gait & Posture*, *121*, 258–265. https://doi.org/10.1016/j.gaitpost.2025.05.013

Chakraborty, S., Nandy, A., & Kesar, T. M. (2020). Gait deficits and dynamic stability in children and adolescents with cerebral palsy: A systematic review and meta-analysis. *Clinical Biomechanics*, *71*, 11–23. https://doi.org/10.1016/j.clinbiomech.2019.09.005

Chang, C., Chen, C., Yeh, K., & Kuo, K. N. (2020). Association of age in motor function outcomes after multilevel myofascial release in children with cerebral palsy. *Biomedical Journal*, *43*(6), 469–475. https://doi.org/10.1016/j.bj.2019.10.003

Chang, F., Rhodes, J. T., & Carollo, J. J. (2010). The Role of Gait Analysis in Treating Gait Abnormalities in Cerebral Palsy. *Orthopedic Clinics of North America*, *41*(4), 489–506. https://doi.org/10.1016/j.ocl.2010.06.009

Cimolin, V., Galli, M., Vimercati, S. L., & Albertini, G. (2011a). Use of the Gait Deviation Index for the assessment of gastrocnemius fascia lengthening in children with Cerebral

Palsy. *Research in Developmental Disabilities*, *32*(1), 377–381. https://doi.org/10.1016/j.ridd.2010.10.017

Cimolin, V., Piccinini, L., Portinaro, N., Turconi, A. C., Albonico, S., Crivellini, M., & Galli, M. (2011b). The Effects of Femoral Derotation Osteotomy in Cerebral Palsy: A Kinematic and Kinetic Study. *HIP International*, *21*(6), 657–664. https://doi.org/10.5301/HIP.2011.8758

Cook, R. E., Schneider, I., Hazlewood, M. E., Hillman, S. J., & Robb, J. E. (2003). Gait analysis alters decision-making in cerebral palsy. *Journal of Pediatric Orthopaedics*, *23*(3), 292–295. https://doi.org/10.1097/01241398-200305000-00004

Cuomo, A. V., Gamradt, S. C., Kim, C. O., Pirpiris, M., Gates, P. E., McCarthy, J. J., & Otsuka, N. Y. (2007). Health-related quality of life outcomes improve after multilevel surgery in ambulatory children with cerebral palsy. *Journal of Pediatric Orthopedics*, *27*(6), 653–657. https://doi.org/10.1097/BPO.0b013e3180dca147

Damiano, D. L. (2014). Meaningfulness of mean group results for determining the optimal motor rehabilitation program for an individual child with cerebral palsy. *Developmental Medicine & Child Neurology*, *56*(12), 1141–1146. https://doi.org/10.1111/dmcn.12505

Davids, J. R., Cung, N. Q., Chen, S., Sison-Williamson, M., & Bagley, A. M. (2019). Control of Walking Speed in Children With Cerebral Palsy. *Journal of Pediatric Orthopaedics*, *39*(8), 429–435. https://doi.org/10.1097/BPO.0000000000000978

Davids, J. R., Oeffinger, D. J., Bagley, A. M., Sison-Williamson, M., & Gorton, G. (2015). Relationship of Strength, Weight, Age, and Function in Ambulatory Children With Cerebral Palsy. *Journal of Pediatric Orthopaedics*, *35*(5), 523–529. https://doi.org/10.1097/BPO.0000000000000320

Davids, J. R., Rogozinski, B. M., Hardin, J. W., & Davis, R. B. (2011). Ankle Dorsiflexor Function After Plantar Flexor Surgery in Children with Cerebral Palsy. *Journal of Bone and Joint Surgery*, *93*(23), e138. https://doi.org/10.2106/JBJS.K.00239

Davis, E. M., Hubley-Kozey, C. L., Landry, S. C., Ikeda, D. M., Stanish, W. D., & Wilson, J. L. A. (2019). Longitudinal evidence links joint level mechanics and muscle activation patterns to 3-year medial joint space narrowing. *Clinical Biomechanics*, *61*, 233–239. https://doi.org/10.1016/j.clinbiomech.2018.12.016

Delp, S. L., Statler, K., & Carroll, N. C. (1995). Preserving plantar flexion strength after surgical treatment for contracture of the triceps surae: A computer simulation study. *Journal of Orthopaedic Research*, *13*(1), 96–104. https://doi.org/10.1002/jor.1100130115

DeLuca, P. A., Davis, R. B., Õunpuu, S., Rose, S., & Sirkin, R. (1997). Alterations in Surgical Decision Making in Patients with Cerebral Palsy Based on Three-Dimensional Gait Analysis. *Journal of Pediatric Orthopaedics*, *17*(5), 608.

Desailly, E., Badina, A., & Khouri, N. (2020). Kinematics after unilateral femoral derotation osteotomy in children with diplegic cerebral palsy. *Orthopaedics & Traumatology: Surgery & Research*, *106*(7), 1325–1331. https://doi.org/10.1016/j.otsr.2019.11.032

Dimakopoulos, R., Syrogiannopoulos, G., Grivea, I., Dailiana, Z., Youroukos, S., & Spinou, A. (2022). Kinematic and Temporospatial Changes in Children with Cerebral Palsy during the Initial Stages of Gait Development. *Developmental Neurorehabilitation*, *25*(1), 10–18. https://doi.org/10.1080/17518423.2021.1914763

Dobson, F., Morris, M. E., Baker, R., & Graham, H. K. (2007). Gait classification in children with cerebral palsy: A systematic review. *Gait Posture*, *25*(1), 140–152. https://doi.org/10.1016/j.gaitpost.2006.01.003

Dreher, T., Buccoliero, T., Wolf, S. I., Heitzmann, D., Gantz, S., Braatz, F., & Wenz, W. (2012). Long-Term Results After Gastrocnemius-Soleus Intramuscular Aponeurotic Recession as a Part of Multilevel Surgery in Spastic Diplegic Cerebral Palsy. *Journal of Bone and Joint Surgery*, *94*(7), 627–637. https://doi.org/10.2106/JBJS.K.00096

Dreher, T., Thomason, P., Švehlík, M., Döderlein, L., Wolf, S. I., Putz, C., Uehlein, O., Chia, K., Steinwender, G., Sangeux, M., & Graham, H. K. (2018). Long-term development of gait after multilevel surgery in children with cerebral palsy: A multicentre cohort study. *Developmental Medicine and Child Neurology*, *60*(1), 88–93. https://doi.org/10.1111/dmcn.13618

Dumas, R., Chèze, L., & Verriest, J.-P. (2007). Adjustments to McConville et al. And Young et al. Body segment inertial parameters. *Journal of Biomechanics*, *40*(3), 543–553. https://doi.org/10.1016/j.jbiomech.2006.02.013

Escalda, C., Ferreira, M., Mateus, R., João, F., & Veloso, A. (2023). Knee joint contact forces to assess the effect of single event multi level surgery over time in crouch gait. *Gait & Posture*, *106*, S56–S57. https://doi.org/10.1016/j.gaitpost.2023.07.070

Fazlali, H., Sadeghi, H., Sadeghi, S., Ojaghi, M., & Allard, P. (2020). Comparison of four methods for determining the cut-off frequency of accelerometer signals in able-bodied individuals and ACL ruptured subjects. *Gait & Posture*, *80*, 217–222. https://doi.org/10.1016/j.gaitpost.2020.06.009

Foroughi, N., Smith, R., & Vanwanseele, B. (2009). The association of external knee adduction moment with biomechanical variables in osteoarthritis: A systematic review. *The Knee*, *16*(5), 303–309. https://doi.org/10.1016/j.knee.2008.12.007

Fox, M. D., Reinbolt, J. A., Õunpuu, S., & Delp, S. L. (2009). Mechanisms of improved knee flexion after rectus femoris transfer surgery. *Journal of Biomechanics*, *42*(5), 614–619. https://doi.org/10.1016/j.jbiomech.2008.12.007

Frank, T. D., Dotov, D. G., & Turvey, M. T. (2010). A Canonical-Dissipative Approach to Control and Coordination in the Complex System Agent-Task-Environment. In P. Danion Frederic & P. Latash Mark (Eds.), *Motor Control: Theories, Experiments, and Applications* (p. 0). Oxford University Press. https://doi.org/10.1093/acprof:oso/9780195395273.003.0003

Franki, I., De Cat, J., Deschepper, E., Molenaers, G., Desloovere, K., Himpens, E., Vanderstraeten, G., & Van den Broeck, C. (2014). A clinical decision framework for the identification of main problems and treatment goals for ambulant children with bilateral spastic cerebral palsy. *Research in Developmental Disabilities*, *35*(5), 1160–1176. https://doi.org/10.1016/j.ridd.2014.01.025

Fregly, B. J. (2021). A Conceptual Blueprint for Making Neuromusculoskeletal Models Clinically Useful. *Applied Sciences*, *11*(5), 2037. https://doi.org/10.3390/app11052037

French, Z. P., Torres, R. V., & Whitney, D. G. (2019). Elevated prevalence of osteoarthritis among adults with cerebral palsy. *Journal of Rehabilitation Medicine*, *51*(8), 575–581. https://doi.org/10.2340/16501977-2582

Fritz, S., & Lusardi, M. (2009). White Paper: "Walking Speed: the Sixth Vital Sign": *Journal of Geriatric Physical Therapy*, *32*(2), 2–5. https://doi.org/10.1519/00139143-200932020-00002

Gage, J. R. (1990). Surgical treatment of knee dysfunction in cerebral palsy. *Clinical Orthopaedics and Related Research*, *253*, 45–54.

Gage, J. R. (1993). Gait analysis. An essential tool in the treatment of cerebral palsy. *Clinical Orthopaedics and Related Research*, *288*, 126–134.

Gage, J. R., & Novacheck, T. F. (2001). An update on the treatment of gait problems in cerebral palsy. *Journal of Pediatric Orthopedics. Part B*, *10*(4), 265–274.

Gage, J. R., Schwartz, M. H., Koop, S. E., & Novacheck, T. F. (2009a). Patient assessment—Introduction and overview. *The Identification and Treatment of Gait Problems in Cerebral Palsy*, *58*(180), 181–285. https://doi.org/10.1001/archpedi.1965.02090030355031

Gage, J. R., Schwartz, M. H., Koop, S. E., & Novacheck, T. F. (2009b). *The Identification and Treatment of Gait Problems in Cerebral Palsy*. Wiley. https://books.google.com/books?id=PiiDMzb551sC

Gibson, B. E., Teachman, G., Wright, V., Fehlings, D., Young, N. L., & McKeever, P. (2012). Children's and parents' beliefs regarding the value of walking: Rehabilitation implications for children with cerebral palsy. *Child: Care, Health and Development*, *38*(1), 61–69. https://doi.org/10.1111/j.1365-2214.2011.01271.x

Gómez-Pérez, C., Font-Llagunes, J. M., Martori, J. C., & Vidal Samsó, J. (2019). Gait parameters in children with bilateral spastic cerebral palsy: A systematic review of randomized controlled trials. *Developmental Medicine and Child Neurology*, *61*(7), 770–782. https://doi.org/10.1111/dmcn.14108

Gómez-Pérez, C., Vidal Samsó, J., Puig Diví, A., Medina Casanovas, J., Font-Llagunes, J. M., & Martori, J. C. (2023). Relationship between spatiotemporal parameters and clinical outcomes in children with bilateral spastic cerebral palsy: Clinical interpretation

proposal. *Journal of Orthopaedic Science*, *28*(5), 1136–1142. https://doi.org/10.1016/j.jos.2022.08.011

Gough, M., Eve, L. C., Robinson, R. O., & Shortland, A. P. (2004). Short-term outcome of multilevel surgical intervention in spastic diplegic cerebral palsy compared with the natural history. *Developmental Medicine & Child Neurology*, *46*(02). https://doi.org/10.1017/S0012162204000192

Graham, H. K., Rosenbaum, P., Paneth, N., Dan, B., Lin, J.-P., Damiano, D. L., Becher, J. G., Gaebler-Spira, D., Colver, A., Reddihough, D. S., Crompton, K. E., & Lieber, R. L. (2016). Cerebral palsy. *Nature Reviews Disease Primers*, *2*(1), 15082. https://doi.org/10.1038/nrdp.2015.82

Gresits, O. Z., Vezér, M., Engh, M. A., Szabó, B., Molnár, Z., Hegyi, P., & Terebessy, T. (2026). Impact of femoral derotation osteotomy on gait in ambulatory children with cerebral palsy: A systematic review and meta-analysis. *Brazilian Journal of Physical Therapy*, *30*(1), 101257. https://doi.org/10.1016/j.bjpt.2025.101257

Haberfehlner, H., Jaspers, R. T., Rutz, E., Harlaar, J., van der Sluijs, J. A., Witbreuk, M. M., van Hutten, K., Romkes, J., Freslier, M., Brunner, R., Becher, J. G., Maas, H., & Buizer, A. I. (2018). Outcome of medial hamstring lengthening in children with spastic paresis: A biomechanical and morphological observational study. *PLoS ONE*, *13*(2), e0192573. https://doi.org/10.1371/journal.pone.0192573

Hamill, J., Selbie, S., & Kepple, T. (2013). Three-Dimensional Kinematics. In *Research Methods in Biomechanics, 2E:* Human Kinetics. https://books.google.com/books?id=gRn8AAAAQBAJ

Hanson, A. M., Nadeau, J. T., Ciccodicola, E. M., Rethlefsen, S. A., Wren, T. A. L., & Kay, R. M. (2025). Impact of Age on Gait Deviations and Function After Single Event Multilevel Surgery in Children With Cerebral Palsy. *Journal of Pediatric Orthopaedics*, *45*(7), 416. https://doi.org/10.1097/BPO.0000000000002973

HAS-Motion. (n.d.). *Visual3D* (Version 2024.03.3) [Computer software]. HAS-Motion.

Hausdorff, J. M., Zemany, L., Peng, C.-K., & Goldberger, A. L. (1999). Maturation of gait dynamics: Stride-to-stride variability and its temporal organization in children. *Journal of Applied Physiology*, *86*(3), 1040–1047. https://doi.org/10.1152/jappl.1999.86.3.1040

Hebda-Boon, A., Tan, X.-L., Tillmann, R., Shortland, A. P., Firth, G. B., & Morrissey, D. (2023). The impact of instrumented gait analysis on decision-making in the interprofessional management of cerebral palsy: A scoping review. *European Journal of Paediatric Neurology*, *42*, 60–70. https://doi.org/10.1016/j.ejpn.2022.11.007

Hedges, L. V. (1981). Distribution Theory for Glass's Estimator of Effect Size and Related Estimators. *Journal of Educational Statistics*, *6*(2), 107–128. https://doi.org/10.2307/1164588

Herskind, A., Ritterband-Rosenbaum, A., Willerslev-Olsen, M., Lorentzen, J., Hanson, L., Lichtwark, G., & Nielsen, J. B. (2016). Muscle growth is reduced in 15-month-old children with cerebral palsy. *Developmental Medicine & Child Neurology*, *58*(5), 485–491. https://doi.org/10.1111/dmcn.12950

Hicks, J. L., Delp, S. L., & Schwartz, M. H. (2011). Can biomechanical variables predict improvement in crouch gait? *Gait and Posture*, *34*(2), 197–201. https://doi.org/10.1016/j.gaitpost.2011.04.009

Himpens, E., Franki, I., Geerts, D., Tack, R., Van Der Looven, R., & Van Den Broeck, C. (2013). Quality of life in youngsters with cerebral palsy after single-event multilevel surgery. *European Journal of Paediatric Neurology : EJPN : Official Journal of the European Paediatric Neurology Society*, *17*(4), 401–406. https://doi.org/10.1016/J.EJPN.2013.02.001

Hobani, S., Alhakami, A. M., Uddin, S., Ahmad, F., Alsobayel, H., Hobani, S., Alhakami, A. M., Uddin, S., Ahmad, F., & Alsobayel, H. (2022). Perceived Application and Barriers for Gait Assessment in Physical Therapy Practice in Saudi Arabia. *Life*, *13*(1). https://doi.org/10.3390/life13010050

Hochberg, Y., & Tamhane, A. C. (1987). *Multiple Comparison Procedures*. Wiley.

Hof, A. L. (1996). Scaling gait data to body size. *Gait & Posture*, *4*(3), 222–223. https://doi.org/10.1016/0966-6362(95)01057-2

Holm, S. (1979). A Simple Sequentially Rejective Multiple Test Procedure. *Scandinavian Journal of Statistics*, *6*(2), 65–70.

Horsch, A., Petzinger, L., Deisenhofer, J., Ghandour, M., Klotz, M., Renkawitz, T., & Putz, C. (2024). The Impact of Operative Correction of Equinus in Cerebral Palsy on Gait Patterns. *Foot & Ankle International*, *45*(2), 130–140. https://doi.org/10.1177/10711007231217273

Hsu, A. T., Perry, J., Gronley, J. K., & Hislop, H. J. (1993). Quadriceps force and myoelectric activity during flexed knee stance. *Clinical Orthopaedics and Related Research*, *288*, 254–262.

Hsu, J. (1996). *Multiple Comparisons: Theory and Methods*. Chapman and Hall/CRC. https://doi.org/10.1201/b15074

Hulleck, A. A., Menoth Mohan, D., Abdallah, N., El Rich, M., & Khalaf, K. (2022). Present and future of gait assessment in clinical practice: Towards the application of novel trends and technologies. *Frontiers in Medical Technology*, *4*. https://doi.org/10.3389/fmedt.2022.901331

Igura, R., Nakamura, J., & Anan, M. (2025). The Impact of Increased Knee Joint Flexion Angle During Loading Response on Mechanical Load of the Knee Joint in Healthy Elderly Individuals: A Cross-Sectional Study. *Cureus*. https://doi.org/10.7759/cureus.90117

Johnson, D. C., Damiano, D. L., & Abel, M. F. (1997). The evolution of gait in childhood and adolescent cerebral palsy. *Journal of Pediatric Orthopedics*, *17*(3), 392–396.

Kainz, H., Mindler, G. T., & Kranzl, A. (2023). Influence of femoral anteversion angle and neck-shaft angle on muscle forces and joint loading during walking. *PLOS ONE*, *18*(10), e0291458. https://doi.org/10.1371/journal.pone.0291458

Karpati, F., Weir, S., & Narayanan, U. (2011). *Gait Outcomes Assessment List (GOAL): Development of a patient prioritycentered outcome measure for children with ambulatory cerebral palsy* [Symposium]. Sixth Annual Bloorview Research Institute Symposium, Holland Bloorview Kids Rehabilitation Hospital, Ontario, Ca. https://hollandbloorview.ca/sites/default/files/migrate/files/Karpatiweb.pdf

Kay, R. M., Rethlefsen, S. A., Ryan, J. A., & Wren, T. A. L. (2004). Outcome of gastrocnemius recession and tendo-achilles lengthening in ambulatory children with cerebral palsy: *Journal of Pediatric Orthopaedics, Part B*, *13*(2), 92–98. https://doi.org/10.1097/00009957-200403000-00006

Kean, C. O., Hinman, R. S., Bowles, K. A., Cicuttini, F., Davies-Tuck, M., & Bennell, K. L. (2012). Comparison of peak knee adduction moment and knee adduction moment

impulse in distinguishing between severities of knee osteoarthritis. *Clinical Biomechanics*, *27*(5), 520–523. https://doi.org/10.1016/j.clinbiomech.2011.12.007

Keawutan, P., Bell, K. L., Oftedal, S., Davies, P. S. W., Ware, R. S., & Boyd, R. N. (2018). Quality of life and habitual physical activity in children with cerebral palsy aged 5 years: A cross-sectional study. *Res Dev Disabil*, *74*, 139–145. https://doi.org/10.1016/j.ridd.2018.01.008

Kerr, C., Parkes, J., Stevenson, M., Cosgrove, A. P., & McDowell, B. C. (2008). Energy efficiency in gait, activity, participation, and health status in children with cerebral palsy. *Developmental Medicine & Child Neurology*, *50*(3), 204–210. https://doi.org/10.1111/j.1469-8749.2008.02030.x

Kerr Graham, H., & Selber, P. (2003). Musculoskeletal aspects of cerebral palsy. *The Journal of Bone and Joint Surgery*, *85*(2), 157–166. https://doi.org/10.1302/0301-620X.85B2.14066

Kim, C. J., & Son, S. M. (2014). Comparison of Spatiotemporal Gait Parameters between Children with Normal Development and Children with Diplegic Cerebral Palsy. *Journal of Physical Therapy Science*, *26*(9), 1317–1319. https://doi.org/10.1589/jpts.26.1317

Ko, F. C., Dragomir, C., Plumb, D. A., Goldring, S. R., Wright, T. M., Goldring, M. B., & van der Meulen, M. C. H. (2013). In Vivo Cyclic Compression Causes Cartilage Degeneration and Subchondral Bone Changes in Mouse Tibiae. *Arthritis & Rheumatism*, *65*(6), 1569–1578. https://doi.org/10.1002/art.37906

Koller, W., Baca, A., & Kainz, H. (2023). The gait pattern and not the femoral morphology is the main contributor to asymmetric hip joint loading. *PLOS ONE*, *18*(9), e0291789. https://doi.org/10.1371/journal.pone.0291789

Kristianslund, E., Krosshaug, T., & van den Bogert, A. J. (2012). Effect of low pass filtering on joint moments from inverse dynamics: Implications for injury prevention. *Journal of Biomechanics*, *45*(4), 666–671. https://doi.org/10.1016/j.jbiomech.2011.12.011

Kurz, M. J., Judkins, T. N., Arellano, C., & Scott-Pandorf, M. (2008). A passive dynamic walking robot that has a deterministic nonlinear gait. *Journal of Biomechanics*, *41*(6), 1310–1316. https://doi.org/10.1016/j.jbiomech.2008.01.007

Kutzner, I., Trepczynski, A., Heller, M. O., & Bergmann, G. (2013). Knee Adduction Moment and Medial Contact Force – Facts about Their Correlation during Gait. *PLoS ONE*, *8*(12), e81036. https://doi.org/10.1371/journal.pone.0081036

Lamberts, R. P., Burger, M., Du Toit, J., & Langerak, N. G. (2016). A systematic review of the effects of single-event multilevel surgery on gait parameters in children with spastic cerebral palsy. *PLoS ONE*, *11*(10), 1–22. https://doi.org/10.1371/journal.pone.0164686

Laracca, E., Stewart, C., Postans, N., & Roberts, A. (2014). The effects of surgical lengthening of hamstring muscles in children with cerebral palsy—The consequences of pre-operative muscle length measurement. *Gait and Posture*, *39*(3), 847–851. https://doi.org/10.1016/j.gaitpost.2013.11.010

Lee, S. Y., Kwon, S. S., Chung, C. Y., Lee, K. M., Choi, Y., Kim, T. G., Shin, W. C., Choi, I. H., Cho, T. J., Yoo, W. J., & Park, M. S. (2014). Rectus femoris transfer in cerebral palsy patients with stiff knee gait. *Gait and Posture*, *40*(1), 76–81. https://doi.org/10.1016/j.gaitpost.2014.02.013

Lehtonen, K., Mäenpää, H., & Piirainen, A. (2015). Does single-event multilevel surgery enhance physical functioning in the real-life environment in children and adolescents

with cerebral palsy (CP)?: Patient perceptions five years after surgery. *Gait and Posture*, *41*(2), 448–453. https://doi.org/10.1016/j.gaitpost.2014.11.005

Lenth, R. V., & Piaskowski, J. (2017). *emmeans: Estimated Marginal Means, aka Least-Squares Means* (p. 2.0.0) [Dataset]. https://doi.org/10.32614/CRAN.package.emmeans

Lieber, R. L., Steinman, S., Barash, I. A., & Chambers, H. (2004). Structural and functional changes in spastic skeletal muscle. *Muscle & Nerve*, *29*(5), 615–627. https://doi.org/10.1002/mus.20059

Lin, C. J., Guo, L. Y., Su, F. C., Chou, Y. L., & Cherng, R. J. (2000). Common abnormal kinetic patterns of the knee in gait in spastic diplegia of cerebral palsy. *Gait and Posture*, *11*(3), 224–232. https://doi.org/10.1016/S0966-6362(00)00049-7

Lofterød, B., Terjesen, T., Skaaret, I., Huse, A.-B. B., & Jahnsen, R. (2007). Preoperative gait analysis has a substantial effect on orthopedic decision making in children with cerebral palsy: Comparison between clinical evaluation and gait analysis in 60 patients. *Acta Orthopaedica*, *78*(1), 74–80. https://doi.org/10.1080/17453670610013448

Lynn, A. K., Turner, M., & Chambers, H. G. (2009). Surgical Management of Spasticity in Persons with Cerebral Palsy. *PM and R*, *1*(9), 834–838. https://doi.org/10.1016/j.pmrj.2009.07.016

Malt, M. A., Aarli, Å., Bogen, B., & Fevang, J. M. (2016). Correlation between the Gait Deviation Index and gross motor function (GMFCS level) in children with cerebral palsy. *Journal of Children's Orthopaedics*, *10*(3), 261–266. https://doi.org/10.1007/s11832-016-0738-4

Marconi, V., Hachez, H., Renders, A., Docquier, P.-L., & Detrembleur, C. (2014). Mechanical work and energy consumption in children with cerebral palsy after single-event

multilevel surgery. *Gait & Posture*, *40*(4), 633–639. https://doi.org/10.1016/j.gaitpost.2014.07.014

Massaad, A., Assi, A., Skalli, W., & Ghanem, I. (2014). Repeatability and validation of Gait Deviation Index in children: Typically developing and cerebral palsy. *Gait & Posture*, *39*(1), 354–358. https://doi.org/10.1016/j.gaitpost.2013.08.001

McCarthy, J., Shrader, M. W., Graham, K., Veerkamp, M., Brower, L., Chambers, H., Davids, J. R., Kay, R. M., Narayanan, U., Novacheck, T. F., Pierz, K., Rhodes, J., Rutz, E., Shilt, J., Shore, B. J., Theologis, T., & Van Campenhout, A. (2020). Establishing surgical indications for hamstring lengthening and femoral derotational osteotomy in ambulatory children with cerebral palsy. *Journal of Children's Orthopaedics*, *14*(1), 50–57. https://doi.org/10.1302/1863-2548.14.190173

McDowell, B. C., Hewitt, V., Nurse, A., Weston, T., & Baker, R. (2000). The variability of goniometric measurements in ambulatory children with spastic cerebral palsy. *Gait & Posture*, *12*(2), 114–121. https://doi.org/10.1016/S0966-6362(00)00068-0

McGinley, J. L., Baker, R., Wolfe, R., & Morris, M. E. (2009). The reliability of three-dimensional kinematic gait measurements: A systematic review. *Gait & Posture*, *29*(3), 360–369. https://doi.org/10.1016/j.gaitpost.2008.09.003

McGinley, J. L., Dobson, F., Ganeshalingam, R., Shore, B. J., Rutz, E., & Graham, H. K. (2012). Single-event multilevel surgery for children with cerebral palsy: A systematic review. *Developmental Medicine and Child Neurology*, *54*(2), 117–128. https://doi.org/10.1111/j.1469-8749.2011.04143.x

McIntyre, S., Goldsmith, S., Webb, A., Ehlinger, V., Hollung, S. J., McConnell, K., Arnaud, C., Smithers-Sheedy, H., Oskoui, M., Khandaker, G., Himmelmann, K., & Group*, the G. C.

P. (2022). Global prevalence of cerebral palsy: A systematic analysis. *Developmental Medicine & Child Neurology*, *64*(12), 1494–1506. https://doi.org/10.1111/dmcn.15346

McMulkin, M. L., & MacWilliams, B. A. (2015). Application of the Gillette Gait Index, Gait Deviation Index and Gait Profile Score to multiple clinical pediatric populations. *Gait & Posture*, *41*(2), 608–612. https://doi.org/10.1016/j.gaitpost.2015.01.005

McNee, A. E., Shortland, A. P., Eve, L. C., Robinson, R. O., & Gough, M. (2004). Lower limb extensor moments in children with spastic diplegic cerebral palsy. *Gait & Posture*, *20*(2), 171–176. https://doi.org/10.1016/j.gaitpost.2003.08.009

Metz, C., Jaster, M., Walch, E., Sarpong-Bengelsdorf, A., Kaindl, A. M., & Schneider, J. (2022). Clinical Phenotype of Cerebral Palsy Depends on the Cause: Is It Really Cerebral Palsy? A Retrospective Study. *Journal of Child Neurology*, *37*(2), 112–118. https://doi.org/10.1177/08830738211059686

Modenese, L., Barzan, M., & Carty, C. P. (2021). Dependency of lower limb joint reaction forces on femoral version. *Gait & Posture*, *88*, 318–321. https://doi.org/10.1016/j.gaitpost.2021.06.014

Molenaers, G. (2006). The Effects of Quantitative Gait Assessment and Botulinum Toxin A on Musculoskeletal Surgery in Children with Cerebral Palsy. *The Journal of Bone and Joint Surgery (American)*, *88*(1), 161. https://doi.org/10.2106/JBJS.C.01497

Molloy, M., McDowell, B. C., Kerr, C., & Cosgrove, A. P. (2010). Further evidence of validity of the Gait Deviation Index. *Gait and Posture*, *31*(4), 479–482. https://doi.org/10.1016/j.gaitpost.2010.01.025

Morrell, D. S., Pearson, J. M., & Sauser, D. D. (2002). Progressive Bone and Joint Abnormalities of the Spine and Lower Extremities in Cerebral Palsy. *RadioGraphics*, *22*(2), 257–268. https://doi.org/10.1148/radiographics.22.2.g02mr19257

Murphy, S. L., Schepens Niemiec, S., Lyden, A. K., & Kratz, A. L. (2016). Pain, Fatigue, and Physical Activity in Osteoarthritis: The Moderating Effects of Pain- and Fatigue-Related Activity Interference. *Archives of Physical Medicine and Rehabilitation*, *97*(9 Suppl), S201-209. https://doi.org/10.1016/j.apmr.2015.05.025

Nagano, H., Tatsumi, I., Sarashina, E., Sparrow, W. A., & Begg, R. K. (2015). Modelling knee flexion effects on joint power absorption and adduction moment. *The Knee*, *22*(6), 490–493. https://doi.org/10.1016/j.knee.2015.06.016

Narayanan, U. G. (2007). The role of gait analysis in the orthopaedic management of ambulatory cerebral palsy. *Current Opinion in Pediatrics*, *19*(1), 38–43. https://doi.org/10.1097/MOP.0b013e3280118a6d

Nieuwenhuys, A., Õunpuu, S., Van Campenhout, A., Theologis, T., De Cat, J., Stout, J., Molenaers, G., De Laet, T., & Desloovere, K. (2016). Identification of joint patterns during gait in children with cerebral palsy: A Delphi consensus study. *Developmental Medicine & Child Neurology*, *58*(3), 306–313. https://doi.org/10.1111/dmcn.12892

Niklasch, M., Döderlein, L., Klotz, M. C., Braatz, F., Wolf, S. I., & Dreher, T. (2015). Asymmetric pelvic and hip rotation in children with bilateral cerebral palsy: Uni- or bilateral femoral derotation osteotomy? *Gait & Posture*, *41*(2), 670–675. https://doi.org/10.1016/j.gaitpost.2015.01.024

Norlin, R., Odenrick, P., & Sandlund, B. (1981). Development of gait in the normal child. *Journal of Pediatric Orthopedics*, *1*(3), 261–266. https://doi.org/10.1097/01241398-198111000-00004

Norlin, R., & Tkaczuk, H. (1985). One-session surgery for correction of lower extremity deformities in children with cerebral palsy. *Journal of Pediatric Orthopedics*, *5*(2), 208–211.

Norman, J. F., Bossman, S., Gardner, P., & Moen, C. (2004). Comparison of the Energy Expenditure Index and Oxygen Consumption Index During Self-Paced Walking in Children with Spastic Diplegia Cerebral Palsy and Children Without Physical Disabilities. *Pediatric Physical Therapy*, *16*(4), 206. https://doi.org/10.1097/01.PEP.0000145930.84009.23

Novacheck, T. F., & Gage, J. R. (2007). Orthopedic management of spasticity in cerebral palsy. *Child's Nervous System*, *23*(9), 1015–1031. https://doi.org/10.1007/s00381-007-0378-6

O'Connell, N. E., Smith, K. J., Peterson, M. D., Ryan, N., Liverani, S., Anokye, N., Victor, C., & Ryan, J. M. (2019). Incidence of osteoarthritis, osteoporosis and inflammatory musculoskeletal diseases in adults with cerebral palsy: A population-based cohort study. *Bone*, *125*, 30–35. https://doi.org/10.1016/j.bone.2019.05.007

Oeffinger, D., Bagley, A., Rogers, S., Gorton, G., Kryscio, R., Abel, M., Damiano, D., Barnes, D., & Tylkowski, C. (2008). Outcome tools used for ambulatory children with cerebral palsy: Responsiveness and minimum clinically important differences. *Developmental Medicine & Child Neurology*, *50*(12), 918–925. https://doi.org/10.1111/j.1469-8749.2008.03150.x

O'Sullivan, R., French, H. P., Rossom, S. V., Jonkers, I., & Horgan, F. (2021). The association between gait analysis measures associated with crouch gait, functional health status and daily activity levels in cerebral palsy. *Journal of Pediatric Rehabilitation Medicine*. https://journals.sagepub.com/doi/full/10.3233/PRM-200676

Ounpuu, S., Muik, E., Davis, R. B., Gage, J. R., & DeLuca, P. A. (1993). Rectus femoris surgery in children with cerebral palsy. Part II: A comparison between the effect of transfer and release of the distal rectus femoris on knee motion. *Journal of Pediatric Orthopedics*, *13*(3), 331–335. https://doi.org/10.1097/01241398-199305000-00011

Õunpuu, S., Solomito, M., Bell, K., DeLuca, P., & Pierz, K. (2015). Long-term outcomes after multilevel surgery including rectus femoris, hamstring and gastrocnemius procedures in children with cerebral palsy. *Gait and Posture*, *42*(3), 365–372. https://doi.org/10.1016/j.gaitpost.2015.07.003

Paley, D. (2002). *Principles of Deformity Correction*. Springer Berlin Heidelberg. https://doi.org/10.1007/978-3-642-59373-4

Palisano, R. J., Kang, L.-J., Chiarello, L. A., Orlin, M., Oeffinger, D., & Maggs, J. (2009). Social and community participation of children and youth with cerebral palsy is associated with age and gross motor function classification. *Physical Therapy*, *89*(12), 1304–1314. https://doi.org/10.2522/ptj.20090162

Palisano, R. J., Rosenbaum, P., Bartlett, D., & Livingston, M. H. (2008). Content validity of the expanded and revised Gross Motor Function Classification System. *Developmental Medicine & Child Neurology*, *50*(10), 744–750. https://doi.org/10.1111/j.1469-8749.2008.03089.x

Park, M. S., Chung, C. Y., Lee, S. H., Choi, I. H., Cho, T. J., Yoo, W. J., Park, B. S. M. Y., & Lee, K. M. (2009). Effects of distal hamstring lengthening on sagittal motion in patients with diplegia. Hamstring length and its clinical use. *Gait and Posture*, *30*(4), 487–491. https://doi.org/10.1016/j.gaitpost.2009.07.115

Patterson, K. K., Parafianowicz, I., Danells, C. J., Closson, V., Verrier, M. C., Staines, W. R., Black, S. E., & McIlroy, W. E. (2008). Gait Asymmetry in Community-Ambulating Stroke Survivors. *Archives of Physical Medicine and Rehabilitation*, *89*(2), 304–310. https://doi.org/10.1016/j.apmr.2007.08.142

Perry, J., Antonelli, D., & Ford, W. (1975). Analysis of knee-joint forces during flexed-knee stance. *JBJS*, *57*(7), 961.

Pinheiro, J. C., & Bates, D. M. (2000). Linear Mixed-Effects Models: Basic Concepts and Examples. In *Mixed-Effects Models in Sand S-PLUS* (pp. 3–56). Springer New York. https://doi.org/10.1007/978-1-4419-0318-1_1

R Core Team. (2025). *R: a language and environment for statistical computing* [Manual]. R Foundation for Statistical Computing. https://www.R-project.org/

Rajagopal, A., Kidziński, Ł., McGlaughlin, A. S., Hicks, J. L., Delp, S. L., & Schwartz, M. H. (2018). Estimating the effect size of surgery to improve walking in children with cerebral palsy from retrospective observational clinical data. *Scientific Reports*, *8*(1), 16344. https://doi.org/10.1038/s41598-018-33962-2

Rasmussen, H. M., Pedersen, N. W., Overgaard, S., Hansen, L. K., Dunkhase-Heinl, U., Petkov, Y., Engell, V., & Holsgaard-Larsen, A. (2019). Gait analysis for individually tailored interdisciplinary interventions in children with cerebral palsy: A randomized controlled

trial. *Developmental Medicine and Child Neurology*, *61*(10), 1189–1195. https://doi.org/10.1111/dmcn.14178

Reinbolt, J. A., Fox, M. D., Arnold, A. S., Õunpuu, S., & Delp, S. L. (2008). Importance of preswing rectus femoris activity in stiff-knee gait. *Journal of Biomechanics*, *41*(11), 2362–2369. https://doi.org/10.1016/j.jbiomech.2008.05.030

Rethlefsen, S. A., Healy, B. S., Wren, T. A. L., Skaggs, D. L., & Kay, R. M. (2006). Causes of intoeing gait in children with cerebral palsy. *The Journal of Bone and Joint Surgery. American Volume*, *88*(10), 2175–2180. https://doi.org/10.2106/JBJS.E.01280

Rethlefsen, S. A., & Kay, R. M. (2013). Transverse Plane Gait Problems in Children With Cerebral Palsy. *Journal of Pediatric Orthopaedics*, *33*(4), 422–430. https://doi.org/10.1097/BPO.0b013e3182784e16

Robbins, S. M. K., & Maly, M. R. (2009). The effect of gait speed on the knee adduction moment depends on waveform summary measures. *Gait & Posture*, *30*(4), 543–546. https://doi.org/10.1016/j.gaitpost.2009.08.236

Robinson, R. O., Herzog, W., & Nigg, B. M. (1987). Use of force platform variables to quantify the effects of chiropractic manipulation on gait symmetry. *Journal of Manipulative and Physiological Therapeutics*, *10*(4), 172–176. Scopus.

Rodda, J. M., Graham, H. K., Carson, L., Galea, M. P., & Wolfe, R. (2004). Sagittal gait patterns in spastic diplegia. *The Journal of Bone and Joint Surgery*, *86*(2), 251–258. https://doi.org/10.1302/0301-620X.86B2.13878

Rose, G. E., Lightbody, K. A., Ferguson, R. G., Walsh, J. C., & Robb, J. E. (2010). Natural history of flexed knee gait in diplegic cerebral palsy evaluated by gait analysis in children

who have not had surgery. *Gait & Posture*, *31*(3), 351–354. https://doi.org/10.1016/j.gaitpost.2009.12.006

Rose, S. A., DeLuca, P. A., Davis, R. B., Õunpuu, S., & Gage, J. R. (1993). Kinematic and Kinetic Evaluation of the Ankle After Lengthening of the Gastrocnemius Fascia in Children with Cerebral Palsy. *Journal of Pediatric Orthopaedics*, *13*(6), 727–732. https://doi.org/10.1097/01241398-199311000-00007

Rutz, E., Baker, R., Tirosh, O., Romkes, J., Haase, C., & Brunner, R. (2011). Tibialis anterior tendon shortening in combination with Achilles tendon lengthening in spastic equinus in cerebral palsy. *Gait Posture*, *33*(2), 152–157. https://doi.org/10.1016/j.gaitpost.2010.11.002

Rutz, E., Donath, S., Tirosh, O., Kerr Graham, H., Baker, R., Graham, H. K., & Baker, R. (2013). Explaining the variability improvements in gait quality as a result of single event multi-level surgery in cerebral palsy. *Gait and Posture*, *38*(3), 455–460. https://doi.org/10.1016/j.gaitpost.2013.01.014

Saglam, Y., Ekin Akalan, N., Temelli, Y., & Kuchimov, S. (2016). Femoral derotation osteotomy with multi-level soft tissue procedures in children with cerebral palsy: Does it improve gait quality? *Journal of Children's Orthopaedics*, *10*(1), 41–48. https://doi.org/10.1007/s11832-015-0706-4

Sanger, T. D., Chen, D., Delgado, M. R., Gaebler-Spira, D., Hallett, M., Mink, J. W., & the Taskforce on Childhood Motor Disorders. (2006). Definition and Classification of Negative Motor Signs in Childhood. *Pediatrics*, *118*(5), 2159–2167. https://doi.org/10.1542/peds.2005-3016

Saraph, V., Zwick, E.-B., Zwick, G., Steinwender, C., Steinwender, G., & Linhart, W. (2002). Multilevel Surgery in Spastic Diplegia: Evaluation by Physical Examination and Gait Analysis in 25 Children: *Journal of Pediatric Orthopaedics*, *22*(2), 150–157. https://doi.org/10.1097/01241398-200203000-00003

Schipplein, O. D., & Andriacchi, T. P. (1991). Interaction between active and passive knee stabilizers during level walking. *Journal of Orthopaedic Research: Official Publication of the Orthopaedic Research Society*, *9*(1), 113–119. https://doi.org/10.1002/jor.1100090114

Schwartz, M. H., & Rozumalski, A. (2008). The gait deviation index: A new comprehensive index of gait pathology. *Gait and Posture*, *28*(3), 351–357. https://doi.org/10.1016/j.gaitpost.2008.05.001

Schwartz, M. H., Viehweger, E., Stout, J., Novacheck, T. F., & Gage, J. R. (2004). Comprehensive treatment of ambulatory children with cerebral palsy: An outcome assessment. *Journal of Pediatric Orthopedics*, *24*(1), 45–53.

Selbie, S., Hamill, J., Kepple, T., & Robertson, D. G. E. (Eds.). (2014). Three-Dimensional Kinetics. In *Research methods in biomechanics* (Second edition). Human Kinetics. https://doi.org/10.5040/9781492595809

Sharma, Y., Cheung, L., Patterson, K. K., & Iaboni, A. (2024). Factors influencing the clinical adoption of quantitative gait analysis technology with a focus on clinical efficacy and clinician perspectives: A scoping review. *Gait & Posture*, *108*, 228–242. https://doi.org/10.1016/j.gaitpost.2023.12.003

Shelly, A., Davis, E., Waters, E., Mackinnon, A., Reddihough, D., Boyd, R., Reid, S., & Graham, H. K. (2008). The relationship between quality of life and functioning for

children with cerebral palsy. *Developmental Medicine and Child Neurology*, *50*(3), 199–203. https://doi.org/10.1111/J.1469-8749.2008.02031.X/FORMAT/PDF

Shore, B. J., Desloovere, K., & Narayanan, U. G. (2020). Outcome Measurement in Ambulatory Cerebral Palsy. In *Improving Quality of Life for Individuals with Cerebral Palsy Through Treatment of Gait Impairment: International Cerebral Palsy Function and Mobility Symposium* (1st ed, p. 36). Mac Keith Press.

Shuman, B. R., Goudriaan, M., Desloovere, K., Schwartz, M. H., & Steele, K. M. (2019). Muscle synergies demonstrate only minimal changes after treatment in cerebral palsy. *Journal of NeuroEngineering and Rehabilitation*, *16*(1), 1–10. https://doi.org/10.1186/s12984-019-0502-3

Šidák, Z. (1967). Rectangular Confidence Regions for the Means of Multivariate Normal Distributions. *Journal of the American Statistical Association*, *62*(318), 626–633. https://doi.org/10.1080/01621459.1967.10482935

Silver, R., De La Garza, J., & Rang, M. (1985). The myth of muscle balance. A study of relative strengths and excursions of normal muscles about the foot and ankle. *The Journal of Bone and Joint Surgery. British Volume*, *67-B*(3), 432–437. https://doi.org/10.1302/0301-620X.67B3.3997956

Skaggs, D. L., Rethlefsen, S. A., Kay, R. M., Dennis, S. W., Reynolds, R. A. K., & Tolo, V. T. (2000). *Variability in Gait Analysis Interpretation*.

Smith, L. R., Lee, K. S., Ward, S. R., Chambers, H. G., & Lieber, R. L. (2011). Hamstring contractures in children with spastic cerebral palsy result from a stiffer extracellular matrix and increased in vivo sarcomere length. *The Journal of Physiology*, *589*(Pt 10), 2625–2639. https://doi.org/10.1113/jphysiol.2010.203364

Smith, S. H. L., Coppack, R. J., van den Bogert, A. J., Bennett, A. N., & Bull, A. M. J. (2021). Review of musculoskeletal modelling in a clinical setting: Current use in rehabilitation design, surgical decision making and healthcare interventions. *Clinical Biomechanics*, *83*(September 2020), 105292. https://doi.org/10.1016/j.clinbiomech.2021.105292

Smithers-Sheedy, H., Badawi, N., Blair, E., Cans, C., Himmelmann, K., Krägeloh-Mann, I., McIntyre, S., Slee, J., Uldall, P., Watson, L., & Wilson, M. (2014). What constitutes cerebral palsy in the twenty-first century? *Developmental Medicine & Child Neurology*, *56*(4), 323–328. https://doi.org/10.1111/dmcn.12262

States, R. A., Salem, Y., Krzak, J. J., Godwin, E. M., McMulkin, M. L., & Kaplan, S. L. (2024). Three-Dimensional Instrumented Gait Analysis for Children With Cerebral Palsy: An Evidence-Based Clinical Practice Guideline. *Pediatric Physical Therapy*, *36*(2), 182–206. https://doi.org/10.1097/PEP.0000000000001101

Steele, K. M., DeMers, M. S., Schwartz, M. S., & Delp, S. L. (2012). Compressive Tibiofemoral Force during Crouch Gait. *Gait & Posture*, *35*(4), 556–560. https://doi.org/10.1016/j.gaitpost.2011.11.023

Steele, K. M., & Schwartz, M. H. (2022). Causal Effects of Motor Control on Gait Kinematics After Orthopedic Surgery in Cerebral Palsy: A Machine-Learning Approach. *Frontiers in Human Neuroscience*, *16*, 846205. https://doi.org/10.3389/fnhum.2022.846205

Stoddart, J. C., Dandridge, O., Garner, A., Cobb, J., & Arkel, R. J. van. (2021). The compartmental distribution of knee osteoarthritis – a systematic review and meta-analysis. *Osteoarthritis and Cartilage*, *29*(4), 445–455. https://doi.org/10.1016/j.joca.2020.10.011

Stout, J. L., Gage, J. R., Schwartz, M. H., & Novacheck, T. F. (2008). Distal Femoral Extension Osteotomy and Patellar Tendon Advancement to Treat Persistent Crouch Gait in Cerebral Palsy: *The Journal of Bone and Joint Surgery-American Volume*, *90*(11), 2470–2484. https://doi.org/10.2106/JBJS.G.00327

Sung, K. H., Kwon, S. S., Chung, C. Y., Lee, K. M., Cho, G. H., & Park, M. S. (2018). Long-term outcomes over 10 years after femoral derotation osteotomy in ambulatory children with cerebral palsy. *Gait and Posture*, *64*(May), 119–125. https://doi.org/10.1016/j.gaitpost.2018.06.003

Sutherland. (1997). The development of mature gait. *Gait & Posture*, *6*(2), 163–170. https://doi.org/10.1016/S0966-6362(97)00029-5

Sutherland, & Davids, J. R. (1993). Common gait abnormalities of the knee in cerebral palsy. *Clinical Orthopaedics and Related Research*, *288*, 139–147.

Thawrani, D., Haumont, T., Church, C., Holmes, L., Dabney, K. W., & Miller, F. (2012). Rectus Femoris Transfer Improves Stiff Knee Gait in Children With Spastic Cerebral Palsy. *Clinical Orthopaedics & Related Research*, *470*(5), 1303–1311. https://doi.org/10.1007/s11999-011-2215-1

Theologis, T. (2013). Lever arm dysfunction in cerebral palsy gait. *Journal of Children's Orthopaedics*, *7*(5), 379–382. https://doi.org/10.1007/s11832-013-0510-y

Theologis, T., Birks, J., Stebbins, J., Thompson, N., Davies, L., Cooper, C., Nogaro, M. C., Wright, J., Beard, D. J., & Perry, D. C. (2025). A UK national prospective cohort study investigating current practices in single-event multilevel surgery for children with bilateral cerebral palsy and its impact on gait and function: The CPinBOSS study. *The*

Bone & Joint Journal, *107-B*(12), 1370–1378. https://doi.org/10.1302/0301-620X.107B12.BJJ-2025-0014.R2

Thibault, M., Robin Poole, A., & Buschmann, M. D. (2002). Cyclic compression of cartilage/bone explants in vitro leads to physical weakening, mechanical breakdown of collagen and release of matrix fragments. *Journal of Orthopaedic Research*, *20*(6), 1265–1273. https://doi.org/10.1016/S0736-0266(02)00070-0

Thomason, P., Selber, P., & Graham, H. K. (2013). Single Event Multilevel Surgery in children with bilateral spastic cerebral palsy: A 5 year prospective cohort study. *Gait and Posture*, *37*(1), 23–28. https://doi.org/10.1016/j.gaitpost.2012.05.022

Tylkowski, C. M., Horan, M., & Oeffinger, D. J. (2009). Outcomes of Gastrocnemius-soleus Complex Lengthening for Isolated Equinus Contracture in Children With Cerebral Palsy. *Journal of Pediatric Orthopaedics*, *29*(7), 771–778. https://doi.org/10.1097/BPO.0b013e3181b76a7c

van de Walle, P., Hallemans, A., Schwartz, M., Truijen, S., Gosselink, R., & Desloovere, K. (2012). Mechanical energy estimation during walking: Validity and sensitivity in typical gait and in children with cerebral palsy. *Gait and Posture*, *35*(2), 231–237. https://doi.org/10.1016/j.gaitpost.2011.09.012

van den Hecke, A., Malghem, C., Renders, A., Detrembleur, C., Palumbo, S., & Lejeune, T. M. (2007). Mechanical work, energetic cost, and gait efficiency in children with cerebral palsy. *Journal of Pediatric Orthopedics*, *27*(6), 643–647. https://doi.org/10.1097/BPO.0b013e318093f4c3

Van Ooteghem, K., Mansfield, A., Inness, E. L., Killingbeck, J., & Sibley, K. M. (2020). Integrating Technology Into Clinical Practice for the Assessment of Balance and

Mobility: Perspectives of Exercise Professionals Practicing in Retirement and Long-term Care. *Archives of Rehabilitation Research and Clinical Translation*, *2*(2), 100041. https://doi.org/10.1016/j.arrct.2020.100041

Van Rossom, S., Kainz, H., Wesseling, M., Papageorgiou, E., De Groote, F., Van Campenhout, A., Molenaers, G., Desloovere, K., & Jonkers, I. (2020). Single-event multilevel surgery, but not botulinum toxin injections normalize joint loading in cerebral palsy patients. *Clinical Biomechanics (Bristol, Avon)*, *76*, 105025. https://doi.org/10.1016/j.clinbiomech.2020.105025

Veerkamp, K., Schallig, W., Harlaar, J., Pizzolato, C., Carty, C. P., Lloyd, D. G., & van der Krogt, M. M. (2019). The effects of electromyography-assisted modelling in estimating musculotendon forces during gait in children with cerebral palsy. *Journal of Biomechanics*, *92*, 45–53. https://doi.org/10.1016/j.jbiomech.2019.05.026

Vuillermin, C., Rodda, J., Rutz, E., Shore, B. J., Smith, K., & Graham, H. K. (2011). Severe crouch gait in spastic diplegia can be prevented: A population-based study. *Journal of Bone and Joint Surgery - Series B*, *93 B*(12), 1670–1675. https://doi.org/10.1302/0301-620X.93B12

West, B. J., & Scafetta, N. (2003). A nonlinear dynamical model of human gait. *Physical Review E*, *67*(5), 051917. https://doi.org/10.1103/PhysRevE.67.051917

Whitney, D. G., Kamdar, N. S., Ng, S., Hurvitz, E. A., & Peterson, M. D. (2019). Prevalence of high-burden medical conditions and health care resource utilization and costs among adults with cerebral palsy. *Clinical Epidemiology*, *11*, 469–481. https://doi.org/10.2147/CLEP.S205839

Whittle, M. W. (2007). *Gait Analysis*. Elsevier. https://doi.org/10.1016/B978-0-7506-8883-3.X5001-6

Williams, D. S., & Martin, A. E. (2019). Gait modification when decreasing double support percentage. *Journal of Biomechanics*, *92*, 76–83. https://doi.org/10.1016/j.jbiomech.2019.05.028

Wilson, N. C., Chong, J., Mackey, A. H., & Stott, N. S. (2014). Reported outcomes of lower limb orthopaedic surgery in children and adolescents with cerebral palsy: A mapping review. *Developmental Medicine & Child Neurology*, *56*(9), 808–814. https://doi.org/10.1111/dmcn.12431

Winter, D. A. (2009). *Biomechanics and Motor Control of Human Movement*. John Wiley & Sons.

Winters, T. F. J., Gage, J. R., & Hicks, R. (1987). Gait patterns in spastic hemiplegia in children and young adults. *The Journal of Bone and Joint Surgery. American Volume*, *69*(3), 437–441.

Wise, B. L., Niu, J., Yang, M., Lane, N. E., Harvey, W., Felson, D. T., Hietpas, J., Nevitt, M., Sharma, L., Torner, J., Lewis, C. E., & Zhang, Y. (2012). Patterns of Compartment Involvement in Tibiofemoral Osteoarthritis in Men and Women and in Caucasians and African Americans: The Multicenter Osteoarthritis Study. *Arthritis Care & Research*, *64*(6), 847–852. https://doi.org/10.1002/acr.21606

Wren, T. A. L., Gorton, G. E., Õunpuu, S., & Tucker, C. A. (2011a). Efficacy of clinical gait analysis: A systematic review. *Gait and Posture*, *34*(2), 149–153. https://doi.org/10.1016/j.gaitpost.2011.03.027

Wren, T. A. L., Otsuka, N. Y., Bowen, R. E., Scaduto, A. A., Chan, L. S., Sheng, M., Hara, R., & Kay, R. M. (2011b). Influence of gait analysis on decision-making for lower extremity orthopaedic surgery: Baseline data from a randomized controlled trial. *Gait and Posture*, *34*(3), 364–369. https://doi.org/10.1016/j.gaitpost.2011.06.002

Wren, T. A. L., Tucker, C. A., Rethlefsen, S. A., Gorton, G. E., & Õunpuu, S. (2020). Clinical efficacy of instrumented gait analysis: Systematic review 2020 update. *Gait and Posture*, *80*(March), 274–279. https://doi.org/10.1016/j.gaitpost.2020.05.031

Zajac, F. E. (1989). Muscle and tendon: Properties, models, scaling, and application to biomechanics and motor control. *Critical Reviews in Biomedical Engineering*, *17*(4), 359–411.

Zelik, K. E., & Adamczyk, P. G. (2016). A unified perspective on ankle push-off in human walking. *The Journal of Experimental Biology*, *219*(23), 3676–3683. https://doi.org/10.1242/jeb.140376

Zeni, J. A., Richards, J. G., & Higginson, J. S. (2008). Two simple methods for determining gait events during treadmill and overground walking using kinematic data. *Gait and Posture*, *27*(4), 710–714. https://doi.org/10.1016/j.gaitpost.2007.07.007

Zwick, E. B., Leistritz, L., Milleit, B., Saraph, V., Zwick, G., Galicki, M., Witte, H., & Steinwender, G. (2004). Classification of equinus in ambulatory children with cerebral palsy-discrimination between dynamic tightness and fixed contracture. *Gait & Posture*, *20*(3), 273–279. https://doi.org/10.1016/j.gaitpost.2003.10.002

Zwick, E. B., Saraph, V., Strobl, W., & Steinwender, G. (2001). [Single event multilevel surgery to improve gait in diplegic cerebral palsy—A prospective controlled trial]. *Z Orthop Ihre Grenzgeb*, *139*(6), 485–489. https://doi.org/10.1055/s-2001-19228